T-4399

ETHYL ISOPROPYL ETHER (EIPE) SYNTHESIS OVER CATION EXCHANGE RESINS: CATALYST EVALUATION AND REACTION KINETICS

by

Nurak Grisdanurak

T-4399

A thesis submitted to the Faculty and the Board of Trustees of the Colorado School of Mines in partial fulfillment of the requirements for the degree of Doctor of Philosophy (Chemical Engineering and Petroleum Refining).

Golden, Colorado
Date March 22, 96

Signed : Nurak Grisdanurak

Approved : Robert M. Baldwin
Thesis Advisor

Approved : Michael S. Graboski
Thesis Advisor

Golden, Colorado
Date April 2, 1996

Robert M. Baldwin
Chemical Engineering
and Petroleum Refining
Department Head

ABSTRACT

Synthesis of ethyl isopropyl ether (EIPE) from ethanol and propylene has been studied in both batch and trickle-bed downflow reactors using macroporous cation exchange resins as catalysts. In the stirred batch reactor, the effects of catalyst loading, reaction temperature and pressure, and feed composition were investigated in the temperature and pressure range of 80-120°C and 700-1000 psi, respectively. The batch reactor data showed that the reaction rate increased with an increase in catalyst concentration and reaction temperature, while total pressure was found to have no effect on the rate under the experimental conditions. In the trickle-bed reactor, the deactivation characteristics of four catalysts (Dowex HCR-w2, Amberlyst-15, supported FCSA and P/Al 0.8) were evaluated at a pressure of 500 psi by temperature sequencing. All catalysts before and after these tests were characterized for total surface area by BET, and for their ion exchange capacity and total carbon content. Insignificant deactivation was observed for the conditions investigated. Dowex and Amberlyst-15 were found to give similar activity and better selectivity in comparison to the other two catalysts. Dowex was found to be the superior resin for EIPE synthesis due to a higher maximum temperature limit and hence a higher overall activity.

The study concerning reaction kinetics for EIPE synthesis was carried out using Dowex HCR-w2 as a catalyst. Rate data were collected in the temperature range of 100-135°C and in a pressure range of 300-650 psi. Under these conditions, propylene was in the gas phase and ethanol was maintained in the liquid phase. The reaction rate data were analyzed using various heterogeneous models based on LHHW-type mechanisms and a pseudo-homogeneous model. Two adequate kinetic models were developed in which

either propylene adsorption or surface reaction was the rate limiting step. The apparent activation energies using the heterogeneous and pseudo-homogeneous models were found to be 97.60 kJ/mol and 105.42 kJ/mol respectively. The major by-product from synthesis of EIPE was found to be diethylether (DEE), hence the reaction kinetics for this product were also investigated. The reaction rate data were analyzed based on a LHHW mechanism and a model employing a dual-site, surface reaction rate controlling step was found to give an adequate representation to the observed data. The apparent activation energy for DEE synthesis was determined to be 98.93 kJ/mol. The effect of recycling DEE in order to improve the selectivity of the reaction for EIPE was studied experimentally. It was found that using a DEE:ethanol molar ratio of 1.0 increased the selectivity for EIPE by 10-20%. Deactivation characteristics for the Dowex ion exchange resin were tested in a temperature sequence lasting over 100 hours of continuous operation at the maximum allowable temperature of 140°C. Coking and/or polymerization was found to decrease both the activity and selectivity of the catalyst.

DEDICATION

This work is dedicated to my mom, Natsukorn and my dad, Manoon.

TABLE OF CONTENTS

LIST OF FIGURES

LIST OF TABLES

ACKNOWLEDGEMENTS

I would like to thank my advisors, Dr. Robert M. Baldwin and Dr. Micheal S. Graboski for their assistance and patience throughout this study. I would also like to thank my committee: Dr. Scott Cowley, Dr. Thomas McKinnon, Dr. James Ely, Dr. Patrick MacCarthy, and Dr. Bruce Honeyman.

In addition, I would like to gratefully reconize Mr. Jatuporn Wittayakun, a Ph.D. candidate in Chemistry at University of Wisconsin (Madison), for the highest attempt to teach me organic chemistry. Also, unforgettable thanks to all my friends at Mines, Aut Sajjamongkol, Lupong Kaewsichan, Kanjanee Gunvachai, Pinsuda Viravathana, Somruthai Cheysaard, Chuthamart Warasin, Malinee Srivilanon, Linda Gossard, and Stephen N. Paglieri for their help.

Finally, I wish to thank the Royal Thai Government and my family for providing me full financial and unconditional support.

Chapter 1
INTRODUCTION

The Clean Air Act (CAA) regulations of 1990 specify that oxygenates must be added to gasoline in ozone and carbon monoxide air pollution non-attainment areas. In general, an oxygenate can be blended into gasoline in the form of either an alcohol or an ether. Alcohols, particularly ethanol and methanol, blend non-ideally into gasoline due to their polarity and exhibit blending Reid vapor pressures (RVP) which are too high to meet the current Environmental Protection Agency (EPA) mandates concerning gasoline vapor pressure. The EPA will be placing additional restrictions on evaporative emissions in the future which will further restrict use of additives which increase the vapor pressure of the blend. On the other hand, the ether-based oxygenates such as methyl tert-butyl ether (MTBE) and ethyl tert-butyl ether (ETBE) blend more ideally with gasoline and exhibit blending vapor pressures which are low enough to meet current and proposed regulations. MTBE and ETBE can be manufactured by reacting isobutylene with methanol and ethanol, respectively. However, isobutylene is currently in short supply and must be manufactured from field butanes. Because considerable quantities of MTBE and methanol are currently being imported, it may be desirable to find an economically competitive fuel additive based on ethanol which can be produced from domestic sources.

1.1 Objective.

This study will be concerned with the production of an MTBE analog, ethyl isopropyl ether (EIPE). This material may be an effective and economical oxygenated

additive for gasoline since it can be produced from cheaper and readily available domestic materials. The primary objective of the research discussed in this dissertation was to investigate the kinetics for the synthesis of EIPE from ethanol and propylene over cation exchange resin catalysts.

The goals of this research program are as follows:

- investigate the thermodynamics of the reaction including all possible side reactions;
- investigate the feasibility of synthesizing EIPE in a batch reactor;
- design and construct a micro-flow continuous reactor for evaluation of catalysts and process conditions;
- screen several candidate catalysts;
- model and obtain a rate expression for the reaction;
- study selectivity improvement;
- investigate catalyst deactivation.

Chapter 2
BACKGROUND

2.1 Clean Air Act Amendment of 1990.

About one-half of the US. population lives in metropolitan regions that have been designated as air quality nonattainment areas. The most widespread urban air quality problem today is ground level ozone. Motor vehicles emit about half of the hydrocarbons and nitrogen oxides that lead to ozone, over half of the toxic air pollutants such as benzene, and about 90 percent of the carbon monoxide which presents a problem for many urban areas.

Past efforts in reducing vehicle emissions have focused on the development of sophisticated engine emission control systems involving catalytic converters. Research has shown that oxygenates added to gasoline can play a role in reducing motor vehicle emissions (Unzelman, 1991). Title II of the 1990 federal Clean Air Act (CAA) Amendment designates the use of oxygenates as one of the primary control strategies for urban areas in order to reduce emissions of pollutants from motor vehicles. There are two provisions of the Acts which involve oxygenates: 1) the oxygenated fuel provision and; 2) the reformulated gasoline program.

The oxygenated fuel program requires that all gasoline sold during the winter months in 41 carbon monoxide nonattainment areas must contain a minimum of 2.7 percent oxygen by weight. This requirement has been in effect since November 1992. These areas account for about one-third of the country. The EPA has projected that the use of oxygenated fuels would reduce vehicle carbon monoxide emissions by 15-20 percent.

For ozone, the act requires that the gasoline sold meet the standards of the reformulated gasoline program. This program sets a minimum oxygen content of 2 percent by weight, limits benzene content to a maximum of 1 percent, and prohibits addition of heavy metals. In addition to controlling evaporative emissions under the simple model, the RVP (Reid vapor pressure) is limited to 8.1 psi in the northern states, and 7.2 psi in the southern states. This requirement has been in effect since January 1995. The program expects to reduce ozone-forming hydrocarbon and toxic emissions by at least 15 percent during the first phase (1995-1999) and by about 25 percent thereafter (Davis, 1992; Chang and Leiby, 1992; Unzelman, 1991). To meet oxygenate and reformulated gasoline fuel mandates, oxygenates such as alcohols and ethers are receiving significant attention.

2.2 Status of Oxygenated Fuel Additives.

It has been reported that vehicles using M85 (a mixture of 85 percent methanol and 15 percent unleaded regular gasoline) produce 30 to 50 percent less of the smog-forming emissions than regular unleaded gasoline-fueled vehicles. Methanol however has the disadvantage of being toxic and corrosive. Fuel supply systems hence must be designed to prevent human exposure to methanol. Mechanics must be trained to properly handle the methanol-containing fuel because the flame is invisible to the human eye. In addition, vehicles need specially designed stainless steel equipment to withstand corrosive effects if they are to run on fuels with high concentrations of methanol. M85 also emits much more formaldehyde from the tailpipe, and emissions of carbon monoxide are equal or higher when compared to conventional unleaded gasoline.

Ethanol, another alternative, is already widely available as a fuel in the form of "gasohol". Like methanol, ethanol produces 30 to 50 percent less smog-forming emissions than similar gasoline-powered vehicles, and can also reduce carbon monoxide

emissions. However, ethanol solubility in water leads to phase separation during storage and transportation (Shelley, 1994). With respect to the blending vapor pressure, blending of methanol into gasoline would increase the vapor pressure by more than 2 psi, which would restrict sale of this fuel if all summer gasoline became limited to 9 RVP. Similarly, an ethanol blend would not be viable if 8 RVP became the summertime standard (Lenssen and Young, 1990). By comparison, the ether oxygenated fuels have lower volatilities and only slightly lower blending octane values than alcohols, as shown in Table 1.

In reformulated gasoline, the primary ether oxygenates are MTBE, ETBE, and tert-amylmethyl ether (TAME). MTBE produced from methanol and isobutylene dominates the market due to the ready availability of isobutylene from catalytic cracking and steam cracking fractions. MTBE's ethanol-derived counterpart ETBE has the same advantages as MTBE, including a lower RVP as shown in Table 1. The need for oxygenates has increased dramatically, and methanol was found to be in short supply late in 1994. As a result, methanol was sold for $1.21 a gallon (Hart's 21 for Century Fuels, 1994) which tended to raise the production costs of MTBE and hence gasoline. Manufacturing of ETBE from synthetic ethanol is very expensive. This leaves the use of fermented ethanol, which is now subsidized by tax credits and allows ETBE to compete economically with MTBE due to ethanol tax credits (Wyman, 1993). TAME, produced by the reaction of methanol with isoamylene, has a limitation due to the availability of isoamylene. TAME has not received consumer acceptance due to its odor (Seddon, 1992).

Isobutylene which is used to produce MTBE and ETBE can be supplied from two main sources: fractionation of natural gas liquids and refinery process gas streams. Natural gas liquids contain butane and isobutane which can be recovered and converted into isobutylene by two processes, butane isomerization and isobutane dehydrogenation.

Table 1. Blending Characteristics of Fuel Oxygenates (Brockwell, 1991).

	Boiling pt. (°C)	Blending RVP (psi)	(R+M)/ 2	Oxygen content wt%	Blending limits wt% O_2
Methanol	64.6	60	120	50	-
Ethanol	78.5	18	115	35	3.7
MeOH blend	63.6/82.4	31	108	35	3.7
TBA	83.0	12	100	21	3.7
MTBE	55.2	8	110	18	2.7
ETBE	71.8	4	111	16	2.7
TAME	86.3	1	106	16	2.7

From this process significant yields of isobutylene and propylene are formed (approximately 70% total). However, the isomerization catalyst can be easily deactivated by feed contaminants such as sulfur, nitrogen, olefins, and heavy metals (Monfils et al., 1992). Isobutylene can also be made from its isomer, n-butylene. The catalyst, fluorinated Al_2O_3, which is used for this process has difficulty in suppressing polymerization reactions (Szabo and Perrotey, 1991). The dehydration of TBA is another source for isobutylene; however, this source does not give as significant an amount of isobutylene as the two processes described above (Dunn, 1993). Generally, TBA is produced as a coproduct of propylene oxide manufacture, in which isobutane and propylene are used as raw materials. From the discussions above, it is obvious that

there are many steps involved in the manufacture of isobutylene. Hence, isobutylene is generally rather expensive as a raw material.

2.3 Status of Feedstock Ethanol.

Ethanol is derived primarily from renewable resources such as corn and grain feedstocks. Production of ethanol is more costly on a per gallon basis than some other alternative fuels. Fermentation methods for the production of ethanol are also, in general, slow and costly. Recently however, Josephson (1992) reported on research from the US National Renewable Energy Laboratory in Golden, Colorado which can improve ethanol production by an enzymatic technique known as Simultaneous Saccharrification Fermentation (SSF). This process requires about 120 hours to produce a 5% aqueous solution of ethanol for recovery by distillation or other techniques. The SSF process cuts equipment costs, chances of contamination, and gives high yields and high concentrations of ethanol. It is believed that with improvement of the technique, SSF will reduce the cost of ethanol from $1.35 a gallon in 1990 to $0.65 a gallon by 2010. Eokhoff (1993) also demonstrated the use of a continuous membrane reactor technology in SSF to decrease total processing time from the current 120 hours to less than 24 hours. By beginning a transition to ethanol, the US could ultimately lessen dependence on foreign sources of energy.

2.4 Ethyl IsoPropyl Ether (EIPE).

EIPE (2-ethoxy propane) is an unsymmetrical ether. A laboratory method to synthesize an unsymmetrical ether is to have an alkoxide undergo a reaction with a primary haloalkane under typical S_N2 conditions. This method is referred to the Williamson synthesis.

EIPE has a structure and physical properties similar to MTBE as shown in Table 2. The synthesis reaction is as follows:

$$\text{Ethanol} + \text{Propylene} \xrightarrow{\text{catalyst}} \text{EIPE}$$

The reaction feedstocks are ethanol and propylene. The reaction employs an acidic catalyst similar to that used for MTBE manufacture.

Table 2. Characteristics of EIPE and MTBE.

	EIPE	MTBE
Structure	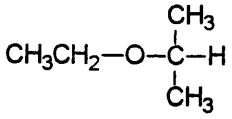	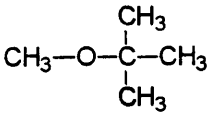
Boiling point °C	57.5[1] 54.0[2]	55.2
Density	0.720	0.741
Blending vapor pressure	7.90[3]	8.00
Octane number	NA	110

[1] : Data observed (Grisdanurak, 1992)
[2] : Bennett et al., 1928
[3] : Estimated data (see appendix A-3)
NA : No data available

EIPE was synthesized first under acidic conditions by Norris (Norris, 1932) by reacting isopropyl alcohol and ethanol in 75% sulfuric acid. The yields of diethyl ether (DEE) and EIPE were 34% and 61%, respectively. Francis et al. (1937) disclosed a commercial method for manufacture of EIPE involving a process by which propylene was utilized as a raw material. By mixing propylene, ethanol, and sulfuric acid, and heating for 4 hours at a temperature of 82.40°C under an initial pressure 570 psi, EIPE, DEE, and diisopropyl ether (DIPE) were produced in a ratio of 89/38/4 respectively. Unfortunately, such methods have a number of disadvantages. These can include: severe corrosion, acid-handling difficulties, high loss of acid, and the costly step of re-concentration of the diluted acid.

Bell (1989) disclosed a method for EIPE production over a β-zeolite catalyst. An equimolar feed of ethanol and propylene was processed through a fixed-bed tubular reactor over β-zeolite (65% extruded with 35% alumina and diluted with sand to provide 0.25 gm./cc active catalyst concentration) under conditions of 150-152°C and 6630 kPa (950 psi). These results are shown in Table 3. To compare the selectivity of zeolite and acid resin, both reactants were charged into a batch reactor over Amberlyst-15 (A-15) in various resin concentrations. These results are shown in Table 4. The molar selectivity for EIPE compared to DEE over β-zeolite is clearly higher than that over A-15. On the other hand, A-15 provides a higher ethanol conversion than when using β-zeolite.

Economic comparisons of EIPE and other oxygenates such as MTBE and ETBE have shown that EIPE production based upon the captured value of propylene and its propylene alkylation value and ethanol at $1.20 per gallon makes the EIPE production cost about 1.5-2.8 cents per gallon more than MTBE. Meanwhile on the same economic basis ETBE costs approximately 6.1-7.6 cents per gallon more than MTBE. These costs also do not also reflect higher methanol market prices (Graboski, 1994).

Table 3. EIPE Reaction Products at 150°C, 950 psi, over β-zeolite (Bell, 1989).

Hr. on stream	2	4	5	23
WHSV(based on olefin and active catalyst)	3.74	1.86	0.93	0.31
conversion %Propylene	13.9	26.1	26.8	56.7
Molar Selectivity				
EIPE / DEE	4.45	4.87	5.01	4.26
Reaction Effluent (wt%)				
Water	0.2	0.2	0.3	0.4
Propylene	37.2	31.8	33.9	18.8
Ethanol	47.9	41.1	36.0	21.9
IPA	0.3	0.6	0.7	1.8
DEE	2.3	3.8	4.2	9.2
EIPE	12.1	22.2	24.8	46.6
DIPE	0.1	0.2	0.1	1.3

Table 4. EIPE Reaction Products at 150°C, 950 psi, over A-15 (Bell, 1989).

Catalyst conc.(gm/cc)	0.06	0.06	0.06	0.25	0.25	0.25
Hr. on stream	2	4	8	3	5	6
WHSV (based on active catalyst)	23.3	11.29	5.41	5.62	2.88	1.43
Conversion %Propylene	17.9	21.2	46.0	60.6	73.5	78.3
Molar selectivity						
EIPE / DEE	2.51	2.76	3.41	3.18	3.19	3.29
Product stream (wt%)						
Water	0.3	0.1	0.3	0.3	0.3	0.4
Propylene	29.3	44.2	24.5	16.9	11.7	9.6
Ethanol	53.8	25.4	25.3	19.5	10.1	7.9
IPA	1.1	1.8	3.4	4.8	5.1	5.4
DEE	3.8	6.5	8.9	11.9	14.6	14.8
EIPE	11.5	21.4	36.2	45.1	55.3	57.9
DIPE	0.1	0.5	1.4	2.9	4.0	NA

Since there are few studies for EIPE production, this study will be based on the technology for available oxygenates including MTBE, ETBE, and oxygenates from propylene.

2.5 MTBE and ETBE Review.

MTBE is formed by the reaction of methanol with isobutylene. Conventional operating conditions for MTBE production over ion exchange resins such as Amberlyst-15 are 40°C and 80-300 psi in order to keep the reaction mixture in the liquid phase; a liquid hourly space velocity (LHSV) of 2 to 50 hr^{-1}, and a molar ratio of methanol to isobutylene equal to 1.0 are also reported (Kirk-Othmer, 1982). Studies of MTBE synthesis in this decade were usually concerned with improvement of catalyst activity. The following reaction summarizes research on MTBE and ETBE.

Chu and Khul (1986) found that MTBE synthesis in the presence of ZSM-5 or ZSM-11 at conditions of 77-105°C and 150-300 psi gave an MTBE yield of about 90-94%. The olefin oligomerization reaction was reduced at the lower temperature (Chu and Khul, 1987). To compare the MTBE production on a conventional catalyst (A-15) and ZSM-5, Pien and Hatcher (1990) found that at a moderate temperature (75°C) the A-15 was approximately 11 times more active than HZSM-5, however, at 100°C the A-15 and HZSM-5 had about the same activity. With HZSM-5, a small amount of DME (dimethyl ether) was produced via methanol dehydration. Chang et al. (1992) reported on an experiment in which the isomorphous substitution of Ti into the zeolite framework was made, and this material was used (Ti-silicate) as a catalyst in MTBE production with temperatures of 70-110°C at atmospheric pressure. An extremely high selectivity to MTBE (essentially 100%) was obtained. No by-products such as DME, diisobutene, or TBA were detected in the reactor effluent stream. The review paper for nafion catalyst, a perfluorinated ion exchange resin, by Waller and Scoyoc (1987) reported that with a

temperature of 80°C and a pressure at 142 psi, a high selectivity to MTBE (100%) was obtained at a methanol conversion level of 82%.

Evans and Edlund (1936) reported on the preparation of over 20 tertiary alkyl ethers using sulfuric acid as a catalyst. They found that by reacting an olefin with a variety of alcohols, a primary alcohol was more reactive than the secondary and tertiary alcohol:

ethanol > isopropanol > tert-butanol

The etherification rates using primary alcohols were shown to be independent of alcohol concentration but dependent on the nature of the alcohols, with less basic alcohols favoring the reaction (Ancillotti, 1977). The reactivity of primary alcohols with isobutylene on A-15 follows the order:

n-butanol > n-propanol > ethanol > methanol

ETBE is a good octane enhancer and is more reactive than methanol. ETBE can enhance the octane number of gasoline at the same level as MTBE, as shown in Table 1. With a higher boiling point, lower RVP, and the lack of an azeotrope with hydrocarbon upon blending, ETBE results in a lowered tendency for engine vapor lock and lower emissions due to evaporative losses. Iborra (1988) summarized several studies of ETBE synthesis in the liquid phase under moderate conditions and with many different kinds of catalysts.

Several acid catalysts were studied to screen their performance in the formation of ETBE (Tau and Davis, 1989). Supported FCSA (Fluorocarbonsulfonic acid), a thermally stable catalyst, was found to be less sensitive to the ethanol-to-isobutylene ratio and to have a better selectivity compared to A-15 for a liquid phase reaction operated at 200-300 psi, 80°C. At 200 psi, it was also found that a ZSM-5 catalyst at 125°C gave conversions which were relatively low compared to A-15 and A-35 for

temperatures up to 60°C, and when compared to a fluorocarbonsulfonic acid catalyst at 80°C.

Rate expressions for MTBE and ETBE synthesis are summarized in Table 5.

Table 5. The Summary of Kinetic Study on MTBE and ETBE.

Production of	Rate Expression	Observation	Reference
MTBE	$k\left(\frac{a_{IB}}{a_{MeOH}} - \frac{a_{MTBE}}{K_a a_{MeOH}^2}\right)$	liquid	Hoffman, 1990
	$k_1 C_{IB} - k_2 C_{MTBE}$	liquid, catalytic distillation	Xu, 1995
ETBE	$k\frac{P_{IB}P_{Et}}{\left(1+K_{IB}P_{IB}+K_{Et}P_{Et}\right)^4}$	gas	Iborra et al., 1992
	$\frac{k\left(a_{IB}\,a_{Et} - a_{ETBE}/K_a\right)}{\left(a_{Et}\right)^3}$	liquid	Tejero et al., 1994

2.6 Oxygenates from Propylene.

IPA, MIPE, and DIPE: In case oxygenates such as MTBE are in short supply, propylene utilization for ether synthesis can be an attractive option for oxygenate production. IPA (isopropanol) is being considered for use as one of the oxygenates; this material can be prepared by the reaction of propylene and water. IPA manufacture has been successfully demonstrated with cation exchange resins (Neier and Woellner, 1972).

According to Hiestand (1961), at low pressure and 130-140°C, no IPA was produced. For satisfactory reaction rates, a mixed phase process with water as liquid and propylene as vapor was suggested.

Sonnemans (1993) conducted the gas phase etherification of propylene with methanol over HZSM-5. The reactions were performed in a fixed-bed reactor using a ratio of feed components of 1.4:0.9:3 for C_3H_6:MeOH:He, respectively (GHSV = 2650). At a temperature of 155°C and a pressure of 2 bars, the reaction gave 2% yield of MIPE (methyl isopropyl ether). Bell (1987) reported on the catalytic reaction of a linear monoolefin (propylene) with a lower alcohol such as methanol to form MIPE. The catalysts used in the reaction were A-15, ZSM-5 and a β-zeolite extrudate. The methanol and 20-100 wt% propylene were fed at a ratio of 0.1-10 on a molar basis. The β-zeolite catalyst was found to be superior for this application, and when operated at 160°C, demonstrated a 60% conversion of propylene to MIPE.

DIPE (diisopropyl ether) is one of the alternative oxygenates which has been found as a by-product of IPA manufacture. German Patent (DEAS) No. 1 210 768 disclosed a process for the continuous production of IPA and DIPE by the catalytic hydration of propylene. In this process, a strongly acidic cation exchange resin consists of a styrene polymerazate crosslinked with about 5 to 20 wt% divinylbenzene and contains about one sulfonic acid group per aromatic ring as the catalyst. In this process, pressure ranges from 17 to 105 atm. At temperatures of 135-157°C, 20 to 90 mole percent of the propylene feed was converted per pass. A conversion of about 35% gave the best selectivity to IPA at 135°C (69 mole percent). The selectivity for the DIPE by-product was found to be about 28%. Huang et al. (1989) converted propylene/propane from a refinery stream (70 mole% propylene, 30 mole% propane) to DIPE. The conditions of propylene conversion employing an extrudate of β-zeolite (85 wt%) bound with silica (15 wt%) were: 160°C, 1800 psi, 0.5 water to propylene mole ratio and 0.5

WHSV based on propylene. The products were DIPE, IPA, oligomor (4-methyl-2-pentene), and water at 63.1, 34.2, 2.1 and 0.6 wt% respectively. With the same process, Huang et al.(1989) prepared DIPE from propylene and isopropanol in the presence of the same catalyst at 166°C, 1000 psi total pressure. The final ether product contained 92.1% DIPE after distillation and extraction.

2.7 Reaction Mechanisms for EIPE Formation.

Ethyl isopropyl ether can be synthesized from propylene and ethanol via a mechanism that involves an acid catalyzed nucleophilic addition reaction. Propylene is first protonated to yield a secondary carbocation. Ethanol then acts as nucleophile and the lone pair of electrons on oxygen are donated to the carbon atom bearing the positive charge to complete the reaction and form ethyl isopropyl ether (Figure 1).

In order to apply this reaction under industrial conditions, use of a solid heterogeneous catalyst as the proton source is normally preferred. Figure 2 illustrates the proposed mechanism for EIPE synthesis over styrene sulfonic acid cation exchange resin.

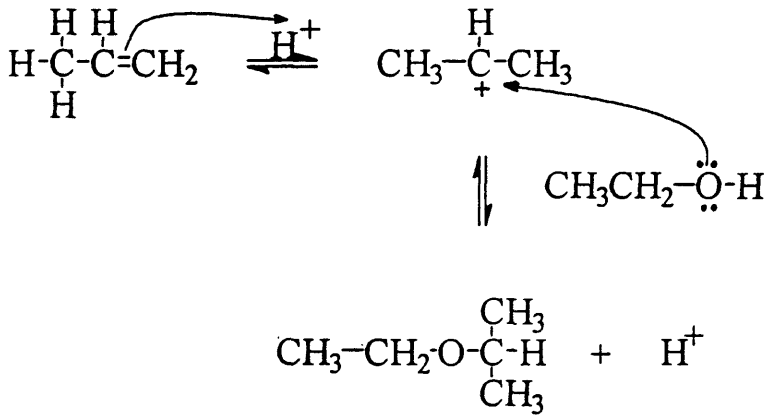

Figure 1. EIPE Synthesis in the Presence of Acid.

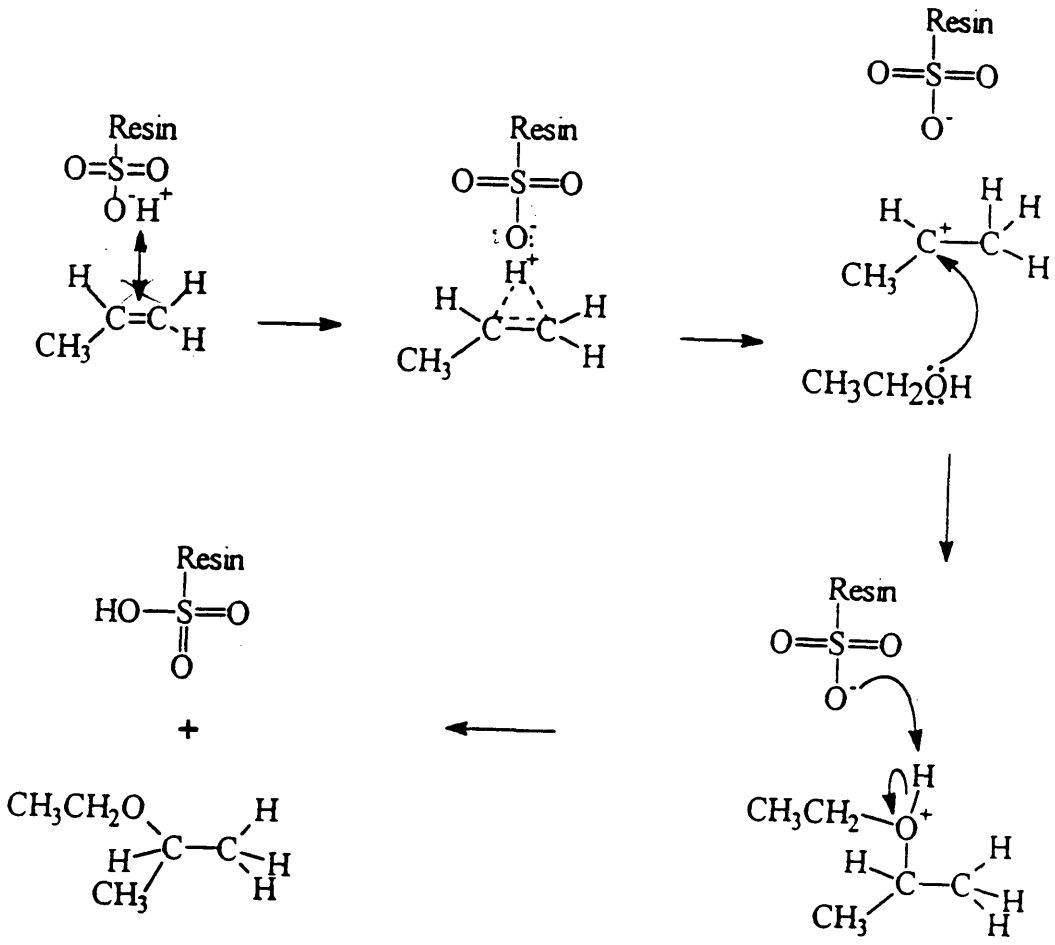

Figure 2. EIPE Synthesis over Cation Exchange Resins.

Cation exchange resins are high-polymeric and tightly cross-linked structures containing fixed polar anionic groups whose negative charges are balanced by cations. Most cation exchange resins are copolymers containing either a phenolic (-OH), carboxylic (-COOH), sulfonic ($-SO_3H$), or phosphonic ($-PO_3H_2$) acid group as integral portions of the resins. Most commercial cationic forms are the sulfonic acids, which are strongly acidic, and the carboxylic acids which are weakly acidic. Therefore, the sulfonic form is the most useful for acid catalyzed reactions in industry since it has high proton donating capabilities (Kunin, 1958). Neier and Woellner (1972) reviewed the advantages of using cation exchange resins as a catalyst instead of using mineral acids as a catalyst. These include the reduction in mineral acid corrosion during acid reconcentration, reduction in energy cost by elimination of reconcentration of acid, and the reduction in air pollution by SO_x and organic sulfur compounds.

A strongly acidic cation exchange resin incorporating sulfonic acid groups is synthesized by copolymerization of styrene with divinylbenzene in suspension, followed by curing. This copolymer is called a host matrix, which is insoluble in an exchange medium. Afterwards, the styrene divinylbenzene copolymer is sulfonated with sulfuric acid. The reactions are as shown in Figure 3.

Dowex HCR-w2 and Amberlyst-15 are commercial names for cation exchange resins. Their properties are presented in Table 6. There are two main different properties for those types of materials, the degree of cross-linking and maximum allowable temperature. The amount of cross-linking determines the adsorptive and swelling capacities of the resins. Highly cross-linked resins have low adsorptive and swelling capacities during the reaction. According to Heiestand (1961), cation exchange resins containing 8 percent cross-linking have sufficient properties to control swelling. One other important property of the catalyst is its thermal stability. Generally, the strong

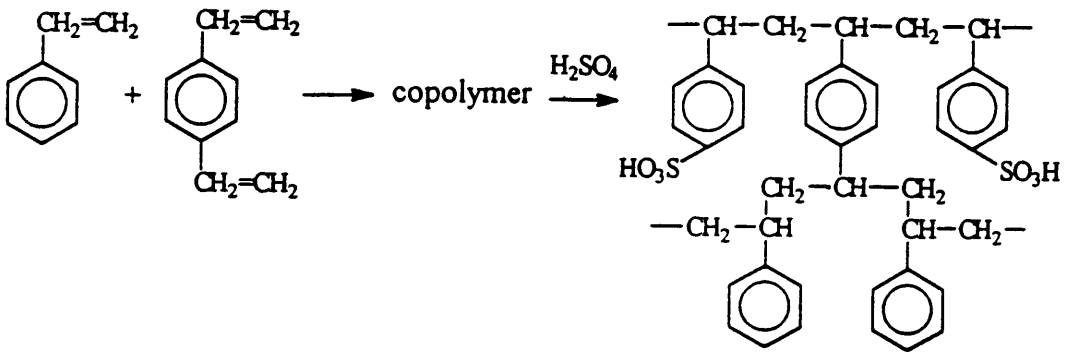

Figure 3. Structure of Cation Exchange Resins (Kunin, 1958).

acid cation exchange resins in all forms are completely stable in water up to 120°C, and their H^+-forms become unstable at 150°C. In this regard, Dowex HCR-w2 has an advantage because the maximum allowable temperature is higher than that of Amberlyst-15.

The third kind of resin is supported FCSA. This catalyst has been under development for several years by the Dow Chemical company and E.I. Dupont de Nemours company. The host matrix of this resin differs from Dowex HCR-w2 and Amberlyst-15. It is a copolymer which contains tetrafluoroethylene, fluorinated vinyl ethers, and fluorosulfonyl groups. The polymer is then converted to the sulfonic acid or sulfonate form by hydrolysis as shown its structure in Figure 4. Polymers of this type possess several properties that are desirable in an acid catalyst, including chemical resistance and thermal stability. Oxidizers, reducing agents, and strong acids have little

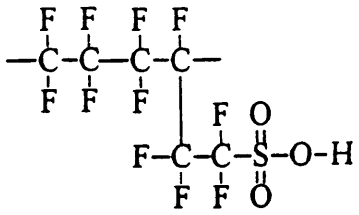

Figure 4. FCSA Structure (Ward, 1988).

effect on the polymer. Operation at temperatures up to 200°C can be maintained without decomposition of the polymer. To increase its mechanical strength, the fluorocarbon is supported on an alumina carrier as a thin coating. A supported FCSA has been found to be effective in catalyzing many different reactions such as the hydration of olefins and the dehydration of alcohols (Weaver al et., 1992). Moreover, in ETBE production, a better yield and selectivity was obtained when using a supported FCSA than when using A-15 and ZSM-5 as catalysts (Tau, 1989).

Since EIPE formation needs a catalyst which has a good proton donating ability, the acidity of the catalyst needs to be considered. A property used to identify the acid strength of concentrated acid solution is Hammett's function (H_o). The function H_o, expresses the tendency of a solution to transfer a proton to a neutral base as the quantity pK_a. This function H_o is defined by the following equation (Rys and Steineger, 1979).

$$H_o = pK_{BH^+} - \log \frac{[BH^+]}{[B]} \quad \text{---------(1)}$$

where pK_{BH+} : the dissociation constant of the conjugate acid (BH^+)

BH^+/B : the ionization ratio

Table 6. Catalyst Properties (Dow Chemical manual, 1994; Kunin, 1962; Weaver,1992; Maholland, 1987).

Catalyst	max. allowable T (°C)	% crosslinkage	acidity function	acidic capacity, meq/g	surface area m^2/g
Dowex HCR-w2	150	8	-2	3.6-4.5	< 1
Amberlyst-15	120	20	-2	4.5	40-45
supported FCSA	200	NA	-12	0.13-0.15	< 1
P/Al 0.8	NA	NA	NA	NA	122-163

The acidity function is similar to pH in that it becomes more negative the greater the acidity of the solution. The Hammett acidity functions for several superacids including A-15 are listed in Table 6. The acidity function of A-15 in water is -2.2. Comparing the H_o value of A-15 with the acidity function of aqueous sulfuric acid, it follows that the

acidity function of A-15 in its H^+ form corresponds to an acidity of 35 to 38% wt sulfuric acid.

The Hammett acidity function of FCSA polymer has been estimated to be -10 to -12 which makes it comparable to or stronger than 100% sulfuric acid (Ward, 1988). Otoma and Arai (1976) reported that the acidity function of HY zeolite is about -4 to -8, which is still less acidic than FCSA polymer.

Chapter 3
EXPERIMENTAL PROCEDURES

3.1 Chemicals and Catalysts.

3.1-1 Chemicals.

Lump sodium, nitric acid, sodium hydroxide, sodium chloride, and KHP were obtained from CSM Chemical stores. Ethyl bromide and Benzoic acid with a minimum purity of 99.5% were obtained from the Aldrich Chemical Co. Ethanol (VWR Scientific), with a minimum purity 95% and dehydrated ethanol absolute-200 proof (McCormick-Distillating Co., Inc.) were used. Propylene, helium, nitrogen, and 4-methyl-2-pentene were supplied by General Air Service & Supply with a minimum purity of 99.99%. DIPE (Banco Standardized), DEE (Mallinckrodt Specialty Chemicals Co.), and HPLC-grade IPA (VWR Scientific), were used for standard samples. EIPE was synthesized at Colorado School of Mines by this author as described below. All chemicals were used as received without further treatment.

Known aliquots of these liquid chemicals were mixed to produce a liquid calibration standard for the gas chromatograph.

Synthesis of EIPE: EIPE was synthesized using the "Williamson" method. In this procedure, metallic sodium and isopropyl alcohol were charged into a flask using a molar ratio of isopropyl alcohol to sodium of 5-8 : 1. To facilitate the reaction, sodium metal was cut into small pieces. The process produced sodium isopropanolate at 50°C under atmospheric pressure. In the second step, alcoholate and unreacted alcohol (used as a solvent) were then boiled in a distilling column under 100% reflux ratio with a stoichiometric quantity of bromoethane for approximately 24 hours. The resulting ether

is purified in several steps. First, liquid is stripped from the product mixture in a simple distillation leaving a sodium bromide salt residue behind. This mixture then was distillated in a B&R spinning band micro distillation column to remove light ends including ethylbromide and some portion of isopropanol. The mid-cut containing ether and isopropanol was then further treated. To remove isopropyl alcohol, esterification with benzoic acid was used. Using these procedures, a yield of greater than 95% EIPE was realized. This product material was checked for purity by mass-spectrometry and it was used as a calibration standard solution to calibrate the gas chromatograph.

3.1-2 Catalysts.

Dowex HCR-w2 ion exchange resins manufactured by the Dow Chemical Co. were obtained from Sigma Chemical Co. Amberlyst-15 ion exchange resins manufactured by Rohm and Haas were obtained from Polysciences, Inc. Supported FCSA was supplied by Dow Chemical Co. P/Al 0.8 was supplied by Prof. Scott Cowley of the Department of Chemistry, Colorado School of Mines.

All catalysts, excluding Amberlyst-15, were dried overnight at 100°C before use. Amberlyst-15 was first washed with an aqueous solution of 6 vol% nitric acid, and then washed with ethanol, and finally dried overnight in an oven at 100°C before use (Datta, 1995).

3.2. Catalytic Reactor Systems.

The experimental investigation of EIPE production was divided into two separate phases. The first phase was performed in a stirred tank batch reactor in order to examine the feasibility of the reaction. The second phase was conducted in a trickle downflow continuous reactor.

3.2-1 A Batch Reactor.

The batch experiments were performed in a 300 cm^3 Autoclave Engineers stainless steel stirred reactor. Figure 5 shows a schematic diagram for the batch system. The temperature was measured with a thermocouple submerged in the liquid phase.

An exact amount of treated catalyst was charged to the autoclave. In this batch study, only Dowex HCR-w2 was used. A defined amount of ethanol was charged to the reactor. The reactor was then closed and pressurized with helium to about 1000 psi to check for leaks and then purged slowly several times. The reactor was then weighed on a 10,000 gm. balance with 0.1 gm. resolution. In order to add propylene into the reactor, the autoclave was chilled to 5°C. This step was carried out to provide a different vapor pressure between the gas supply cylinder and the reactor so that the propylene will be in liquid phase when it was charged to the autoclave, thus facilitating addition of the desired amount. The autoclave was weighed, and then set into a heater and brought as rapidly as possible up to operating temperature, typically between 80-130°C. At this time the motor-drive stirrer was turned on. Temperature and pressure were recorded periodically. The reactor was operated until the reaction reached equilibrium or for some desired time. In the first case, the reaction was assumed to be at equilibrium when the gauge pressure did not change. After taking the autoclave out off the heater, it was chilled down to 5°C again and weighed. Unreacted propylene was vented slowly and the autoclave was weighed again before removing liquid products. At this step the autoclave temperature was still at about 5-10°C. For each experiment, the mass balance was important. Leakage was checked by comparing weights before and after the test.

Analytical: A 0.2 microliter sample of each product was analyzed on a Varian 3700 gas chromatograph equipped with a thermal conductivity detector. A 6 foot x 1/8 in ID, stainless steel column, packed with porapak Q 80%, was used. The

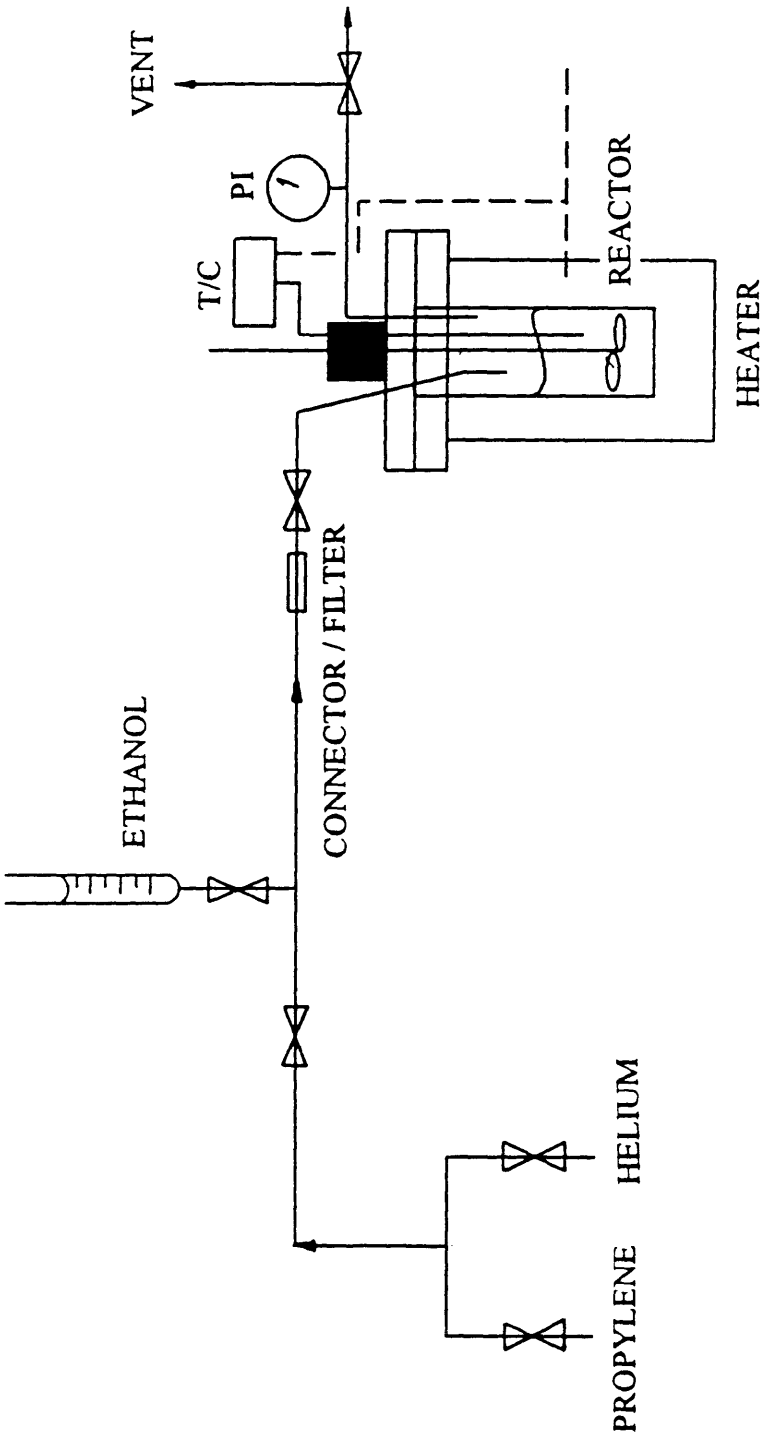

Figure 5. Schematic Diagram for a Batch System.

detector was connected to an HP 3390 integrator directly giving the areas of the different peaks. The GC was calibrated with a standard sample before every injection. The column was temperature programmed with a 1-min. initial hold at 100°C followed by a 25°C/min. ramp up to 185°C with an isothermal hold at the upper temperature for 15 min.

3.2-2 A Trickle-Bed Downflow Reactor.

Experimental measurements were also conducted in a continuous trickle-bed downflow reactor system. The liquid and gas flow rates are important in the design of this reactor. In the trickle-flow regime, the liquid flows down the column on the surface of packing (catalyst) while the gas phase travels in the remaining void space. The gas phase is continuous and the liquid phase dispersed. Increasing the gas flow rate leads to pulsed flow. If, for a given liquid flow rate, the gas flow rate is increased too much, spray flow will be obtained. For higher liquid throughputs, the liquid phase may be continuous and the gas phase dispersed: this is called bubble flow. The flow rate of gas and liquid lead to different hydrodynamic regimes as shown in Figure 6. According to hydrodynamics, operation in the trickle-flow region gives lower pressure drop and prevents flooding of the bed (Ng, 1987). The flow rates which give rise to trickle-flow behavior (see Figure 7) are a liquid superficial flow rate of less than 10^4 kg/m^2-hr and a gaseous flow rate (superficial) of less than 10^4 kg/m^2-hr. In our work, the reactor was designed to operate where the maximum liquid ethanol flow rate was 18.78 kg/m^2-hr. and the maximum gaseous propylene flow rate was 5.0×10^3 kg/m^2-hr. which insured that the hydrodynamics were in the trickle-flow regime.

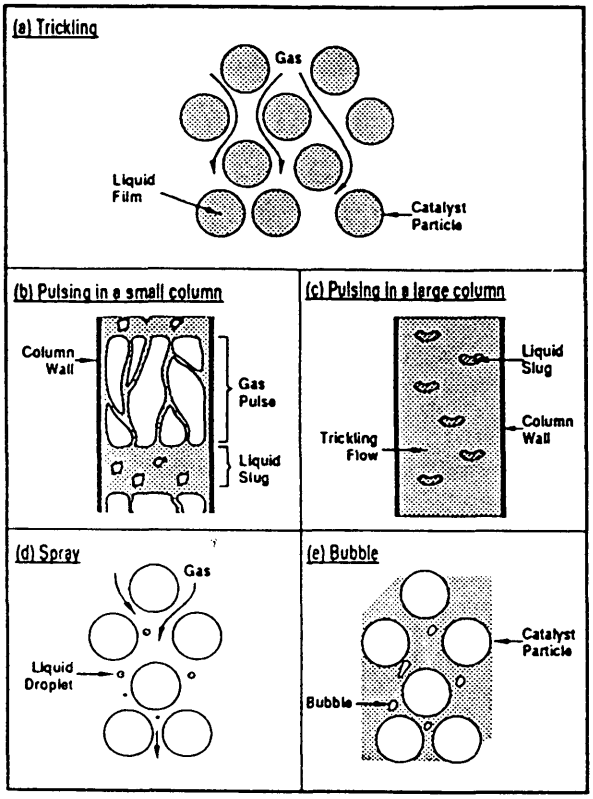

Figure 6. Flow Regimes in Trickle-Bed Reactor (Ng and Chu, 1987).

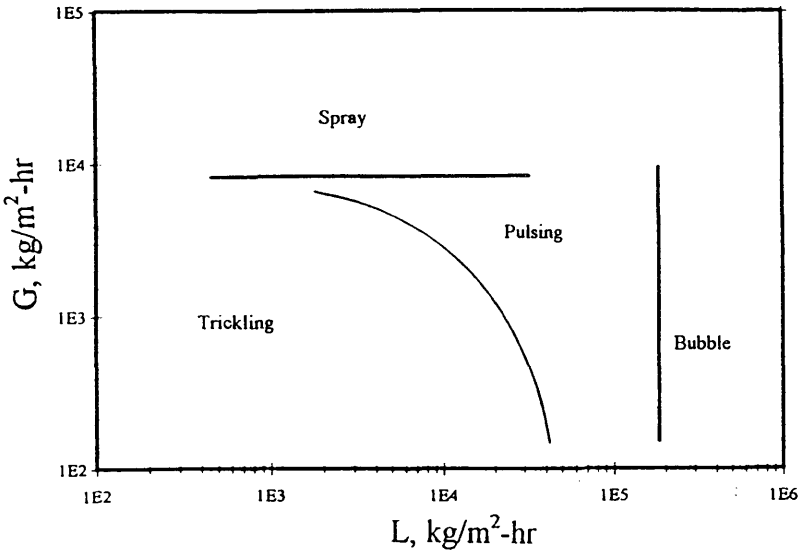

Figure 7. Flow Map for a Typical Trickle-Bed Reactor at Moderate Pressure (Ng and Chu, 1987).

A schematic diagram of the trickle-flow reactor system constructed by this author is shown in Figure 8. The reactor was constructed from a 1/2-in-OD, 16 gauge stainless steel tube 24 inches long. A Lindberg Model 55035 tube furnace was used to heat the reactor tube. In the reactor, the catalyst bed occupied the central 1-2 inch of the isothermal zone. The configuration of catalyst bed is shown in Figure 9. The catalyst with a specific particle size was diluted first with same particle size of inert quartz chips in 1:1 volume ratio. The catalyst was placed on a stainless steel 100 mesh screen which was supported by a layer of quartz chips. Below the steel screen, a plug of glass wool was used to prevent elutriation of catalyst. In order to maintain a good distribution and good mixing of ethanol and propylene in the catalyst bed, the feed inlet was packed with quartz chips followed with a plug of glass wool placed on the top of catalyst bed.

A liquid mini-pump (LDC/Milton Roy CO.) was used to regulate the ethanol or ethanol solution feed rate. Propylene from the siphon tank was fed to a precision HPLC pump (Isco Model LC-5000) for delivery into the system. Ethanol or ethanol solution was sprayed on the top of the distributing zone by a 0.02-in. diameter nozzle. Propylene was heated in the transfer line and then was fed to the side of the distributing zone. The mixture of ethanol and propylene was preheated along the tube before entering the catalyst zone. A type K thermocouple probe was placed at the exit of the reactor and at the center of the catalyst bed while other probes were attached to the outside of the reactor. Temperatures were scanned using an Omega 5 position selector switch and monitored on an Omega Model 400B series digital temperature indicator. The reactor could be considered to be isothermal due to the positioning of the catalyst bed in the isothermal zone as shown in Figure 10. Pressure inside the reactor was controlled by a back pressure regulator Model 5200 (Go, Inc.) which was placed at the end of the system. Pressure was indicated using an Autoclave Engineers pressure indicator Model AEC1-5000-01-PE10.

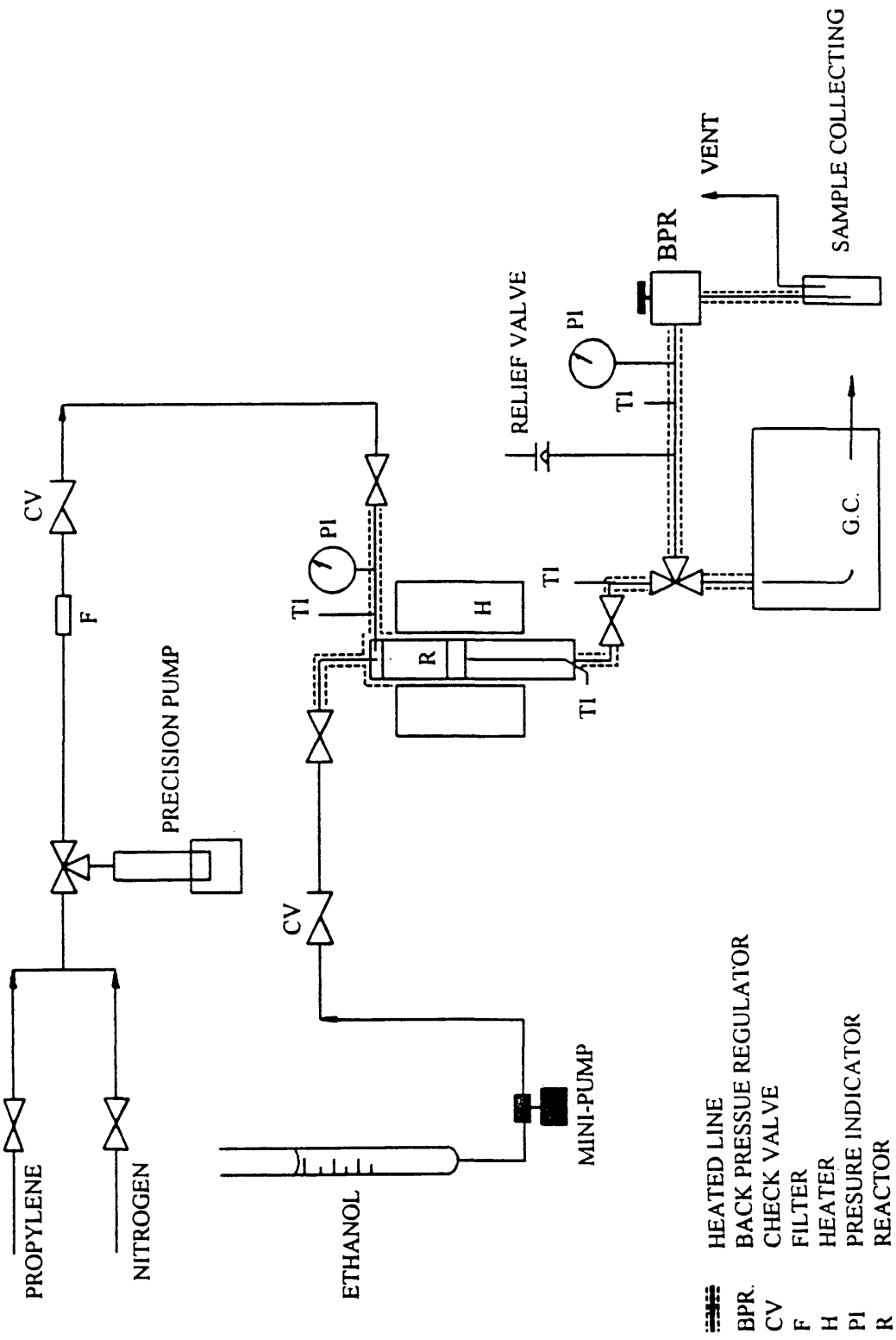

Figure 8. Schematic Diagram for a Flow System.

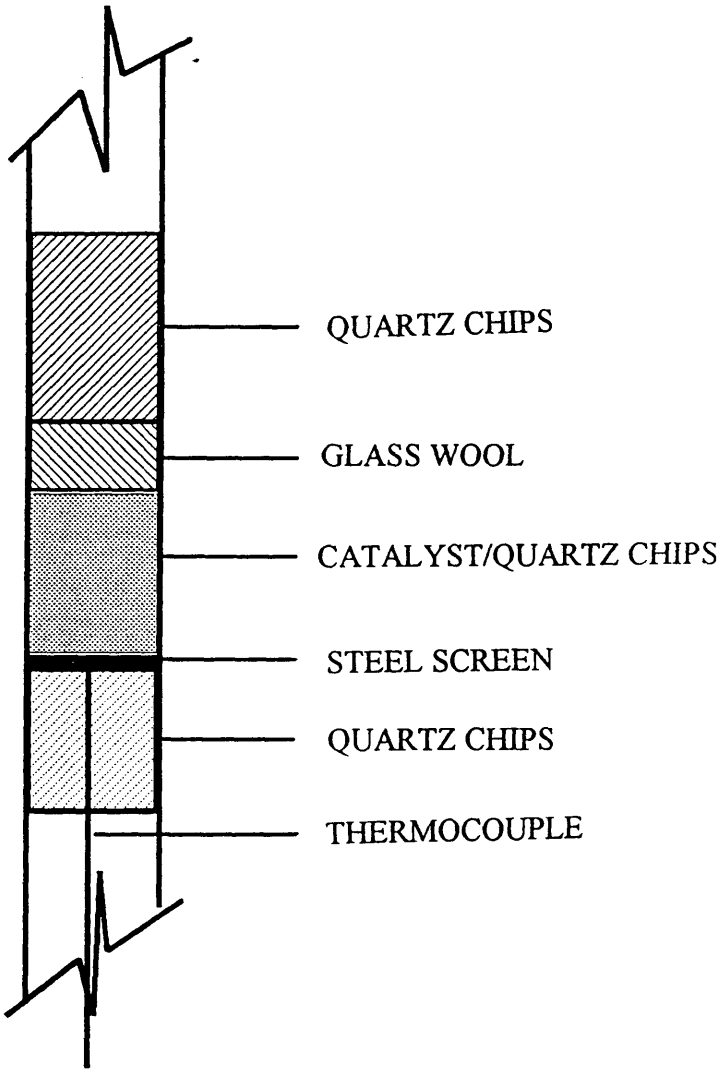

Figure 9. Catalyst Bed Configuration.

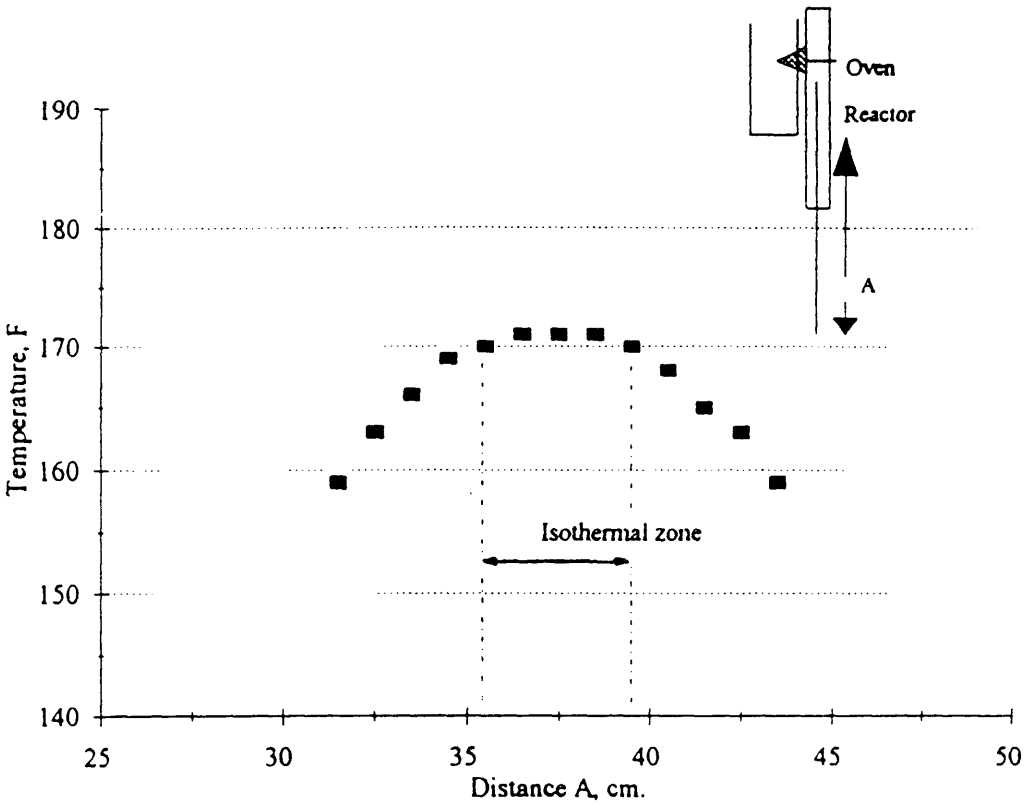

A: The distance measured from the end of oven to the 2 -ft T/C handle

Figure 10. Temperature Profile Inside the Reactor.

The mixture of products was passed directly for analysis to the gas chromatograph.

Analytical: The experimental data were collected for a series of steady state material balance periods (see Appendix C-2). To determine steady state for the reaction, samples of the products were taken for analysis every 20-30 minutes. During each steady state period, all operating variables were held constant. The variables studied are listed in Table 7. The mixture of products was heated in order to vaporize all the liquid products before passing to a 10 μl sample loop. A 6 foot x 1/8 in ID, stainless steel column, packed with porapak Q 80% installed in a Hewlett Packard 5890 gas chromatograph equipped with a thermal conductivity detector was used for analysis of reaction products. A temperature program consisting of a 1-min. initial hold at 60°C followed by a 13°C/min. ramp up to 175°C and a final temperature hold for 5 minutes was employed.

Table 7. Studied Variables and Ranges.

Process Variables	Range
Reactor Temperature, °C	40-240
Reactor Pressure, psi	14.7-700.0
Weight of Catalyst, g.	0.5-6.0
EtOH feed rate, ml/hr.	0.6-2.0
Propylene Feed Rate, ml/hr.	2.0-6.0
WHSV (based on ethanol flow), hr^{-1}	0.06-2.0

3.3 Catalyst Analysis.

3.3-1 BET Surface.

The BET surface area of catalyst was measured using an Omnisorp 100. This apparatus is a fixed volume system where the amount adsorbed can be calculated from the change in the system pressure. Nitrogen was used as an absorbent. The catalyst before the test was dried overnight at 110°C and then put in the sample vessel to degas overnight (120°C for Amberlyst-15 and 150°C for P/Al 0.8). Data were recorded by an on-line computer and the surface area was calculated using the linear part of the adsorption isotherm as follows:

$$S_{cat} = \left[\frac{N_o}{(I+s)V}\right]\alpha \qquad \text{---- (2)}$$

where N_o = Avorgadro's number, 6.02×10^{23}

α the projected area of a molecule on the surface, 16.2 $\mathring{A}^2$

V volume per mole of gas at conditions of measuring, 22,400 $cm^3/gmol$

I intercept

s slope

then $S_{cat} = \dfrac{4.35}{I + s}$ m^2/g solid catalyst

3.3-2 Acid Capacity Determination (Dow Chemical manual, 1994).

A 0.5-1.0 g sample of the catalyst was washed free of reactants or other contaminates. The sample was dried very thoroughly in a vacuum oven at the maximum temperature that can be used (refer to Table 5) for at least 4 hours. This is a critical step since residual water or other materials will cause error in the calculations. The dried sample was weighed on an analytical balance and then transferred to the titration vessel. It was stirred with 10 ml of water containing about 1 g of NaCl and heated to 50-60°C

for 15-20 minutes. During this time, HCl was generated by ion exchange; therefore, care was taken to prevent loss of solution by spillage. The cooled solution was titrated with standardized 0.01 N NaOH (standardized by exact concentration of KHP) to a phenopthalein end point. Since diffusion is slower than ion exchange, the endpoint usually fades at first. The titration is considered complete when the endpoint persists for ten minutes. Best results are obtained when the catalyst particles are as small as possible. The acid capacity can be calculated as follows:

$$\text{Acid Capacity} = [NaOH]\frac{miliequivalents\ of\ NaOH\ added}{weight\ sample} \quad \text{----(3)}$$

Units for acid capacity are miliequivalent per gram.

3.3-2 Total Carbon Analysis.

Carbon was determined by combustion in oxygen by Huffman Laboratory of Golden, CO. An automatic CO_2 coulometer was used to detect and quantify the evolved CO_2. This technique and apparatus have been described in detail elsewhere (Huffman, 1977).

Chapter 4
RESULTS OF THERMODYNAMIC CALCULATIONS

The reaction of ethanol with propylene over an acid catalyst has not been widely discussed. In order to examine the feasibility of this reaction, the equilibrium constants for the main reaction and several possible side reactions were calculated. Side reactions as shown in Figure 11 considered were as follows:

a. propylene dimerization, with formation of 4-methyl-2-pentene
b. ethanol dehydration, with formation of DEE and water
c. propylene hydration, with formation of IPA
d. IPA dehydration, with formation of DIPE and water

Because the dimerization of propylene was observed to be very small during our initial testing, this reaction was considered to be negligible.

There are two important considerations for these calculations. The first is to determine the possibility of making EIPE after assuming that all reactions have taken place in the gas phase and at atmospheric pressure. The second consideration is to find the possibility of making EIPE in a mixed-phase system where ethanol is in the liquid phase and propylene is in the gas phase.

4.1 Gas Phase Reaction Calculation.

In order to examine the feasibility of each reaction, thermodynamic data (C_p, H_f, G_f) must be known. These data then permit calculation of the equilibrium constant at reaction conditions from $\Delta G^\circ_{reaction}$ and $\Delta H^\circ_{reaction}$. The objective of this part of the study was to determine the equilibrium constant (K_a) for the possible reactions which can take

a. EIPE Synthesis with Ion Exchange Resins as the Catalyst

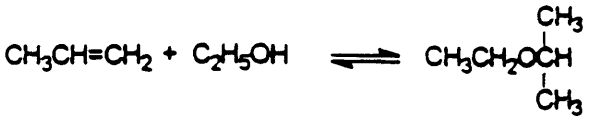

propylene ethanol(EtOH) ethyl isopropyl ether (EIPE)

Condition: Temperature 60°C and 1 atm gas phase $\Delta H_{reaction}$ = -68.15 kJ/mol

b. Propylene Dimerization

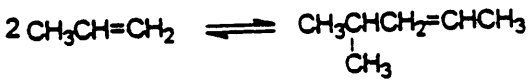

4-methyl-2-pentene

c. Ethanol Dehydration

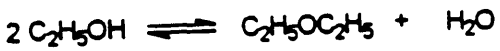

diethyl ether (DEE)

d. Propylene Hydration

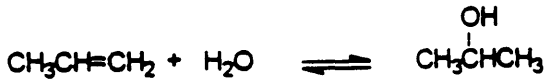

isopropyl alcohol (IPA)

e. IPA Dehydration

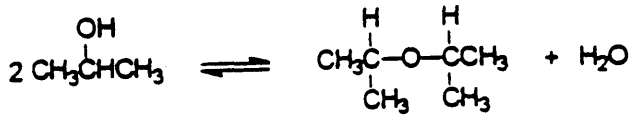

diisopropyl ether (DIPE)

Figure 11. Reactions Involving in the Addition of Ethanol to Propylene.

place. Since the thermodynamic data for most of the species (EtOH, H_2O, IPA, DEE, and DIPE) were available from standard sources, reactions involving these species were computed.

Unfortunately, there are no measured data on the thermodynamic properties (C_p, H_f, G_f) for EIPE. Necessary thermodynamic properties (heat of formation and Gibbs free energy of formation) for this compound were therefore estimated using Joback's group contribution methods as shown in Appendix A-2. The heat of formation was also estimated from SPARTAN 4.0 (semi-empirical, AM1) and the heat of formation using group contribution was found to differ from that computed by SPARTAN by about 0.23 kJ/mol (ΔH_f^o (group contribution) = -284.03 kJ/mol, ΔH_f^o (SPARTAN) = -283.08 kJ/mol). From the computed thermodynamic information, $\Delta H^o_{reaction}$ and $\Delta G^o_{reaction}$ were estimated, and the equilibrium constant calculated at room temperature according to the following expression:

$$K_{298} = \exp\left[\frac{-\Delta G^o_{298}}{298R}\right] \qquad \text{-----(4)}$$

Equilibrium constants at different temperatures were obtained through the Van't Hoff equation.

$$\frac{d \ln K}{d T} = \frac{\Delta H^\circ_{reaction}}{R T^2} \qquad \text{----- (5)}$$

where

$$\Delta H^\circ_{reaction} = \sum_{i=1}^{n} v_i \left[(\Delta H^\circ_{f,298})_i + \int_{298}^{T} (C^\circ_p)_i \, dT \right] \qquad \text{-----(6)}$$

Equation 5 was integrated where the C_p values were dependent on temperature. The calculations are shown in Appendix B.1-B.4 and the results for the EIPE, DEE,

DIPE, and IPA equilibrium constants are shown in Figure 12. The results were compared to those obtained from a commercial software package CHETAH (7.0) which was designed for gas phase thermodynamic calculations. Figure 12 presents the results of both calculations, with the lines showing the results from CHETAH and the symbols representing the results from our calculations. As shown, these two methods give almost exactly the same results. Equilibrium constants for all reactions decrease as temperature increases because all reactions are exothermic. In the temperature range of interest, 25-120°C, equilibrium constants of EIPE and IPA are the same order of magnitude and are relatively low compared to that for ethanol dehydration forming DEE.

In order to further examine the conversion of ethanol to EIPE and DEE, the equilibrium constants for each reaction were used to calculate ethanol fractional conversion by solving the two equilibrium expressions simultaneously in the temperature range from 25 to 120°C. The calculation procedure and one example calculation are shown in Appendix B-5. The results in Figure 13 show that under the assumption of a totally gas phase reaction, the equilibrium conversion of ethanol to EIPE is only in the range of 1 to 30% while ethanol converts to DEE between 60 and 80%. From the above thermodynamic data and calculations, it can be concluded that formation of DEE dominates the system and that EIPE formation is not favorable under gas phase conditions.

4.2 Mixed-Phase Calculations.

Mixed-phase calculations were done using the ASPEN Plus (release 9.0) simulation package. The calculations were done employing RGIBBS which can be used for simultaneous phase and chemical equilibrium calculations based on Gibbs free energy minimization. The RK-ASPEN equation of state was used due to the polarity of some of the species involved. The calculations were done at pressure of 147 psi and temperature

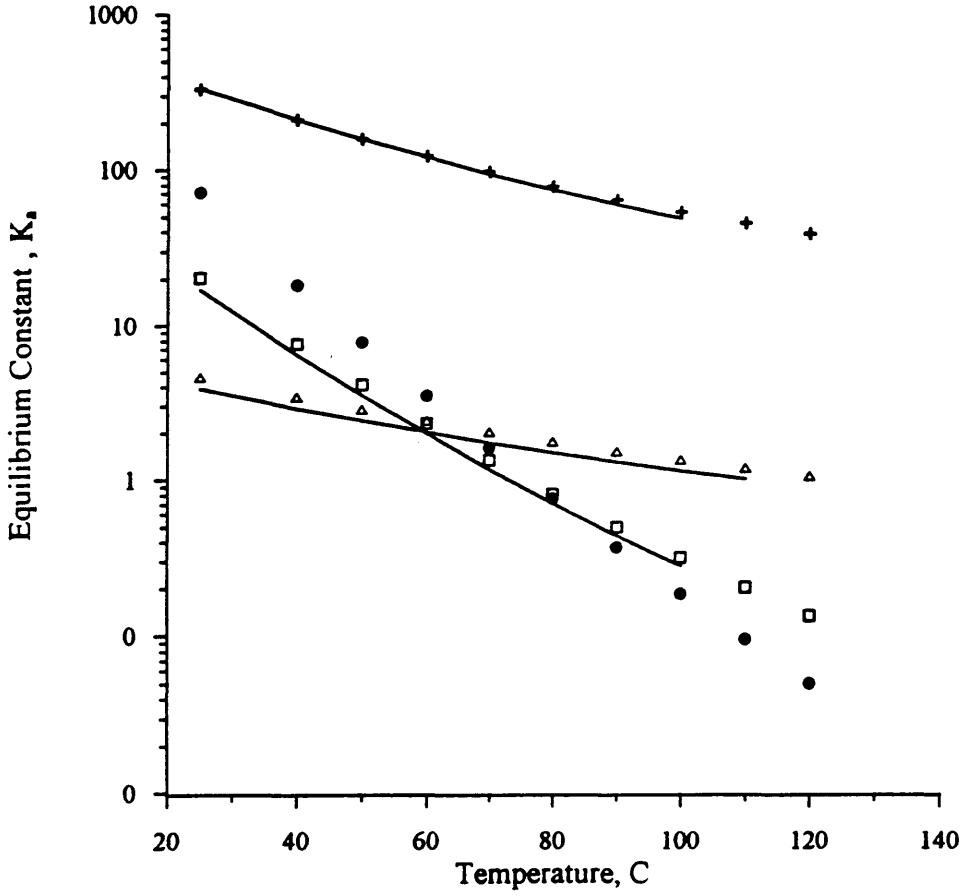

Figure 12. Equilibrium Constant for Gas Phase Reaction.

+ DEE • EIPE □ IPA Δ DIPE

—— Data from Cheetah.

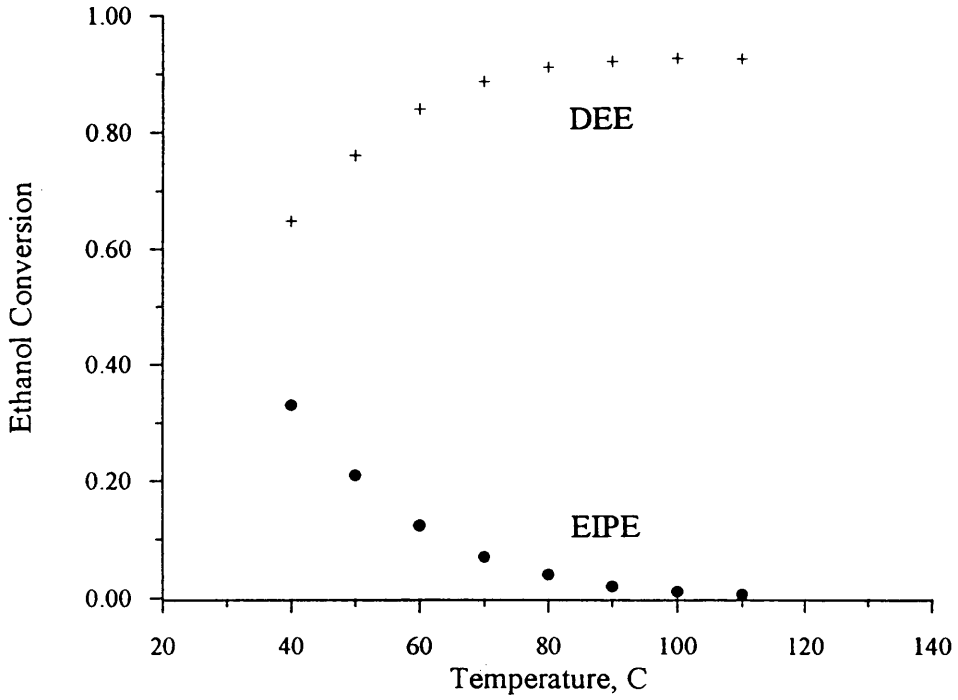

Figure 13. Equilibrum Conversion of Ethanol to EIPE and DEE for Gas Simultaneous Reactions.

range of 25-130°C thus insuring that the system was in the mixed phase. The equilibrium constant results from the ASPEN simulation for each reaction are shown in Figure 14. The results show that the equilibrium constant for EIPE formation is higher than those of other reactions at temperatures below 110°C. However, at temperature above 110°C the equilibrium constant for DEE formation starts to dominate. From Figure 14, we can conclude that only EIPE and DEE reactions will be important under the conditions where ethanol is in the liquid phase and propylene is in the gas phase (mixed-phase). Using K_x from two reactions and calculating the ethanol conversion as before, it was found that the formation reactions for EIPE and DEE were competitive when the temperature was increased as shown in Figure 15. The result at a temperature of 110°C demonstrates for example, that EIPE selectivity is about 70% while ethanol could be converted almost quantitatively to EIPE at room temperature. The comparisons of ethanol conversion between the gas phase and mixed-phase reaction systems show that the formation of EIPE in the mixed-phase is favored relative to that in the gas phase. These equilibrium calculations suggest that the conditions that can be used to optimize EIPE formation are in the mixed-phase where ethanol and EIPE are liquids and propylene is in the gas phase.

Hence, high pressures may favor formation of EIPE relative to DEE under thermodynamic control. To investigate this hypothesis, equilibrium constant calculations at a pressure of 1000 psi were done for EIPE and DEE formation using ASPEN and the results of equilibrium constants were then used to calculate ethanol conversions. As shown in Figure 16, increasing the pressure to a very high level will improve ethanol conversion to EIPE dramatically. Ethanol conversions to EIPE of greater than 90% can be achieved at temperature from 25 to 110°C at a pressure of 1000 psi. Comparing the results at the same temperature but a pressure of 147 psi to the results at 1000 psi, it can be readily seen that an increase in pressure directly increases ethanol conversion to EIPE.

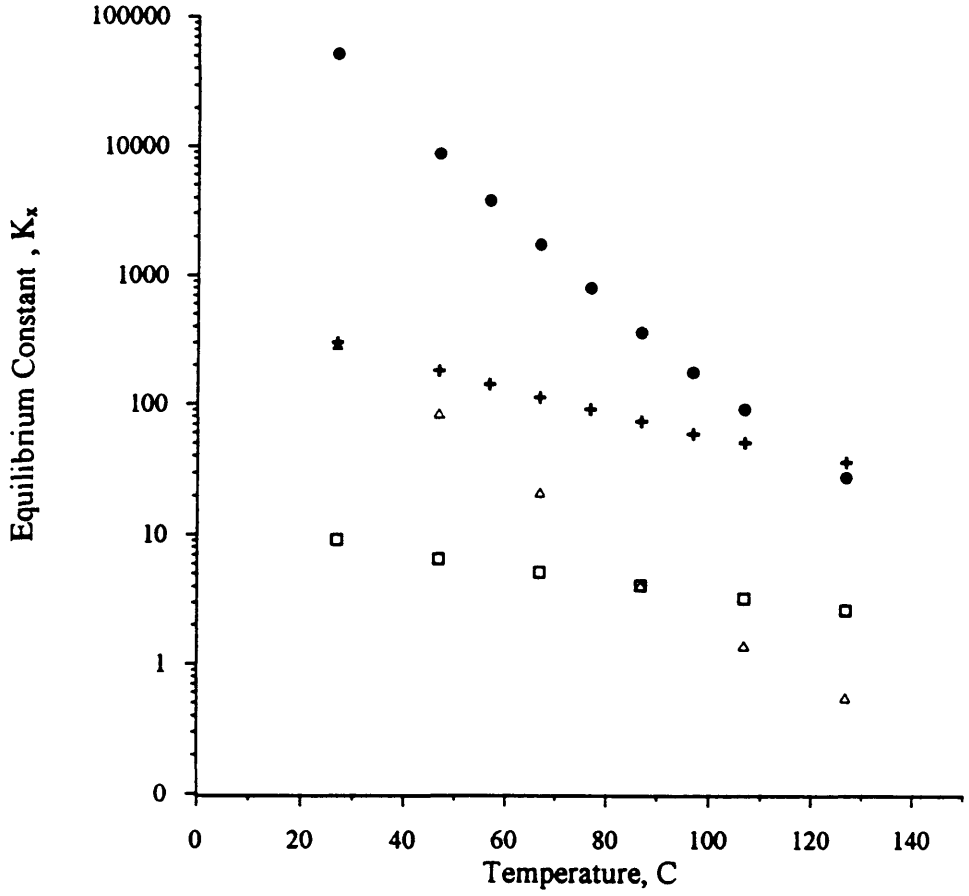

Figure 14. Equilibrium Constant at 147 psi Mixed Phase System.

• EIPE + DEE Δ IPA □ DIPE

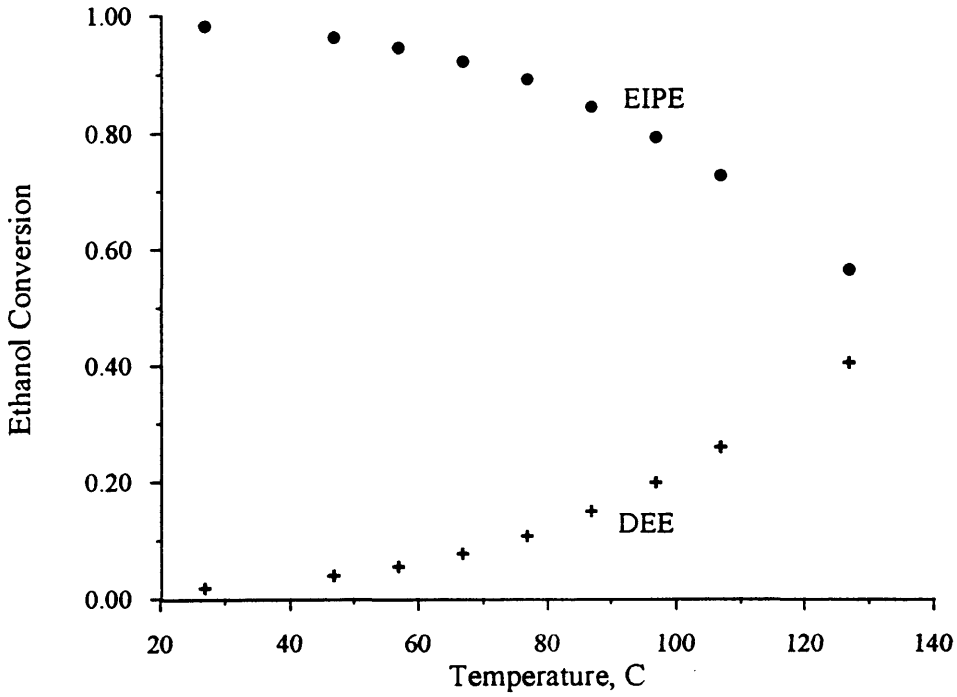

Figure 15. Equilibrium Conversion of Ethanol to EIPE and DEE at 147 psi Mixed Phase System.

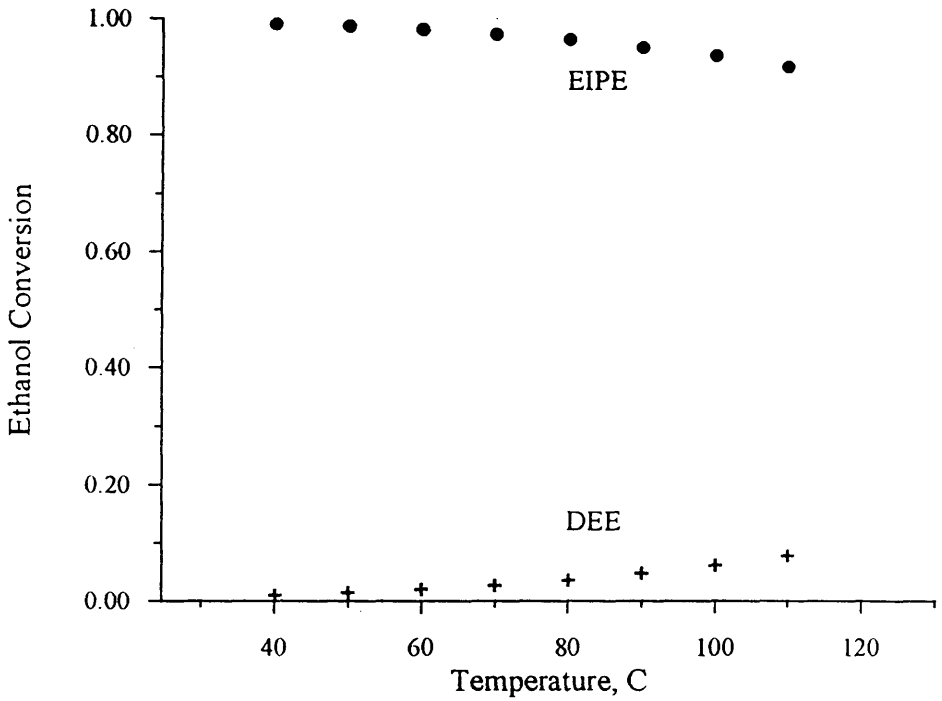

Figure 16. Equilibrium Conversion of Ethanol to EIPE and DEE at 1000 psi Mixed Phase.

This is due, in part, to the increasing solubility of propylene in liquid ethanol as shown in Figure 17. These equilibrium solubility data were generated from the propylene-ethanol phase diagrams computed by Aspen 9.0 (shown in Appendix B-6). However, when the pressure is above the critical locus, increasing the pressure further does not result in an increase in ethanol conversion to EIPE. For example at 100°C, the equilibrium (estimated from Aspen 9.0) conversion to EIPE is 92% at 700 psi, while only a 93% conversion is estimated at 1000 psi. This result of conversion being invariant with pressure is expected due to the phase equilibria prevailing in the reactor at higher pressures. Since at these conditions, propylene and ethanol exist as a dense (liquid-like) single phase mixture, the composition of the fluid in contact with the catalyst reflects most directly the composition of the feed. Thus the reaction rate and conversion depend only on the composition of the feed and not pressure. This is not the case at lower pressures when 2 discrete phases exist and pressure effects on propylene solubility and diffusion rate can be expected to directly affect the rate of reaction. Experimental runs examining the effect of pressure on the rate are discussed in Section 5.1-5.

Figure 18 shows the results of calculations for the vapor pressure of EIPE (estimated by group contribution methods, see Appendix A-4), ethanol and propylene. These data can be used to identify the conditions where ethanol and EIPE are in the liquid phase and propylene is in the gas phase. Since the critical temperature of propylene is 91°C, propylene will behave as a fluid no matter what the pressure is for reaction temperatures in excess of this temperature. In addition, it is necessary to keep reactor pressure high enough to prevent the vaporization of ethanol. Therefore, the reaction condition ranges of interest used in this research (100-140°C and 300-1000 psi) will occupy the mixed-phase region as shown by the shaded area in Figure 18.

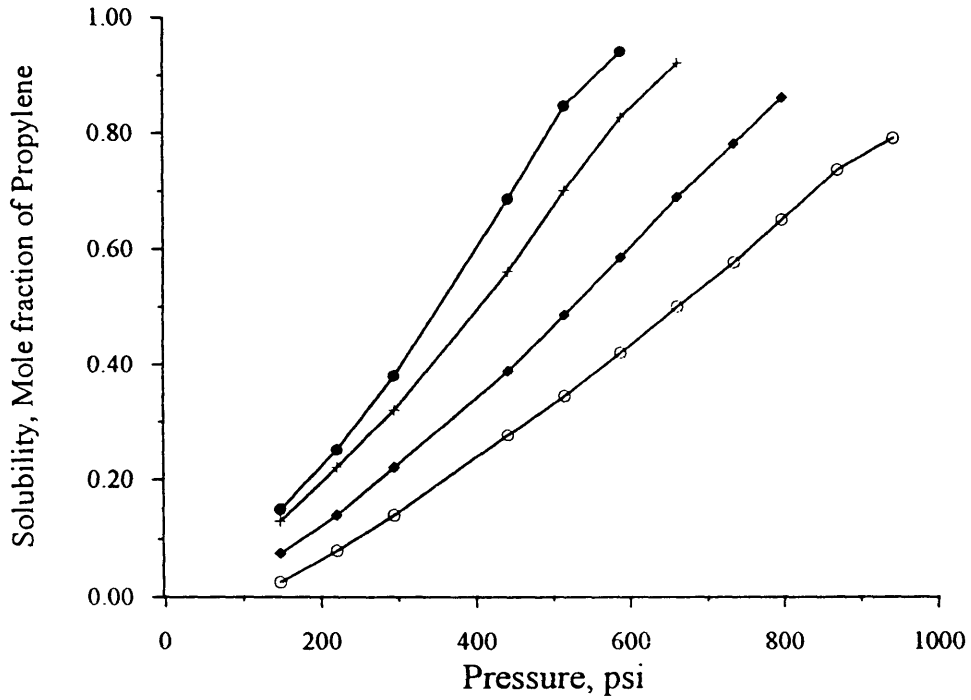

Figure 17. Solubility of Propylene in Ethanol.

• 90°C + 100°C
◊ 120°C ° 140°C

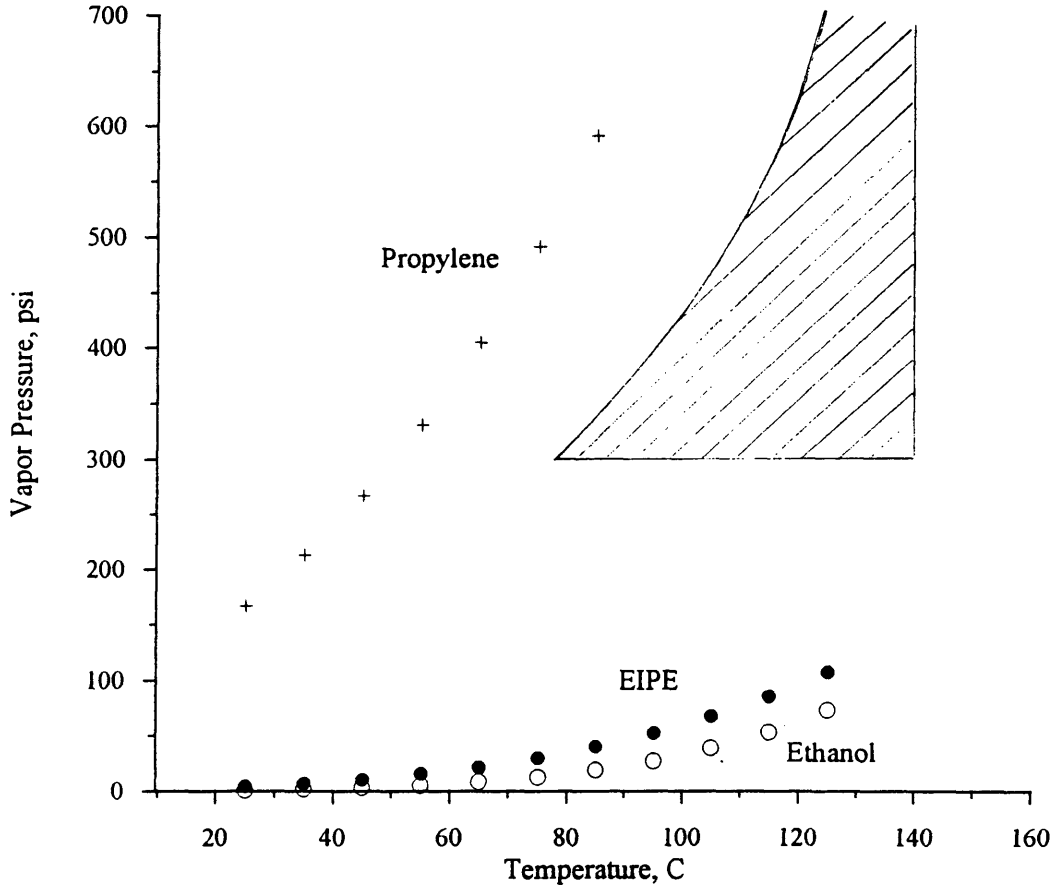

Figure 18. Vapor Pressure of Propylene, EIPE and Ethanol.

Chapter 5
RESULTS AND DISCUSSIONS

The reaction between ethanol and propylene can produce many kinds of products. By using strongly acidic cation exchange resins, etherification will be the governing reaction. By-products formed in the conversion are other ethers such as DEE, DIPE and traces of water and alcohol, principally IPA. Synthesis of EIPE from ethanol and propylene was investigated in two systems; a 300 cm^3 batch reactor and a continuous packed bed micro-reactor.

Experimental data obtained from the gas chromatograph were converted using the response factors (as described in Appendix C.1) and are reported in terms of conversion and selectivity. Conversion and selectivity for the reaction are defined as follows:

$$X(\text{Conversion}) = \frac{\text{moles of ethanol reacted}}{\text{moles of ethanol fed}} \quad \text{---(7)}$$

$$S_i\ (\text{Selectivity}) = \frac{\text{moles of desired product (i) formed}}{\text{moles of ethanol reacted}} \quad \text{---(8)}$$

5.1 Batch System Investigation.

The objectives for studying the reaction in a batch system were to evaluate the feasibility of synthesizing EIPE from propylene and ethanol and to identify reaction conditions which could be used for further study in a bench-scale continuous process.

The effects of four variables were investigated: temperature (80-125°C), initial pressure (700-1000 psi), catalyst (Dowex HCR-w2)/EtOH mass ratio (0.1-1.0), and propylene/EtOH molar ratio (0.5-4.0). While investigating these effects only the relevant parameter was varied while the others were held constant.

5.1-1 Reaction In Absence of Catalyst.

Homogeneous synthesis of EIPE was investigated by performing runs in the batch reactor without catalyst. Conditions of temperature and initial pressure were changed in the range of 80-120°C and 700-1000 psi, respectively, while the propylene/EtOH molar ratio was kept constant at 4.0. Over the entire range of conditions investigated, no product was detected. This indicated that the homogeneous reaction between propylene and ethanol is extremely slow, and that the metal reactor body was non-catalytic toward EIPE formation.

5.1-2 Kinetic Control Region.

External mass transfer: Of particular concern in this system was the effect of the interphase mass transport on the data being measured. The classical method used to examine external mass transfer limitations is to investigate the effect of stirring speed on the reaction rate (Goto, 1993; and Piccoli, 1995). During initial runs, it was found that changing the stirrer speed had no effect on the rate of disappearance of propylene above 350 r.p.m. as shown in Figure 19. Hence, it can be concluded that, in the range of stirrer speeds above 350 to 600 r.p.m., the reaction rate was not affected by the liquid film resistance. At high stirring speeds such as 550 r.p.m., the resin showed good mechanical strength since the resin was found to be intact following runs where this agitation rate was utilized. Thus for all experimental runs, a stirrer speed of 550 r.p.m. was employed.

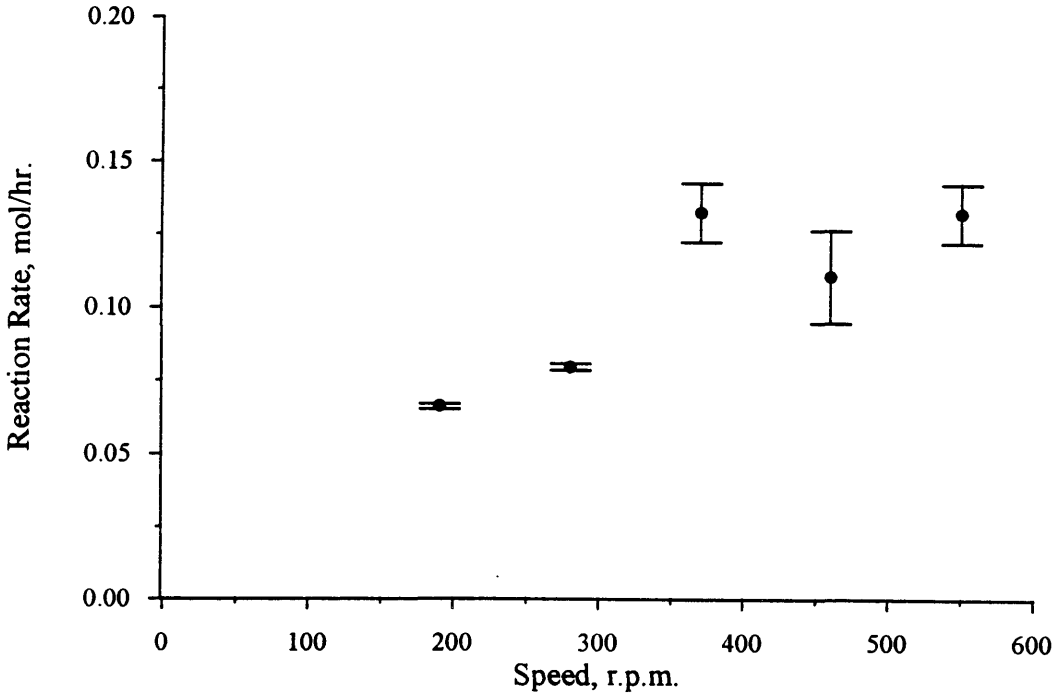

Figure 19. Effect of Agitation Rate on Reaction Rate.

Note : Each point represents the average of three different runs.

The error bar represents the range of the experimental data within one standard deviation.

Internal Mass Transfer: The most general technique to experimentally evaluate the effect of internal mass diffusion is to decrease the particle size and observe the change in reaction rate. Most papers published with this kind of ion exchange resin have ignored internal diffusion limitations. This is because of the nature of catalyst which is macroporous with a large average pore size. For these types of resins, mean pore diameters have been reported to be about 280 A (Kunin, 1958) with a surface area of less than 1.0 m^2/g. For these reasons, internal mass transfer limitations can normally be neglected. Mass transfer limitations for this reaction were, however, investigated experimentally and analytically as described in Section 5.2-3.

5.1-3 Effect of Catalyst Loading.

The first parameter that was tested was the catalyst amount in order to determine the optimum catalyst loading to use for studying other parameters. Reaction rate was computed from the pressure drop divided by time. This study was carried out at 115°C at initial pressure of 850 psi and the ratio of ethanol to propylene was maintained at 1.5. The rate was found to increase as the ratio of catalyst/EtOH increased from 0.1 to 1.0 see Figure 20.

When the ratio of catalyst/ethanol is low, ethanol more likely reacts with the acid groups thus forming solvated protons (ROH_2^+) which are less active acid species than the acid group ($-SO_3H$) in the resins according to Gates and Rodriguez (1973). Therefore, the reaction rate was slower at lower loading of catalyst compared to ethanol. As the ethanol decreased relative to the amount of catalyst, the mechanism gradually shifted to catalysis by SO_3H. Thus, the rate of EIPE formation increased with an increase in SO_3H group concentration. The reaction rate increased until ethanol was no longer able to affect the reaction rate when the ratio of catalyst to ethanol was greater than 0.8.

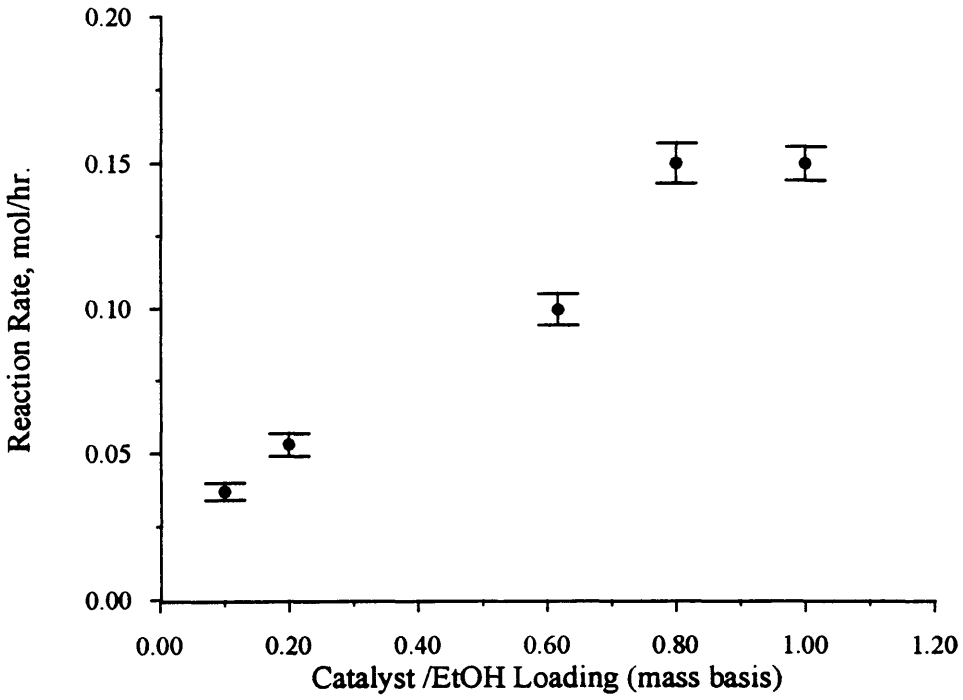

Figure 20. Effect of Catalyst/ethanol Loading.

Note : Each point represents the average of three different runs.

The error bar represents the range of the experimental data within one standard deviation.

5.1-4 Effect of Temperature.

The effect of temperature on the conversion and selectivity for EIPE formation is shown in Figure 21. The reaction temperature was varied in the range from 80 to 125°C. The experiments were not carried out at temperatures over 140°C due to the restriction of catalyst thermal stability. Raising temperature higher than 125°C most probably would not increase conversion and selectivity much since the reactions are close to the thermodynamic control region as shown by the line in Figure 21. This indicates that fractional conversion of ethanol increases substantially with an increase in temperature, and the selectivity for conversion of ethanol to EIPE increases slightly with an increase in temperature.

5.1-5 Effect of Pressure.

The initial reactor pressure was varied in the range from 700 to 1100 psi. Under a constant temperature of 125°C and with a catalyst-to-ethanol mass ratio of 0.8, it was observed that there was no significant change in conversion and selectivity with changing initial pressure (Figure 22). These results agree with the solubility calculations previously discussed. At 125°C, pressures higher than 600 psi will not influence the solubility of propylene in ethanol since propylene and ethanol already exist as a dense single phase mixture as discussed in Section 4.2.

5.1-6 Effect of Propylene to Ethanol Ratio.

The study of the effect of feed ratio (propylene/ethanol) was carried out in the range of 0.5 to 2.5 (mole basis) at a temperature of 125°C, and at 1000 psi initial pressure. From Figure 23, it can be observed that the final conversion is higher when the ratio of propylene to ethanol is higher. Two effects, one physical and one chemical, can be used to explain this observation. First, it has been reported that high alcohol

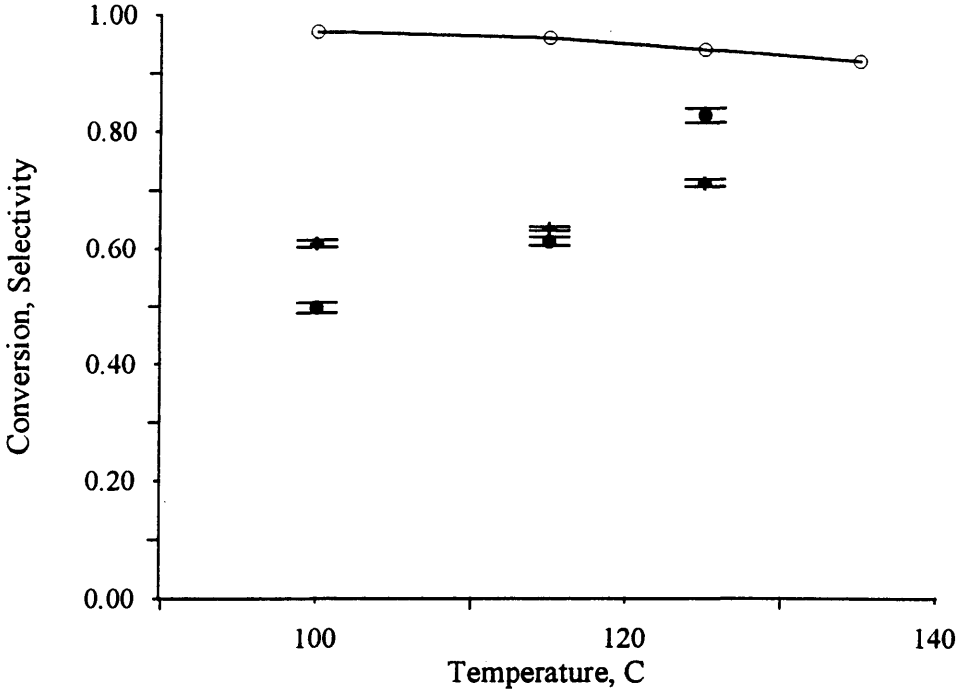

Figure 21. Effect of Temperature.

• Conversion + Selectivity

° Equilibrium Conversion

Note : Each point represents the average of three different runs.

The error bar represents the range of the experimental data within one standard deviation.

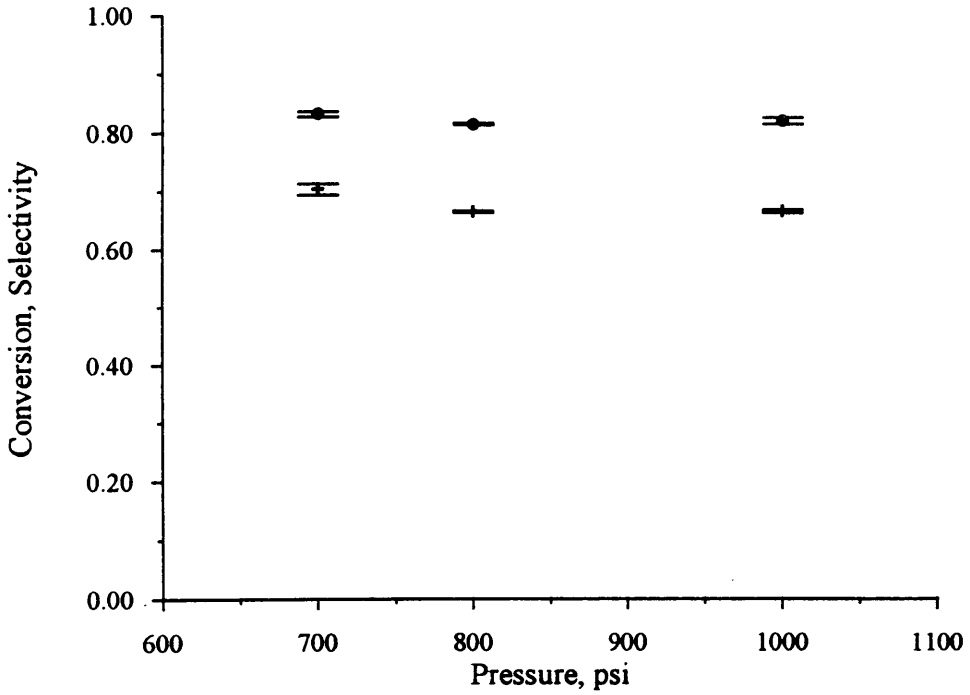

Figure 22. Effect of Initial Pressure.

• Conversion + Selectivity

Note : Each point represents the average of three different runs.

The error bar represents the range of the experimental data within one standard deviation.

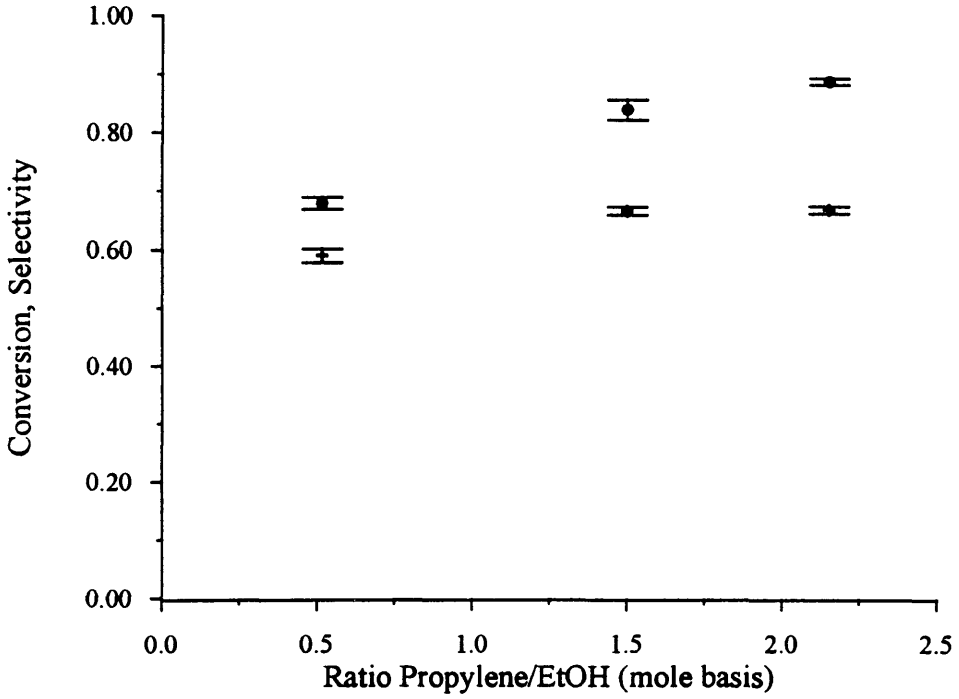

Figure 23. Effect of Feed Composition, Propylene/EtOH (mole basis).

•Converion + Selectivity

Note : Each point represents the average of three different runs.

The error bar represents the range of the experimental data within one standard deviation.

concentrations in contact with ion exchange resins can result in formation of "solvated protons" according to the following equilibrium (Gates and Rodriguez, 1973):

$$ROH + SO_3H \rightleftharpoons ROH_2^+ + SO_3^-$$

Solvated protons are far less acidic compared to the sulfonic group, hence the protonation of olefin would be less rapid at high alcohol concentrations leading to an overall slower reaction rate. Second, the surface coverage of the resin by ethanol at high EtOH/Propylene ratios may physically block access of propylene to the active acidic sites on the resin. This would also lead to an overall slower rate of reaction, as was observed.

5-1.7 Product Distribution.

The results of the investigations of the effects discussed above suggest that the best EIPE production conditions are mixed-phase with 1:1 catalyst/EtOH mass loading and a 1.5:1.0 propylene/EtOH molar ratio. In order to better understand the rate of production of various species, several runs were stopped at intermediate times. The results at 125°C and an initial pressure of 1000 psi are shown in Figure 24. The results show that most of the products are EIPE (about 70%) and DEE (about 20%). Other products (totalling less than 10%) are IPA, water, and DIPE. The products of IPA, water, and DIPE were found because DEE production was responsible for producing water, and this water in turn promoted hydration of propylene to form IPA and DIPE. These data also show that the EIPE product increases monotonically with time and approaches a final value within 90 minutes. Hence, the approximate time required for this reaction is on the order of 60-90 minutes, a time which is comparable to that for synthesis of MTBE.

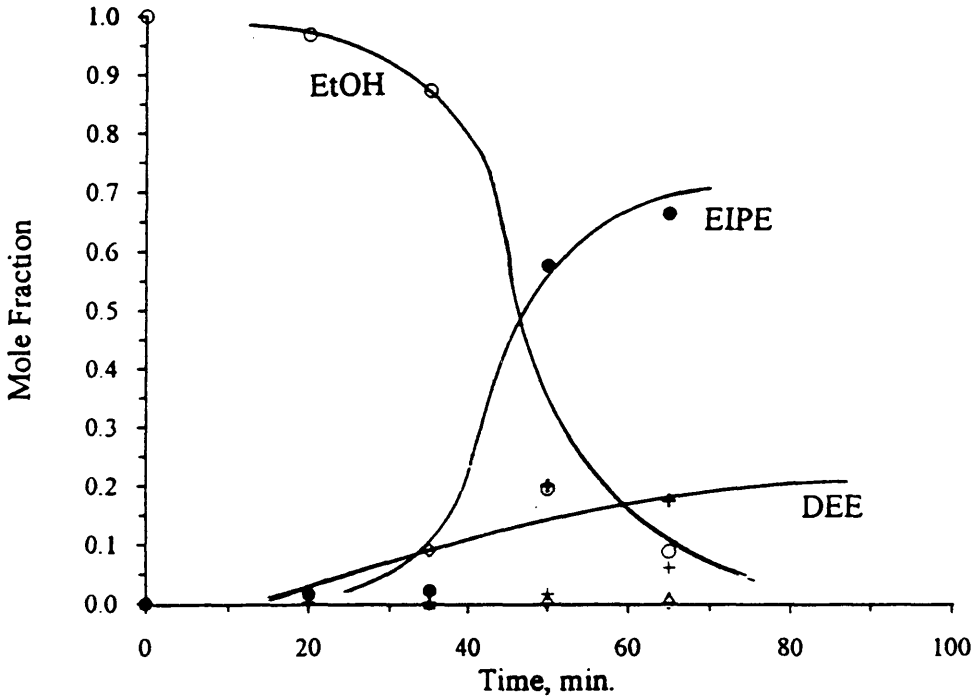

Figure 24. Product Distribution in Mole Fraction Basis.

5.2 Continuous Flow Reactor.

5.2-1 Reactor Configuration.

The second part of this study was carried out in a packed-bed catalytic micro-reactor which was operated in the trickle-flow regime. Both upflow and downflow configurations were tried initially and it was found that downflow operation was preferred due to the fact that there was no limitation on the flow rate imposed by flooding limits.

5.2-2 Blank Run.

The blank (no catalyst) run was performed with the reactor packed with different amounts of quartz chips. The system was run at 70 to 130°C and pressures from 150 to 670 psi. No reaction could be detected in the presence of quartz chips. This indicated that there were no surface reactions occurring and that the stainless steel wall of the reactor was non-catalytic.

5.2-3 Mass and Heat Transfer Limitations.

The measurement of chemical reaction kinetics in the presence of a solid catalyst has to be done in the absence of temperature and concentration gradients associated with mass and heat transfer limitations. Accordingly, mass transfer limitations for external and pore diffusion and heat transfer limitations were investigated both analytically and experimentally.

External Mass Transfer: Assuming an ideal trickle-bed reactor, it can be assumed that the catalyst pellets are completely bathed with liquid. Hence, the concentration profile for reactants in the gas and the liquid phase can be assumed to be as shown in Figure 25. This figure shows that the overall external mass transfer consists of the resistances between gas-liquid and liquid-solid phase. From the steady state mass flux

relationships (Equation 9), the overall external mass transfer coefficient may be expressed as Equation 10 with the assumption that areas for the transfer at each interface are the same at moderate liquid flow rates (Smith, 1983). Satterfield (1975) found that the gaseous reactant is usually present in substantial stoichiometric excess and in relatively high concentration. The product of H k_G then is much greater than either k_L or k_s and Equation 10 then reduces to Equation 11.

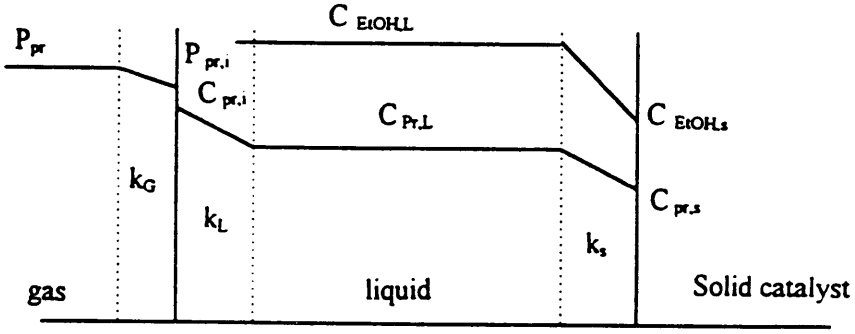

Figure 25. Concentration Distribution of a Gaseous and Liquid Reactant.

$$\text{Rate} = k_G a_L (P_{Pr} - P_{Pr,i}) = k_L a_L (C_{Pr,i} - C_{Pr,L}) = k_s a_s (C_{Pr,L} - C_{Pr,s}) \quad \text{----(9)}$$

$$\frac{1}{a_s k_{Ls}} = \frac{1}{a_L k_G H} + \frac{1}{a_L k_L} + \frac{1}{a_s k_s} \quad \text{----(10)}$$

$$\frac{1}{k_{Ls}} = \frac{1}{k_L} + \frac{1}{k_s} \quad \text{----(11)}$$

Satterfield (1970) used k_{Ls} to propose a criterion for external mass transfer for trickle flow. This criterion, assuming complete wetting of the pellet, suggests that external mass transfer through the liquid film will not be a significant resistance unless the following inequality holds.

$$\left[\frac{10 d_p}{c^* k_{ls}}\right] r (1-\varepsilon) > 1 \qquad \text{----(12)}$$

This criterion was first utilized to calculate preliminary estimates of the importance of intraparticle mass transfer for the laboratory reactor. These calculations are presented in Appendix D.1. As shown, the calculated interphase mass transport parameter was found to be 0.146, which is reasonably far removed from the critical value of 1.00. As some uncertainty was present in estimation of diffusivities for this parameter, it was decided to further investigate the importance of interphase mass transport experimentally in order to identify the conditions where this effect can be ignored. The influence of external mass transport was examined by investigating the effect of varying the space velocity in the reactor. Preliminary experiments were made at the maximum allowable temperature for Dowex HCR-w2 (140°C). Runs were carried out by maintaining a constant feed composition and W/F_{Ao} ratio, but by varying the catalyst mass. When film resistance is important, the rate will vary with changing space velocity. Results of these tests are shown in Figure 26. As can be seen, the reaction rate does not depend on flow rate for WHSV > 0.2 hr^{-1}. The limiting number is very low which corresponds well with the result from the criterion calculation which was also far away from the critical value. These data also show that at WHSV< 0.2 hr^{-1} the system exhibits a first order relationship between rate and the WHSV, suggesting that external mass transfer is the rate limiting step.

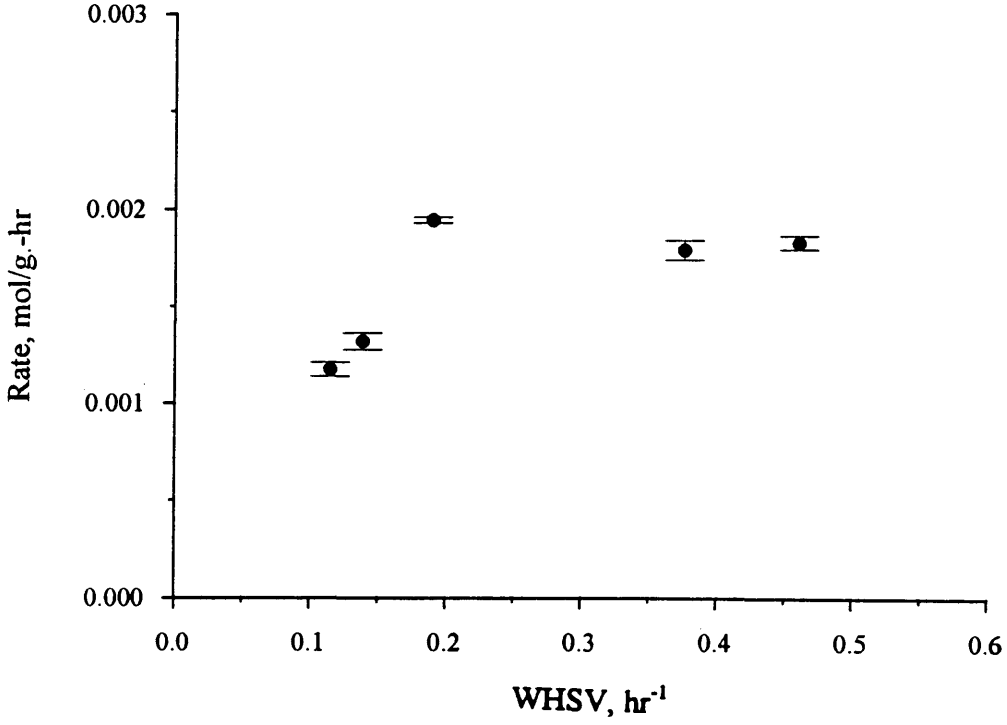

Figure 26. Effect of Liquid Flow Rate on Reaction Rate.

Note : Each point represents the average of three different runs.

The error bar represents the range of the experimental data within one standard deviation.

Internal Mass Transport: Internal diffusion limitations are commonly expressed in terms of a catalyst effectiveness factor, defined as the ratio of the observed rate of reaction to that which would be observed in the absence of any internal diffusion limitations. The Weisz-Prater parameter was modified by Satterfield by adding the void fraction factor for trickle-flow behavior as:

$$\frac{(d_p/2)^2\, r\,(1-\varepsilon)}{D_{eff}\, c_s} < 1 \qquad \text{-----(13)}$$

Calculations for this system utilizing the modified Weisz parameter are shown in Appendix D.2. The calculated modified Weisz parameter (for the severe assumption) is 0.75 which is still far from the critical value of 1.00. As a result, it can be concluded that mass transfer limitations due to pore diffusion will not be significant. However, these limitations were also examined experimentally in order to verify the estimation.

A series of experiments was carried out at constant contact time and feed composition with the dimensions of the catalyst particles decreasing from one run to the next. The observations were made in the range of experimental conditions where the effect of interphase mass transport limitations could be ignored. In the region controlled by chemical reaction, conversion remains constant, whereas in the region of internal diffusion control, conversion is proportional to the catalyst size. As can be seen in Figure 27, the rate was unchanged, within the limit of the experimental error, for all particle sizes tested. This behavior was not unexpected because ethanol can permeate the catalyst easily, and as a result, the resins swells to a large extent in the presence of the alcohol. Hence, the average particle size chosen for evaluating the reaction kinetics in subsequent testing was 0.35 mm. (40-70 mesh size).

Heat Effect: Heat transfer effects can be both external and internal, and can exist when mass transfer limitations are significant (Smith, 1985). As shown above, conditions for this study were set so as to be sure that the effects of internal and external

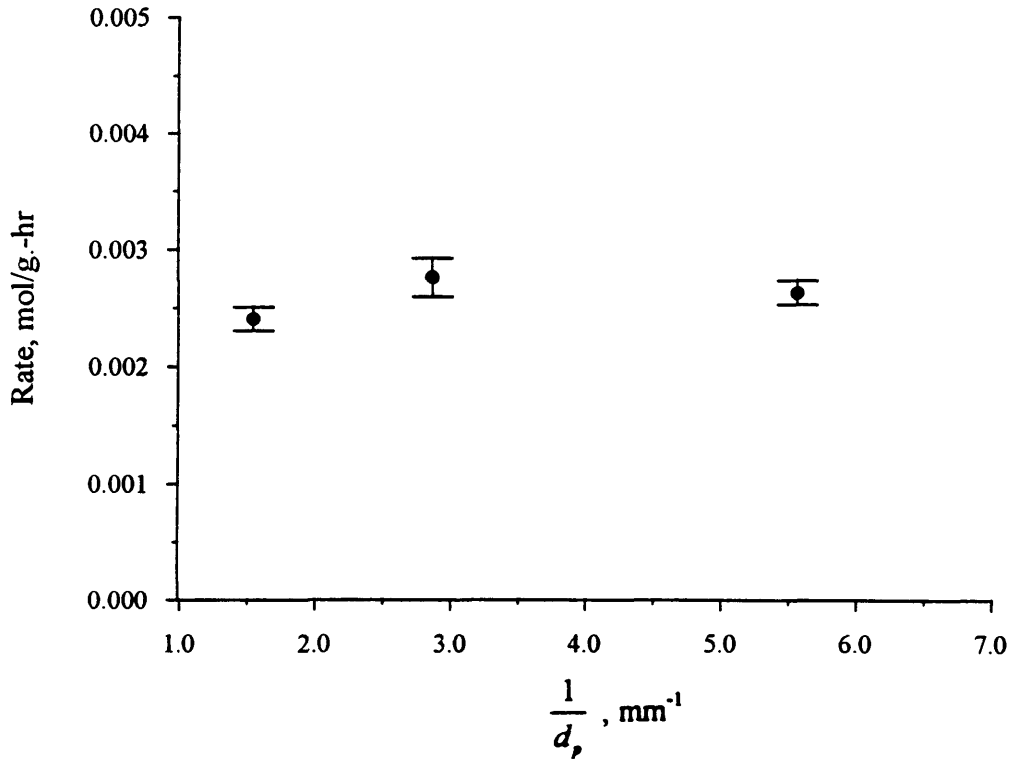

Figure 27. Effect of Particle Size on Reaction Rate.

Note : Each point represents the average of three different runs.

The error bar represents the range of the experimental data within one standard deviation.

mass transport were minimized. The catalyst bed was also packed with diluent quartz chips (50:50 by volume) in order to dilute the catalyst and minimize thermal gradient. Calculations for heat transfer limitations were carried out as shown in Appendix D.3. It was found that the estimated difference between the catalyst surface and the bulk temperature was about 0.2 degree Celsius. This result confirms that there were no heat transfer limitations under the conditions used.

Axial Dispersion: The evaluation of kinetic data from a fixed-bed catalytic reactor is usually based on the assumption of plug flow. However, deviations from plug flow can occur in packed-bed reactors due to axial dispersion. Mears (1974) presented the following criterion for the minimum h/d_p ratio required to hold the reactor length within 5% of that needed for plug flow.

$$\frac{h}{d_p} > \frac{20\,m}{Pe_L} \ln \frac{c_{in}}{c_{out}} \qquad \text{-----(14)}$$

The calculation in Appendix D.4 shows that there is no effect due to axial dispersion for this work.

5.2-4 Catalyst Screening.

Three cation exchange resins (Dowex HCR-w2, Amberlyst-15, and supported FCSA) and one inorganic catalyst (P/Al 0.8) were evaluated as catalysts for EIPE synthesis. The objective of this portion of the study was to screen several candidate catalysts and then select only one catalyst for the further study with respect to reaction kinetics. Since the thermal stability for each catalyst was different, the experimental plan was formulated to test each catalyst at the maximum allowable temperature while the other variables (pressure, space time, feed composition, and time on stream) were held constant. A pressure of 500 psi, WHSV of 0.8 hr^{-1} based on ethanol flow rate and

catalyst dry basis, 4.5 cm^3/hr propylene flow rate, and a particle size of 0.21 to 0.42 mm (40-70 mesh size) were used as fixed parameters for this study.

In addition to evaluating the activity and selectivity of these materials, we decided to first check for deactivation. This was necessary since the activity testing was to be carried out at temperature near the thermal stability limits of each catalyst. Hence, deactivation could be severe due to coking, or other physico-chemical changes in the catalyst leading to erroneous conclusions regarding activity in our subsequent runs.

Deactivation Testing: The conventional method often used to study catalyst life is to set the experiment to run continuously for 50-100 days, and then compare catalyst performance based on conversion and selectivity. With limited time, catalyst life can be studied by temperature sequencing each catalyst. The temperature sequence experiment involves reaction at one low temperature, then increasing temperature to the maximum for a particular catalyst for a period of time and then decreasing temperature to the original value. Each time period for the test was held at 10-12 hours, and a comparison of the conversion and selectivity at low temperature before and after operation at the maximum temperature was used to investigate deactivation. The maximum operating temperature for each catalyst is shown in Table 6. Figures 28 to 31 show the temperature sequences and present the results for conversion and selectivity for each catalyst.

Dowex HCR-w2: EIPE synthesis was first examined at 60°C and 500 psi. These conditions were found to promote very low conversion (less than 1%), but at this condition there were no other by-products detected in the effluent hence selectivity to EIPE was 100%. However, at this low temperature it was concluded that these data were not especially useful for deactivation comparisons. By increasing temperature to 100°C, conversion was increased to about 10% while the selectivity decreased from 100% to about 60%. Subsequently, the reactor was held at 140°C for 15 hours, and

then temperature was decreased to 100°C. The conversion and selectivity at 100°C after running at 140°C remained at 10% and 60% respectively as shown in Figure 28.

Amberlyst-15: The maximum allowable temperature is 120-125°C, therefore the tests were done following a 100-120-100°C temperature sequence. The conversion given by A-15 at 120°C was about 20-25 % with a selectivity of about 60-70%. Comparing the conversions and selectivities of 100°C before and after operation at 120°C, it was found that both conversion and selectivity were maintained between 8 to 10% and 60 to 70%, respectively as shown in Figure 29. These results indicate that there is very slight deactivation with respect to selectivity after running the experiment at the higher temperature.

Supported FCSA: The maximum allowable temperature for this catalyst is 200°C. The temperature sequence hence was set for testing FCSA at temperatures of 100-140-180-140°C. The reaction was found to be very slow at 100°C which gave low conversions (less than 1%), but the selectivity was 100%. The reaction shows very high conversion (80-85%) at 180°C, but shows low selectivity to EIPE (about 20-40%). There were no differences noted in conversion and selectivity before and after testing at 180°C as shown in Figure 30.

P/Al 0.8: Alumina-aluminum phosphate-supported catalysts have been shown to give good performance for ethanol dehydration (Cowley, 1995). Hence, this material was tested as an EIPE synthesis catalyst. With the high thermal stability of this catalyst, the experiment can be run at temperatures as high as 240°C. The results in Figure 31 show that the activity and selectivity were very low, 25% and 10-15% respectively at 240°C. The observations do not show a loss of activity.

From the temperature sequence studies, there was no clear evidence suggesting that deactivation of catalysts will be a problem. However, physical properties were also examined in order to gain more insight into possible mechanisms of catalyst deactivation.

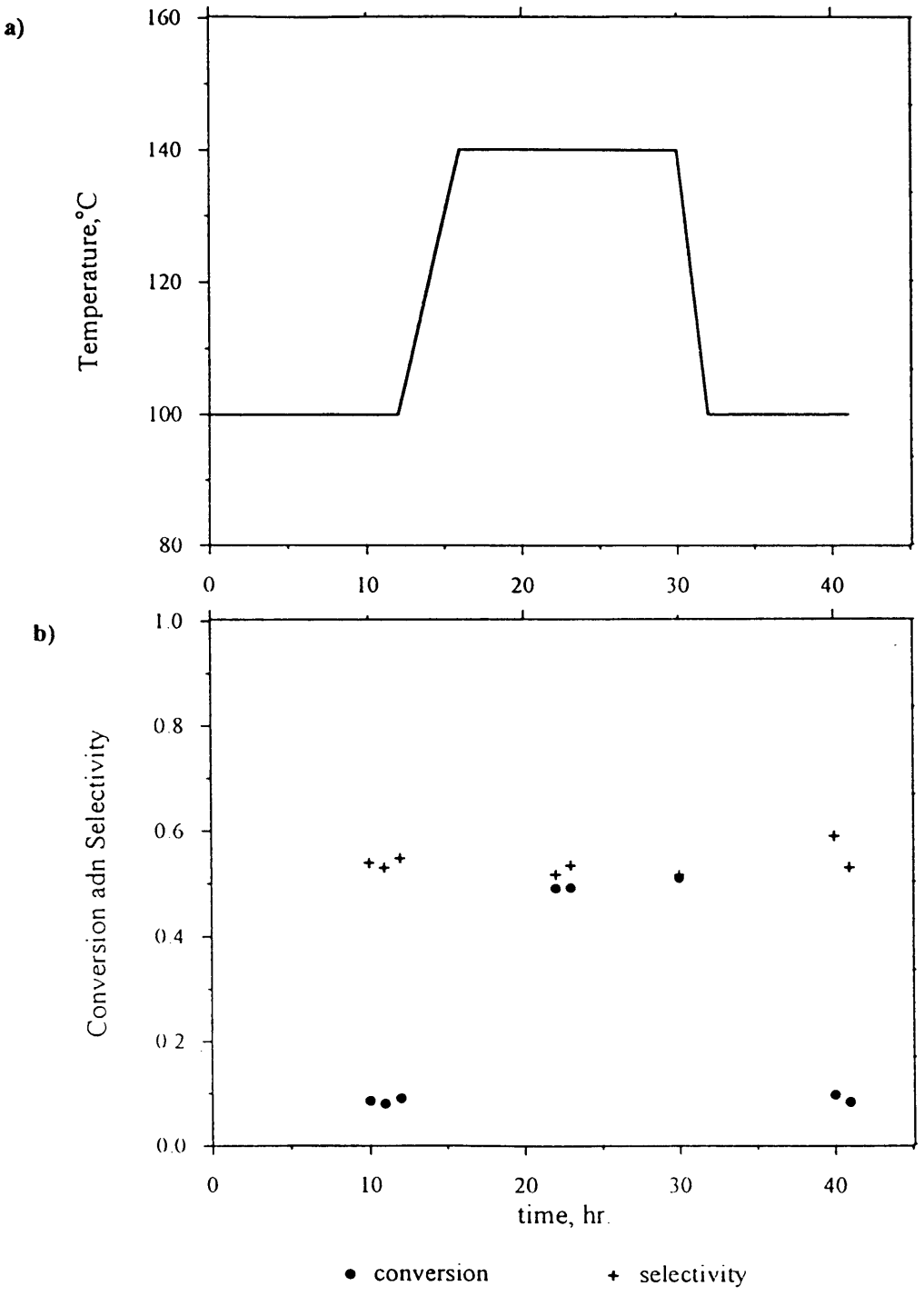

Figure 28. Catalyst (Dowex HCR-w2) Evaluation. a) Temperature Test Sequence b) Conversion and Selectivity.

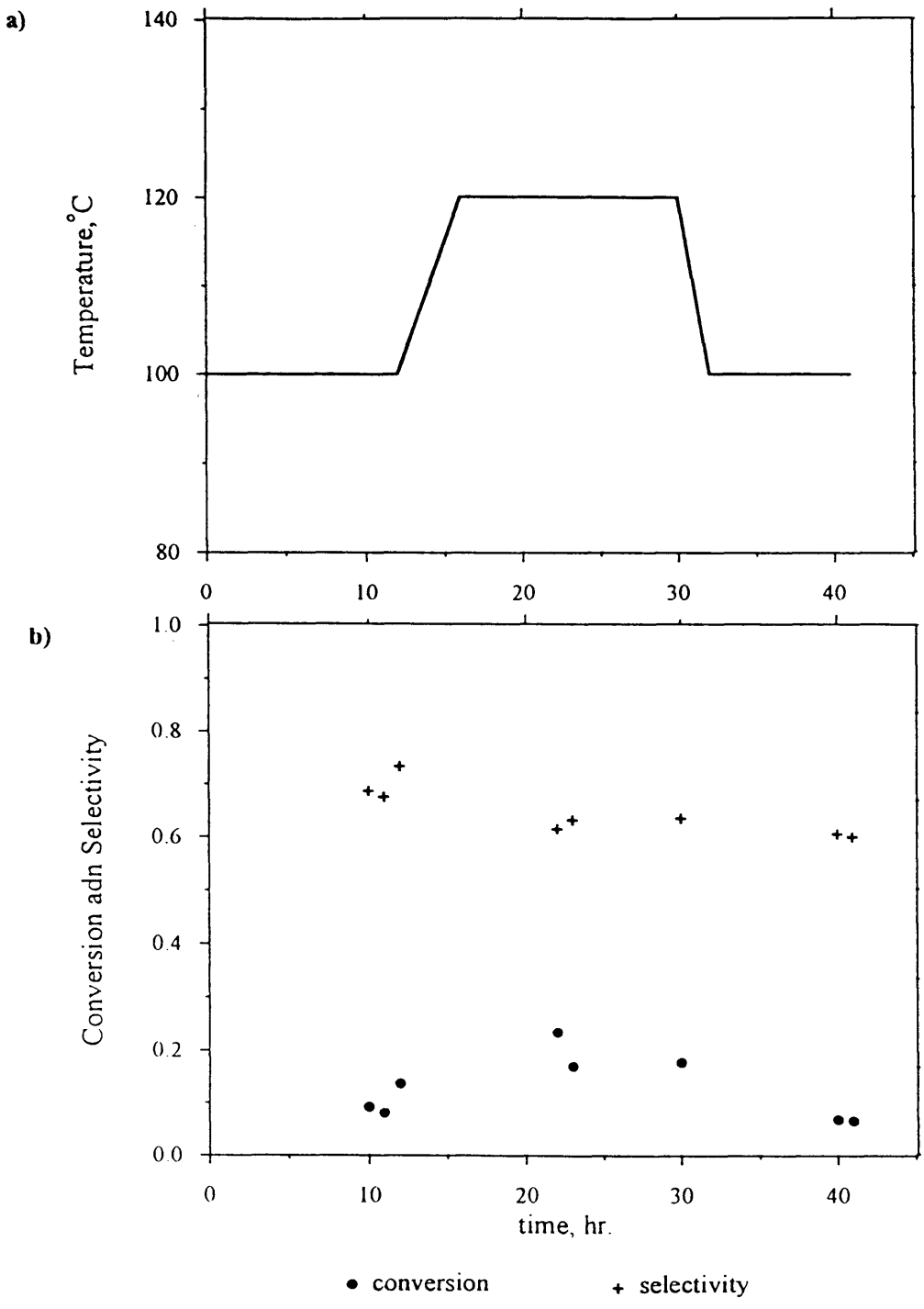

Figure 29. Catalyst (Amberlyst-15) Evaluation. a) Temperature Test Sequence b) Conversion and Selectivity.

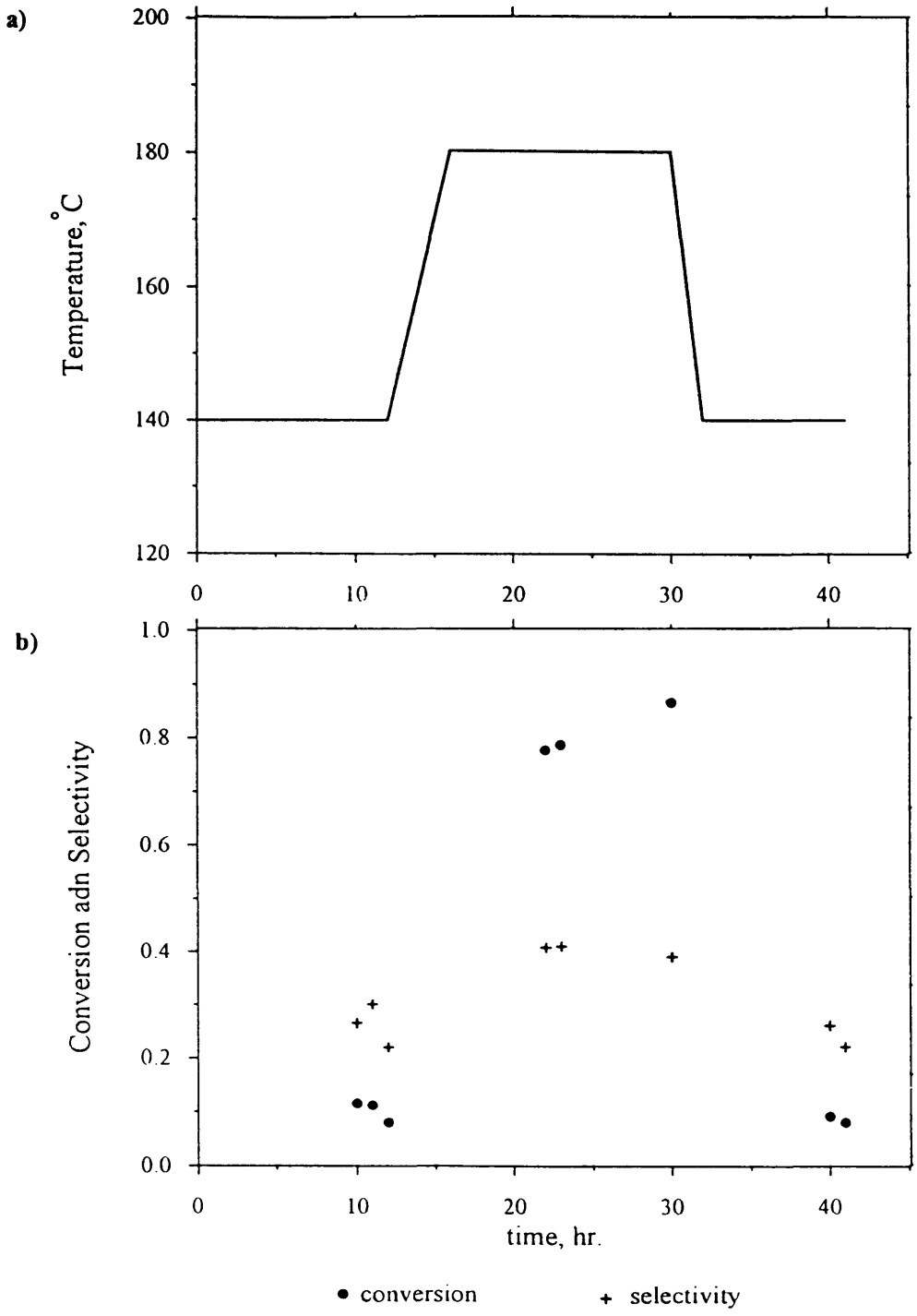

Figure 30. Catalyst (supported FCSA) Evaluation. a) Temperature Test Sequence b) Conversion and Selectivity.

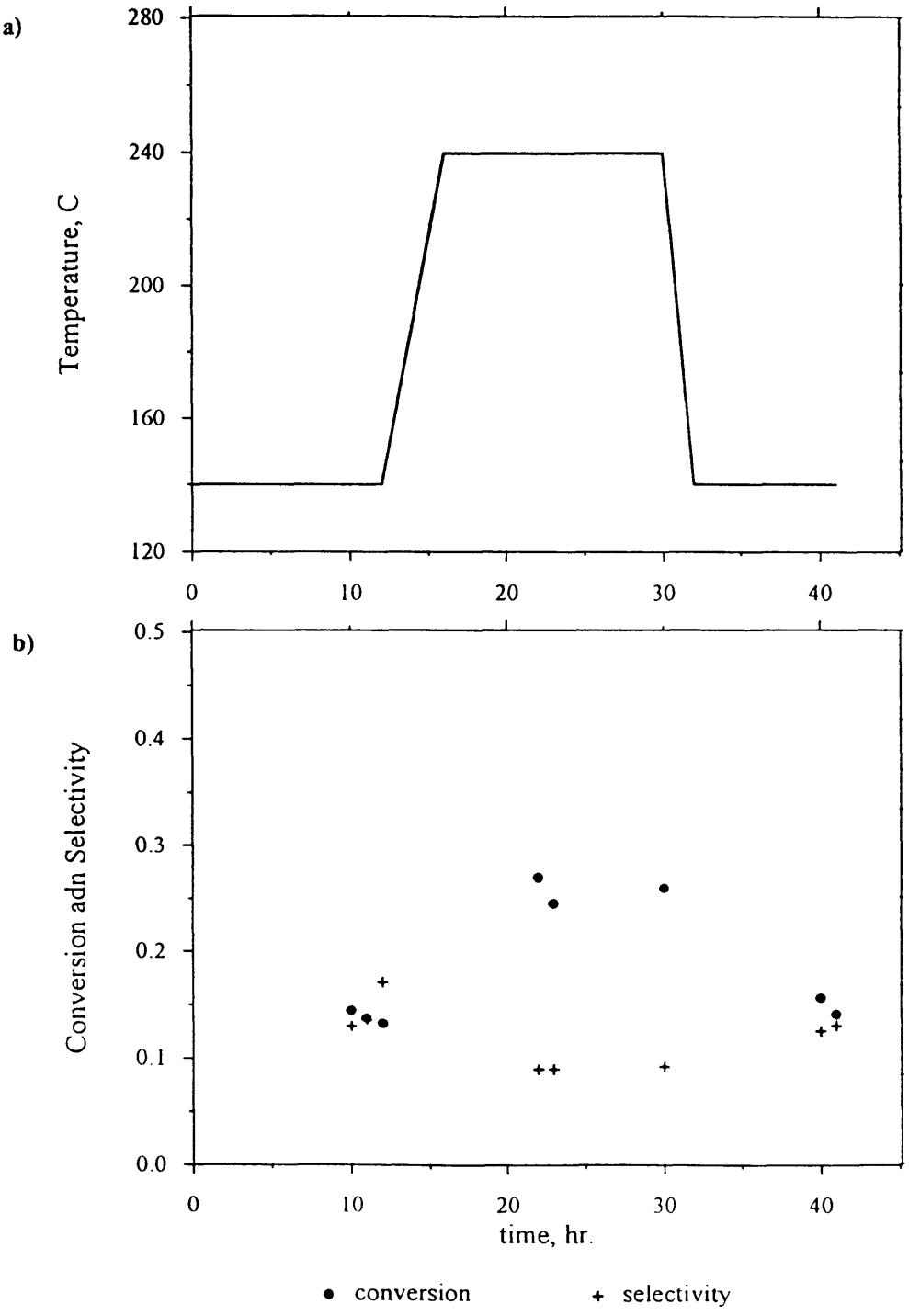

Figure 31. Catalyst (P/Al 0.8) Evaluation. a) Temperature Test Sequence b) Conversion and Selectivity.

To investigate loss of catalyst activity, several properties of catalysts before and after reaction were examined. One cause leading to decreasing conversion and selectivity with time is loss of ion exchange capacity (active sites). The method which is generally used to determine ion exchange capacity has been described previously in section 3.3-2. The catalyst after reaction was in the same physical condition, but a small brown spot appeared on some areas of the catalyst surface. One possible reason for this color change might be coke formation which is able to block the active sites. Spent catalysts were thus subjected to total carbon and BET surface area analysis.

BET Surface Area Analysis: All catalysts (fresh and used) were analyzed for total surface area by the BET method. Unfortunately, data only for Amberlyst-15 and P/Al 0.8 could be obtained. For Dowex HCR-w2 and FCSA, reliable results could not be obtained since their surface areas were too low (less than 1.0 m^2/g). Figures 32 and 33 show the BET plots for A-15 and P/Al 0.8 for both fresh and used catalysts. The surface areas for A-15 and P/Al 0.8 were not found to decrease.

Ion Exchange Capacity: Fresh and spent catalysts were treated with sodium chloride in water solution to form HCl. HCl then was titrated with NaOH using phenolphthalein as an indicator. The amount of H^+ was then calculated from the amount of NaOH consumed and the results (96% confidence level) are presented in Table 8. The greatest loss was for Dowex HCR-w2, with a change of -0.225 meq/g after 42 hours on-stream, while Amberlyst-15 and FCSA showed negligible changes. These losses are small, and suggest that changes in ion exchange capacity will not be of significance in terms of catalyst screening criteria.

Total Carbon Analysis: The results for total carbon content of catalysts are presented in Table 9. Carbon amounts in spent Dowex HCR-w2 and P/Al 0.8 catalysts were increased by about 0.50% compared to the fresh catalysts. Carbon could be produced from the polymerization of propylene, however, the increase of carbon was

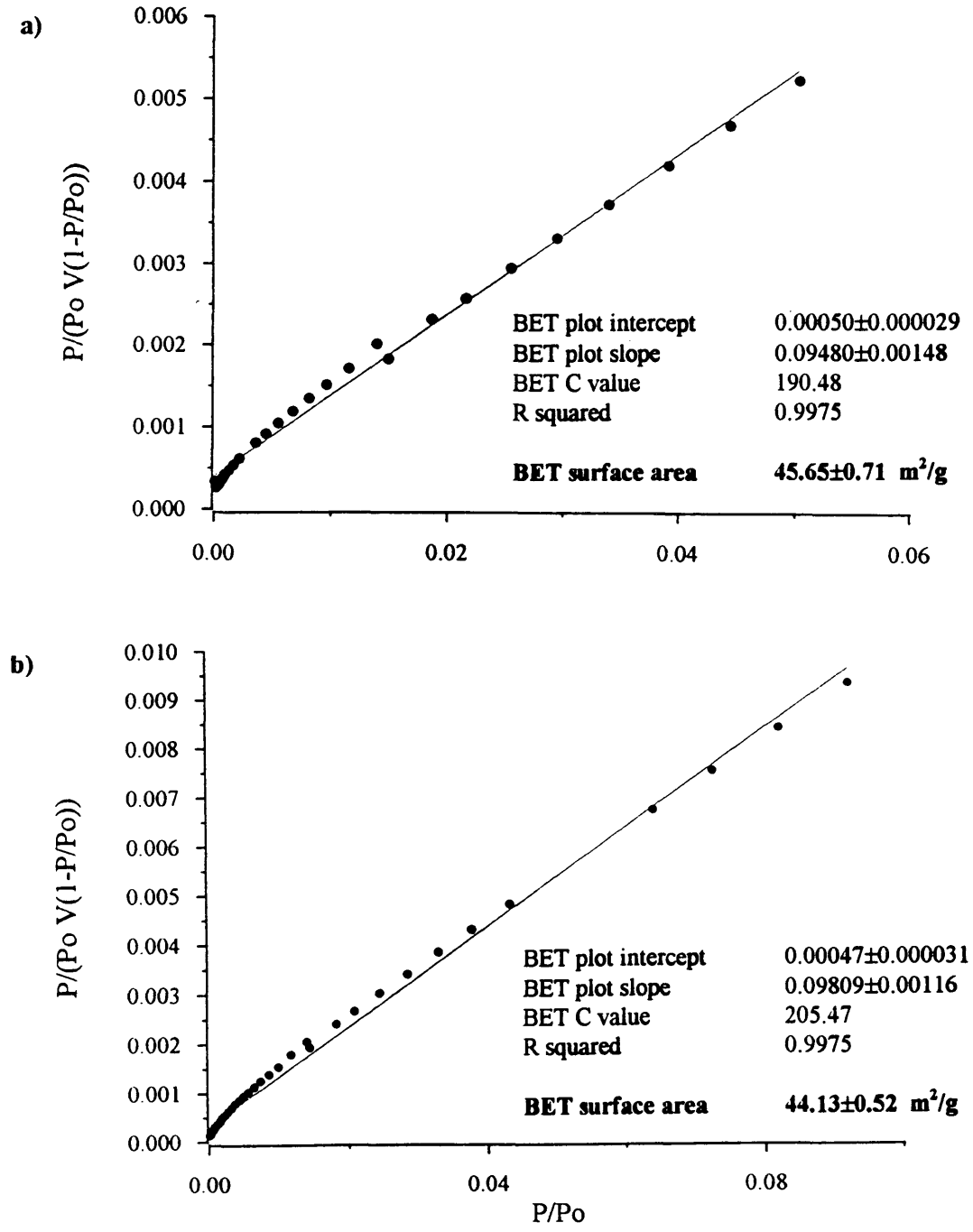

Figure 32. BET of Nitrogen Adsorption Data for Amberlyst-15
a) Fresh b) Used.

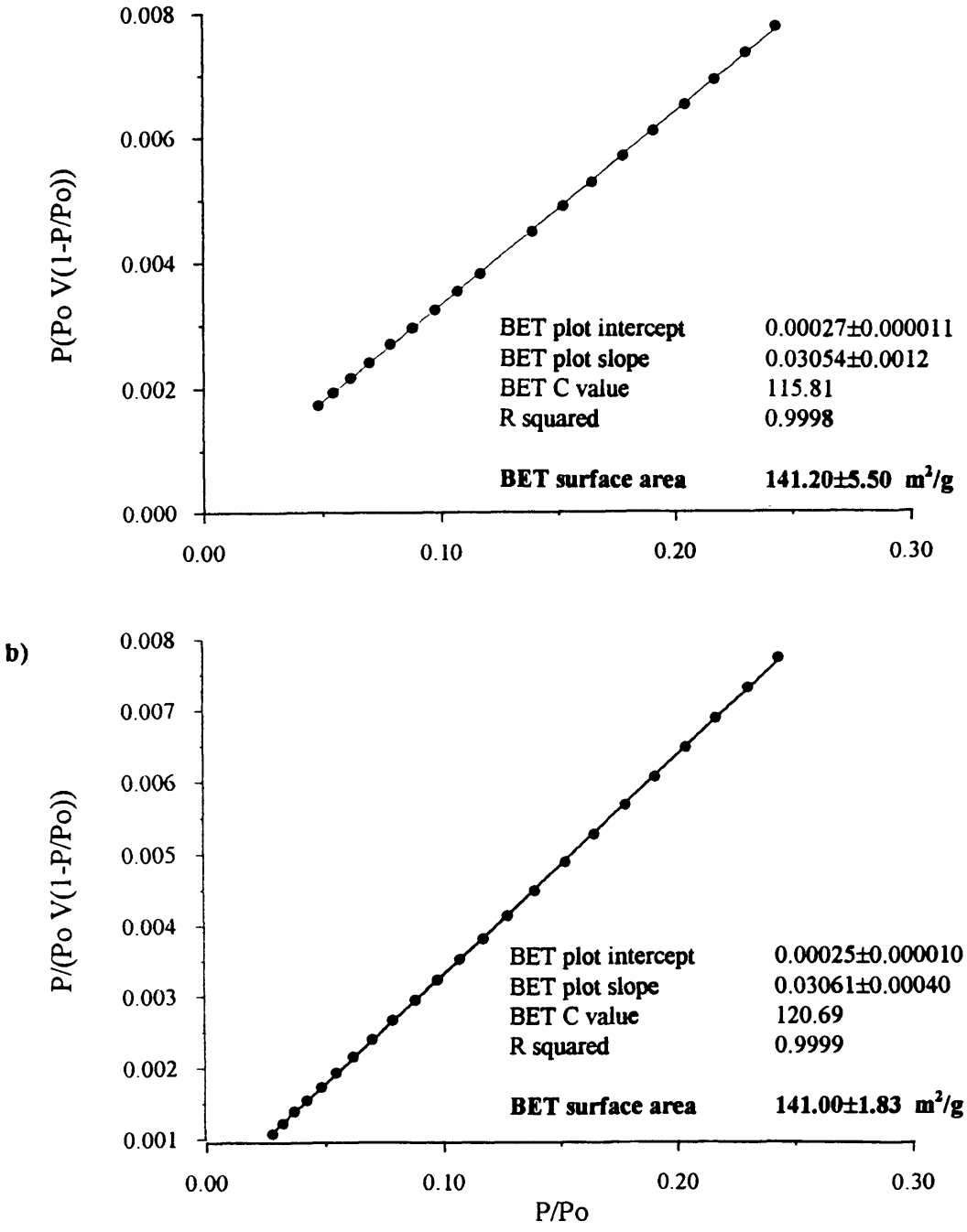

Figure 33. BET of Nitrogen Adsorption Data for P/Al 0.8
a) Fresh b) Used.

Table 8. Ion Exchange Characteristic of Resins (dry basis).

Catalyst	Exchange Capacity, meq/g average	
Dowex HCR-w2	Fresh	5.08
	Used*	4.86
Amberlyst-15	Fresh	4.77
	Used*	4.74
Supported FCSA	Fresh	0.14
	Used*	0.13

Note: *: after 42 hours reaction time.

The data for P/Al 0.8 are not available.

Table 9. Total Carbon Analysis.

Catalyst	Total Carbon, %
Dowex HCR-w2	Fresh 40.81 Used* 41.34
Amberlyst-15	Fresh 46.67 Used* 46.54
Supported FCSA	Fresh 3.16 Used* 3.11
P/Al 0.8	Fresh 0.00 Used* 0.53

Note: * after 42 hour reaction time.

insignificant. For Amberlyst-15 and FCSA, the carbon amount was found to be constant within experimental error.

Summary: From the above comparisons concerning loss of catalyst activity, there is no clear evidence which can be used to judge between the four catalysts. This leaves the decision regarding the best catalyst to be based on conversion and selectivity results. According to Figures 28 to 31, the selectivity to EIPE on FCSA and P/Al 0.8 was found to be in the range of 40 and 20% respectively which was much lower than for Dowex HCR-w2 and Amberlyst-15. Comparing Dowex and A-15 at 120°C, these catalysts were found to give similar results for both conversion and selectivity. However, at the maximum allowable temperature for Dowex (140°C) and A-15 (120°C), performing the reaction using Dowex was found to give higher conversion (about 50% compared to about 20% by using A-15) at the same level of selectivity (50-60%). Therefore, from a practical viewpoint, using Dowex catalyst can produce more EIPE per unit volume of catalyst than can A-15. Hence, for the evaluation of kinetics, Dowex HCR-w2 was selected as the catalyst to be used.

5.2-5 Kinetic Analysis

Kinetic analysis for EIPE:

Experiments for collection of reaction rate data were carried out in the trickle-bed downflow reactor with propylene in gas phase and ethanol in the liquid phase. The reactions were performed far from the limitation of thermodynamic equilibrium and without heat and mass transfer limitations. The operating conditions generally employed are given in Table 10. Conditions were adjusted such that steady-state conversions lower than 15 % were obtained for reactions using a binary feed (ethanol and propylene) and also for experiments where DEE was added to the feed. For these conditions, radial and axial temperature gradients were lower than 0.5°C, and byproducts such as 4-methyl-2-pentene, IPA, and DIPE were not detected in the reactor effluent. Considering the reactor to be a differential plug flow reactor, the reaction rate was computed from ethanol conversion by the relationship :

$$-r_A = \frac{X\, F_{Ao}}{W} \qquad ---(15)$$

During each run, the outlet stream was frequently analyzed to assure that the reaction reached steady state. After steady state was attained, reactant flow rates were maintained for 4-5 hr. and samples were analyzed every 30 minutes in order to obtain average composition data. Table 11 shows one example of typical data collection. Afterwards, a new experiment condition was established. Since the activity of the resin may have decreased, the catalyst was replaced after two or three runs.

The average results for each run are presented in Appendix C.2.4. Validation of the results was determined from carbon, hydrogen, and oxygen balances which closed to nearly 100 percent in every case. These conversion results and conditions were then converted to reaction rate using Equation 15. Figure 34 is a plot of the reaction rate

Table 10. Reaction Parameters for Collection of Rate Data.

Process Variable	Ranges
Catalyst	Dowex HCR-w2
Weight of Catalyst, g.	0.5
Catalyst Size, mesh size	40-70
Reactor Temperature, °C	100-135
Reactor Pressure, psi	350-650
Propylene Feed Rate, $cm^3/hr.$	4.00-5.25
EtOH mixture Feed Rat, $cm^3/hr.$	1.5-2.0
WHSV (based on ethanol flow rate), hr^{-1}	3-4

Table 11. Example of Data Collection for Run Number 31.

Injection Component	1	2	3	4	5	X ± S
Propylene	54.13	57.06	54.31	53.08	54.77	54.46 ± 1.33
EtOH	21.95	21.07	24.31	22.00	23.84	22.59 ± 1.38
DEE	5.14	5.58	5.49	5.01	5.21	5.29 ± 0.24
H_2O	4.30	4.30	4.78	4.77	4.30	4.49 ± 0.26
EIPE	11.30	1.09	11.21	12.30	10.81	11.31 ± 0.60
IPA	1.10	0.94	0.97	1.02	0.89	0.98 ± 0.08
DIPE	0.90	0.87	0.90	0.88	0.81	0.87 ± 0.04

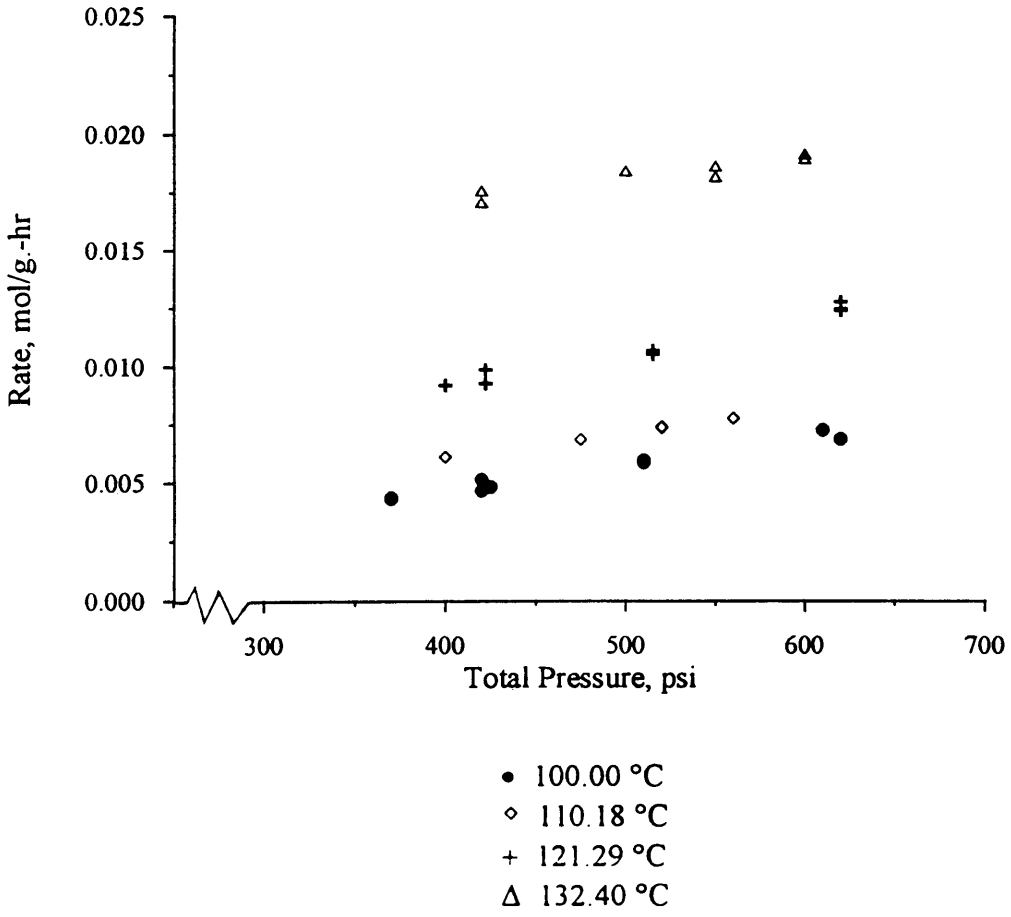

Figure 34. Differential Results from Runs Made with Pure Ethanol Feed at Various Pressures and Temperatures.

with respect to total pressure for various temperatures. Figure 35 shows the reaction rate with respect to total pressure at 100°C for two different feed concentrations of ethanol.

As shown, the yields of DEE and EIPE are dependent on total pressure. In Figure 18, the vapor pressures for ethanol, DEE and EIPE were shown to be relatively low compared to the vapor pressure of propylene. Therefore, the total pressure can be assumed to be equal to the partial pressure of propylene and Figure 34 thus gives data that show how the rate depends on the concentration of propylene. On the other hand, Figure 35 shows that reaction rate was inversely proportional to the concentration of ethanol when the total pressure was kept constant.

These observations show qualitatively how the rate depends on propylene and ethanol concentrations; however, a more quantitative description for the reaction was next developed by deriving Langmuir-Hinshelwood-Hougen-Watson (LHHW) rate expressions.

The LHHW rate equations are based on a series of steps in a multiple sequence including adsorption, chemical reaction, or desorption. It is assumed that the overall rate is controlled by the single slow step and all the other steps are at equilibrium with respect to the rate limiting step. Various plausible kinetic models can be derived based on assumptions concerning the rate controlling step (adsorption, surface reaction, desorption).

Possible reaction mechanisms for this reaction include only dual-site mechanisms. Four kinetic models were derived based on adsorption of ethanol, adsorption of propylene, surface reaction, or desorption of EIPE as the rate controlling step (see Appendix C.2.7). Single-site mechanisms (e.g. Eley-Rideal) for this reaction were not considered because the rate expressions derived from these mechanisms collapsed into simple power-law expressions. The concentration of propylene and ethanol in the

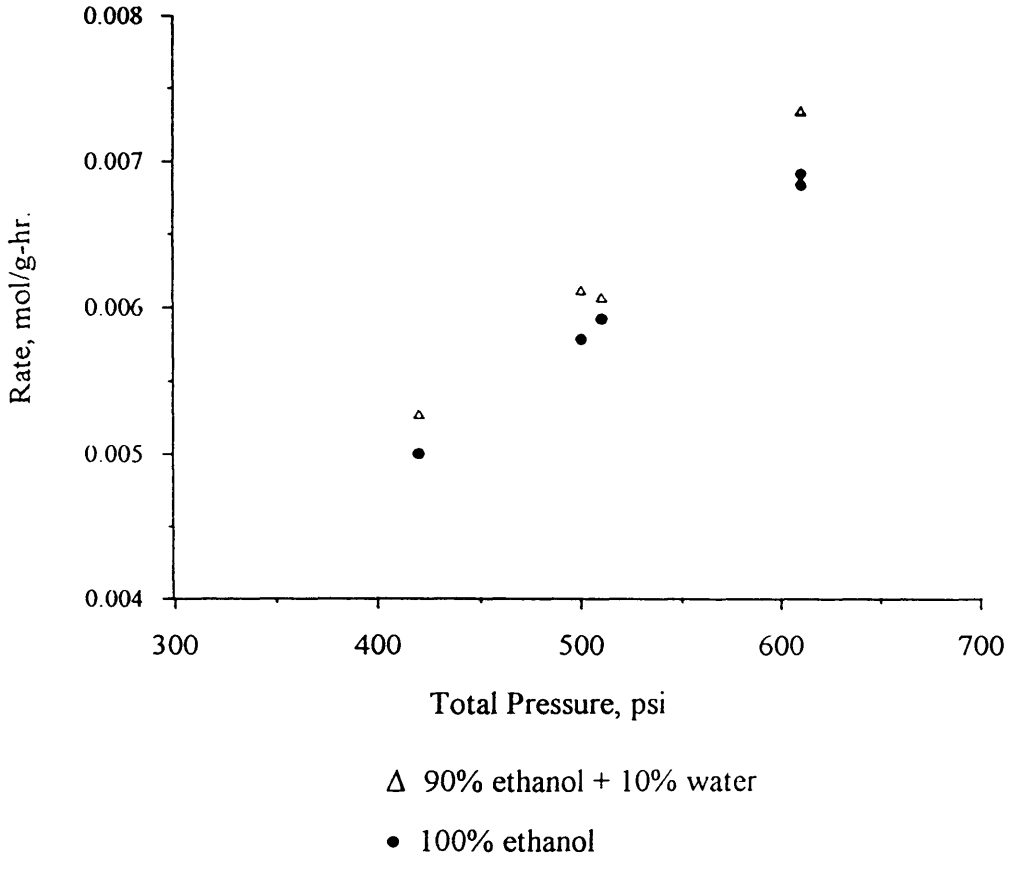

Figure 35. Reaction Rate for 90and 100% Ethanol at 100°C.

proposed expressions are referenced to the surface concentrations ($C_{s,Et}$ and $C_{s,Pr=}$). According to the above discussions, all experiments were run at conditions which minimized internal and external mass transfer and heat transfer limitations (page 59) hence the concentrations of both reactants could be assumed to be equal to the the bulk concentrations ($C_{s,Et} = C_{l,Et}$ and $C_{s,Pr} = C_{l,Pr}$). Propylene concentration was calculated from Henry's Law ($C_{l,Pr} = C_{g,Pr}/H$). Therefore, concentrations for ethanol and propylene in the LHHW rate equations can be expressed in terms of the measured concentrations as:

$$C_{s,Et} = C_{l,Et} \quad \text{and} \quad C_{s,Pr} = C_{g,Pr}/H \text{ where } C_{g,Pr} = P/RT$$

In addition, the experiments were carried out at conditions which produced low conversion, so it could be assumed that the concentration of products was negligible. This assumption agrees well with the high thermodynamic equilibrium constant for this reaction as described in Chapter 4. The kinetic models were then reduced from the reversible forms (left hand side in Table 12) to the irreversible expressions shown in the right hand side of the same table. To identify which kinetic model was the best possible representation for EIPE formation, an evaluation of kinetic parameters was needed.

The most common method for analyzing kinetic parameters for such complex models (Fogler, 1992) is non-linear least squares (NLE). This method searches for the kinetic parameters which minimize the sum of the squared difference betweeen the calculated rate and the observed rate.

An iteration process was then performed. The starting values chosen for the parameters that were to be estimated were extremely important in assuring convergence. In this work, the starting points (kinetic parameters) were all in the range of $1x10^{-3}$ to $1x10^{2}$. The computer program is provided in Appendix E. The results of kinetic parameters were then used to compute the reaction rate and then this calculated rate was

Table 12. Proposed Reaction Rate Expressions for EIPE Formation.

reaction mechanism

Dual site

Model 1 Adsorption of EtOH controlling

$$-r = \frac{C_{*tot}\left(k_{Et}C_{Et} - \frac{k_{Et}^{'}K_E C_E}{KK_{\mathrm{Pr}}C_{\mathrm{Pr}}}\right)}{1 + K_{\mathrm{Pr}}C_{\mathrm{Pr}} + K_E C_E + \frac{K_E C_E}{KK_{\mathrm{Pr}}C_{\mathrm{Pr}}}} \qquad -r^{'} = \frac{k^{'}C_{l,Et}}{1 + \frac{K_{\mathrm{Pr}}}{H}C_{g,\mathrm{Pr}}}$$

where $k^{'} = k_{Et}C_{*tot}$

Model 2 Adsorption of Propylene controlling

$$-r = \frac{C_{*tot}\left(k_{\mathrm{Pr}}C_{\mathrm{Pr}} - \frac{k_{\mathrm{Pr}}^{'}K_E C_E}{KK_{Et}C_{Et}}\right)}{1 + K_{Et}C_{Et} + K_E C_E + \frac{K_E C_E}{KK_{Et}C_{Et}}} \qquad -r^{'} = \frac{k^{'}C_{g,\mathrm{Pr}}}{1 + K_{Et}C_{Et}}$$

where $k^{'} = k_{\mathrm{Pr}}C_{*tot}$

Model 3 Surface rxn. controlling (LHHW)

$$-r = \frac{k_s C_{*tot}\left(K_{Et}K_{\mathrm{Pr}}C_{Et}C_{\mathrm{Pr}} - \frac{K_E}{K}C_E\right)}{\left(1 + K_{\mathrm{Pr}}C_{\mathrm{Pr}} + K_{Et}C_{Et} + K_E C_E\right)^2} \qquad -r^{'} = \frac{k^{'}C_{g,\mathrm{Pr}}C_{l,Et}}{\left(1 + \frac{K_{\mathrm{Pr}}}{H}C_{g,\mathrm{Pr}} + K_{Et}C_{l,Et}\right)^2}$$

where $k^{'} = k_s K_{Et}\frac{K_{\mathrm{Pr}}}{H}C_{*tot}$

continued next page.

Table 12 continued

Model 4 Desorption of EIPE controlling

$$-r = \frac{C_{*tot}\left(k_E K K_{Pr} K_{Et} C_{Pr} C_{Et} - k_E' C_E\right)}{1 + K_{Pr} C_{Pr} + K_{Et} C_{Et} + K_{Pr} K_{Et} K_E C_{Pr} C_{Et}}$$

$$-r' = \frac{k' C_{g,Pr} C_{l,Et}}{1 + \frac{K_{Pr}}{H} C_{g,Pr} + K_{Et} C_{l,Et} + K'' C_{g,Pr} C_{l,Et}}$$

where $k' = k_E K'' C_{*tot}$, $K'' = K_s K_{Pr} K_{Et} / H$

compared to the reaction rate from experimental data. Comparisons between models were made by looking at the multiple R^2 correlation coefficient for goodness of fit. The results for the kinetic parameters, SSE, and R^2 for each temperature and model are presented in Tables 13 to 16.

Decisions between the various models were based upon the requirement that all kinetic, adsorption, and desorption constants had to be positive, and that R^2 values should be close to 1.00. Considering model 1, the values of R^2 were close to zero for every temperature. Therefore, model 1 was eliminated from consideration leaving models 2, 3, and 4 for further study. Comparing three models (2, 3, and 4) based on R^2, models 2 and 3 gave results close to 1.00 while R^2 values for models 4 were in the range of 0.30 to 0.95. Therefore, model 4 was eliminated leaving models 2 and 3 for further study.

Table 13. Kinetic constants for Model 1 Computed from Non-linear Least Squares Method.

Adsorption of EtOH Controlling.

$$-r' = \frac{k' C_{l,Et}}{1 + \frac{K_{Pr}}{H} C_{g,Pr}} \quad \text{where} \quad k' = k_{Et} C_{*tot}$$

T (°C)	kinetic parameter	SSE	R^2
100.00	k′ = 0.00032 $K_{Pr}/H = 10^{-4} - 10^{-7}$	1.0×10^{-4}	0.03
110.18	k′ = 0.00044 $K_{Pr}/H = 10^{-4} - 10^{-7}$	2.2×10^{-4}	3.7×10^{-3}
121.29	k′ = 0.00068 $K_{Pr}/H = 10^{-4} - 10^{-7}$	1.8×10^{-4}	0.02
132.40	k′ = 0.0012 $K_{Pr}/H = 10^{-4} - 10^{-7}$	3.6×10^{-4}	1.04×10^{-3}

Table 14. Kinetic constants for Model 2 Computed from Non-linear Least Squares Method.

Adsorption of Propylene Controlling.

$$-r' = \frac{k' C_{g,\mathrm{Pr}}}{\left(1 + K_{Et} C_{l,Et}\right)} \qquad \text{where } k' = k_{\mathrm{Pr}} C_{*tot}$$

T (°C)	kinetic parameter	SSE	R^2
100.00	k′ = 0.017 K_{Et} = 0.13	2.6×10^{-7}	.97
110.18	k′ = 0.024 K_{Et} = 0.15	2.3×10^{-6}	.88
121.29	k′ = 0.034 K_{Et} = 0.13	2.3×10^{-6}	.85
132.40	k′ = 0.087 K_{Et} = 0.25	1.1×10^{-6}	.85

Table 15. Kinetic constants for Model 3 Computed from Non-linear Least Squares Method.

Surface Reaction Controlling.

$$-r' = \frac{k' C_{g,\mathrm{Pr}} C_{l,Et}}{\left(1+\frac{K_{\mathrm{Pr}}}{H} C_{g,\mathrm{Pr}} + K_{Et} C_{l,Et}\right)^2} \qquad \text{where } k' = k_s K_{Et} \frac{K_{\mathrm{Pr}}}{H} C_{*tot}$$

T (°C)	kinetic parameter	SSE	R^2
100.00	k′ = 0.0076 $K_{Pr}/H = 10^{-4} - 10^{-7}$ K_{Et} = 0.23	2.7×10^{-7}	.97
110.18	k′ = 0.0178 $K_{Pr}/H = 10^{-4} - 10^{-7}$ K_{Et} = 0.34	2.4×10^{-6}	.92
121.29	k′ = 0.0376 $K_{Pr}/H = 10^{-4} - 10^{-7}$ K_{Et} = 0.41	7.1×10^{-7}	.89
132.40	k′ = 0.0970 $K_{Pr}/H = 10^{-4} - 10^{-7}$ K_{Et} = 0.53	3.5×10^{-6}	.81

Table 16. Kinetic Constants for Model 4 Computed from Non-linear Least Squares Method.

Desorption of EIPE Controlling.

$$-r' = \frac{k' C_{g,\mathrm{Pr}} C_{l,Et}}{\left(1+\frac{K_{\mathrm{Pr}}}{H} C_{g,\mathrm{Pr}} + K_{Et} C_{l,Et} + K'' C_{g,\mathrm{Pr}} C_{l,Et}\right)}$$

where $k' = k_E K'' C_{*tot}$, $K'' = K_{\mathrm{Pr}} K_{Et} K / H$

T (°C)	kinetic parameter	SSE	R^2
100.00	k′ = .00085 $K_{Pr}/H = 10^{-4} - 10^{-7}$ K_{Et} = 0.10 K″ = $10^{-4} - 10^{-7}$	3.5×10^{-7}	.96
110.18	k′ = .0011 $K_{Pr}/H = 10^{-4} - 10^{-7}$ K_{Et} = 0.10 K″ = $10^{-4} - 10^{-7}$	3.3×10^{-6}	.30
121.29	k′ = .0023 $K_{Pr}/H = 10^{-4} - 10^{-7}$ K_{Et} = 0.15 K″ = $10^{-4} - 10^{-7}$	1.7×10^{-6}	.95
132.40	k′ = .0044 $K_{Pr}/H = 10^{-4} - 10^{-7}$ K_{Et} = 0.17 K″ = $10^{-4} - 10^{-7}$	5.8×10^{-7}	.27

The difference between models 2 and 3 is that model 3 contains an adsorption term for propylene while model 2 does not. However, since the adsorption equilibrium constant for propylene in model 3 was very small (0.0001), eliminating this term had no effect on the overall fit. The small value of the adsorption equilibrium constant for propylene infers that propylene is not strongly adsorbed on the catalyst surface. The SSE and R^2 given by both models were essentially the same and in the range of 10^{-7}-10^{-6} and 0.80-0.97, respectively. It thus was concluded that both models were adequate to represent the reaction kinetics. For further study, it was decided to use only one of the models (based on the smallest SSE), model 3. A parity plot for model 3 is shown in Figure 36, which further validates the choice.

A confidence test (F-test) was used to compare the results of model 3 and the observed data (Neter et al., 1983). Table 18 shows the confidence level for each temperature in model 3. Values of $F_{observed}$ were within the range of tabulated F values at a 95% confidence interval.

Figure 37 shows the dependence of k′ on temperature. The fit of the Arrhenius law to k` values gives the expression

$$k' = 3.447 \times 10^{11} \exp\left(\frac{-11{,}743}{T}\right) \qquad \text{---------(16)}$$

From these data an apparent activation energy of 97.60 kJ/mol was obtained. The value of E_a' for this reaction is large and also shows high temperature sensitivity for the reaction. In the literature, activation energies of etherification have been reported for the reactions catalyzed by both liquid acids and acidic resins. As shown in Table 19, values E_a' have been reported in the range from 70-80 kJ/mol for MTBE and 70-90 kJ/mol for ETBE. Compared to the apparent activation energy (E_a') for similar etherification

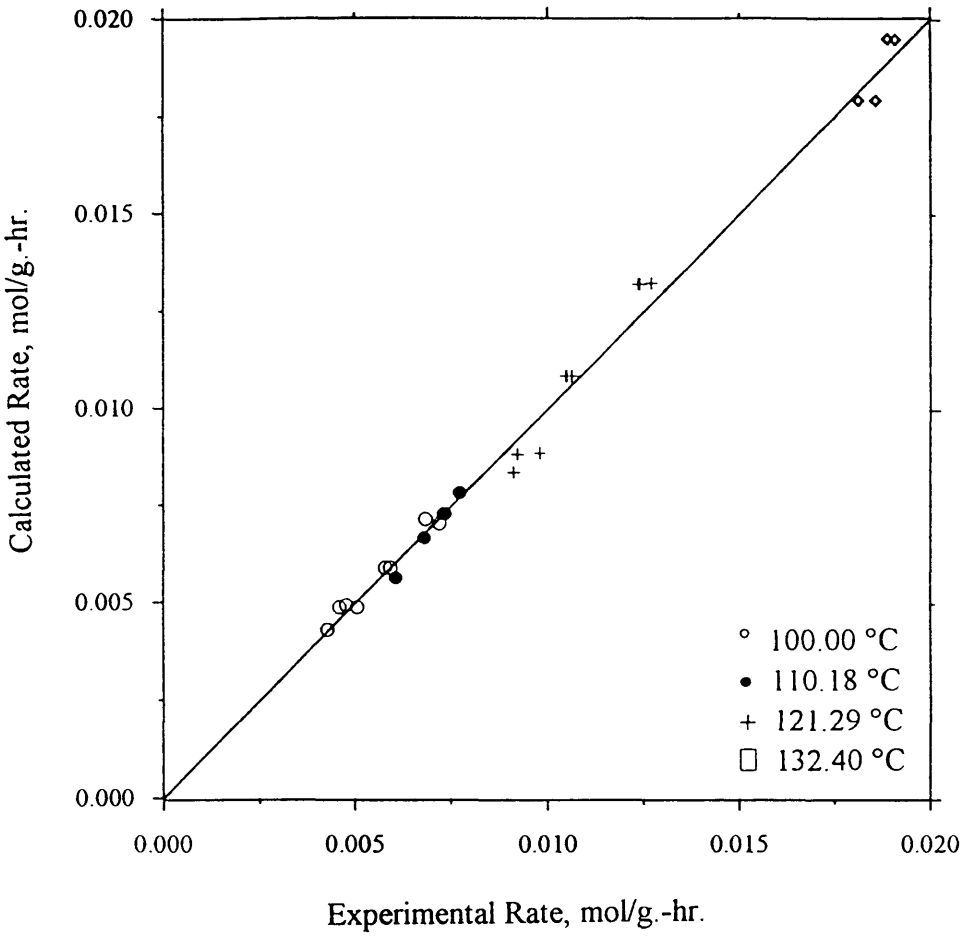

Figure 36. Parity Plot for Model 3 at Different Temperatures.

Table 17. Confidence Interval Test for Model 3.

T (°C)	df	F	% confidence interval
100.00	8	1.011	> 95
110.18	5	1.737	> 95
120.29	8	2.036	> 95
132.40	3	4.644	95

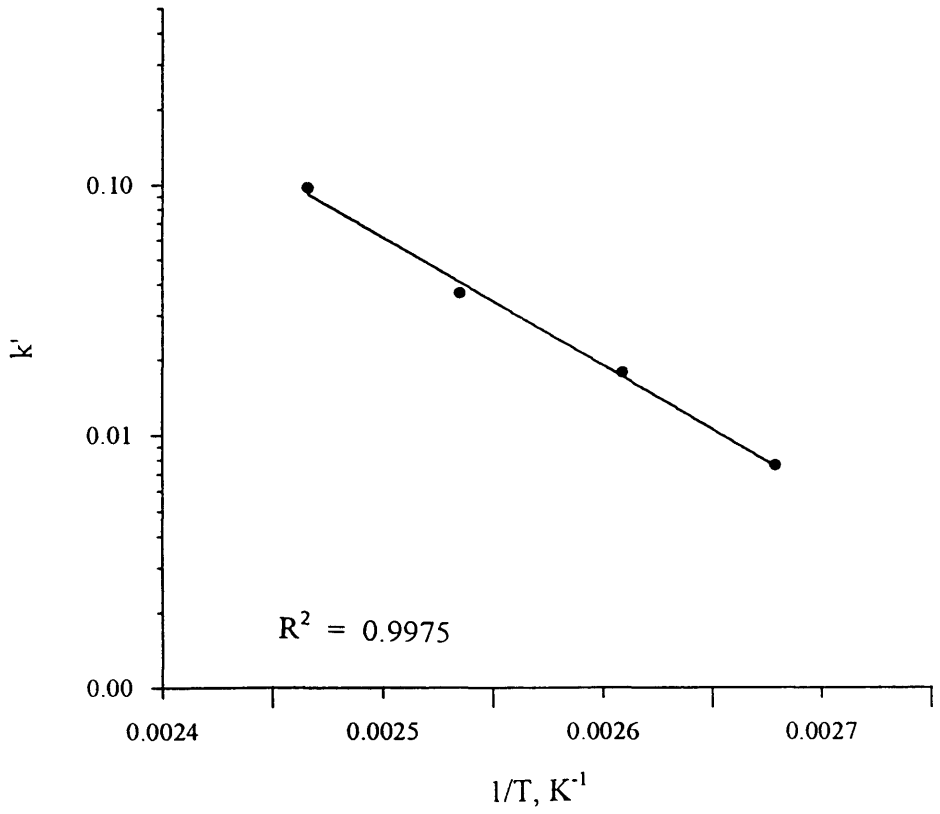

Figure 37. Temperature Dependence of k'.

Table 18. Apparent Activation Energy for EIPE Synthesis and Comparison with Literature Data.

product	reference	catalyst	E_a' (kJ/mol)	observation
EIPE	this work	Dowex HCR-w2	97.6	gas-liquid phase
MIPE	Sonnemans, 1993	H-ZSM-5	113.0	gas phase
MTBE	Ancillotti, 1977	A-15	71.2	liquid phase
	Pien, 1990	H-ZSM-5	71.1	liquid phase
ETBE	Tejero, 1994	K 2631	86.1	liquid phase
	Ancillotti, 1977	A-15	74.0	
	Tejero, 1989	A-15	65.0	gas phase

reactions, E_a' for this study is higher than E_a' for the tertiary ethers (MTBE and ETBE). This difference in activation energy (approximately 20-30 kJ/mol) might due to the effect of the lower stability of secondary relative to tertiary carbonium ions.

In addition, E_a' for MIPE was found to be 113 kJ/mol (Sonnemans, 1993). For a comparison of the formation of MIPE and EIPE, it was found that E_a' for EIPE performed in the gas-liquid phase is lower than that for MIPE performed in the gas phase. The solvation of carbonium ions by the polar ethanol solution stabilizing the intermediate should be taken into account in this comparison.

Power Law Model: The rate expression for the synthesis of EIPE as shown previously (model 3) is complex due to the incorporation of adsorption terms for propylene and ethanol on the catalyst surface. For industrial application (design and scale-up), a simple "power-law" model is often the preferred form for rate expressions. In such a model, it is customary to re-cast the rate expression as a pseudo-homogeneous model in the following manner.

Comparing the adsorption terms in model 3, the adsorption equilibrium constant involving propylene ($K_{Pr} = 10^{-4}$-10^{-7}) was found to be much smaller than that for ethanol at every temperature. For this reason, the adsorption term involving propylene seems to be insignificant; hence this term can be neglected. The LHHW expression can thus be reduced to

$$-r' = \frac{k' C_{g,\mathrm{Pr}} C_{l,Et}}{\left(1+K_{Et} C_{l,Et}\right)^2} \qquad \text{--------(17)}$$

With the assumption that liquid ethanol fully wets the catalyst surface, it can then be assumed that the product of the ethanol concentration and the adsorption equilibrium constant is significantly larger than unity. The rate expression (Equation 17) may now be reduced to

$$-r' = \frac{k' C_{g,\mathrm{Pr}}\, C_{l,Et}}{\left(K_{Et} C_{l,Et}\right)^2} \qquad \text{-------(18)}$$

$$\text{or} \qquad -r' = k'' C_{g,\mathrm{Pr}}^{1} C_{l,Et}^{-1} \qquad \text{where } k'' = k'/K_{Et}^{2} \qquad \text{-----(19)}$$

which shows that the reaction rate is proportional to the concentration of propylene and inversely proportional to the ethanol concentration.

The method of linear least squares analysis was used to evaluate the parameters in this model. Equation 19 was linearized and then regression analysis between (*-r'*) and C_{Pr}/C_{Et} ratio was carried out to solve for k'. Results for k' in terms of an Arrhenius plot are shown in Figure 38. The resulting power law expression can be written as

$$-r' = 2.75x10^{12} \exp\left(\frac{-12,680}{T}\right) \frac{C_{g,Pr}}{K_{Et}^2 C_{l,Et}} \quad \text{------(20)}$$

The apparent activation energy found in the power law expression is not the same as that obtained from the LHHW rate expression; however, the values are very close. As shown in Table 19, it was found that this power law model was an adequate expression compared to those in Table 15 (LHHW expressions) and the F-statistics for all temperatures are all significant at a confidence level of 95% or greater. These findings suggest that the assumptions made in simplifying the LHHW model are reasonable.

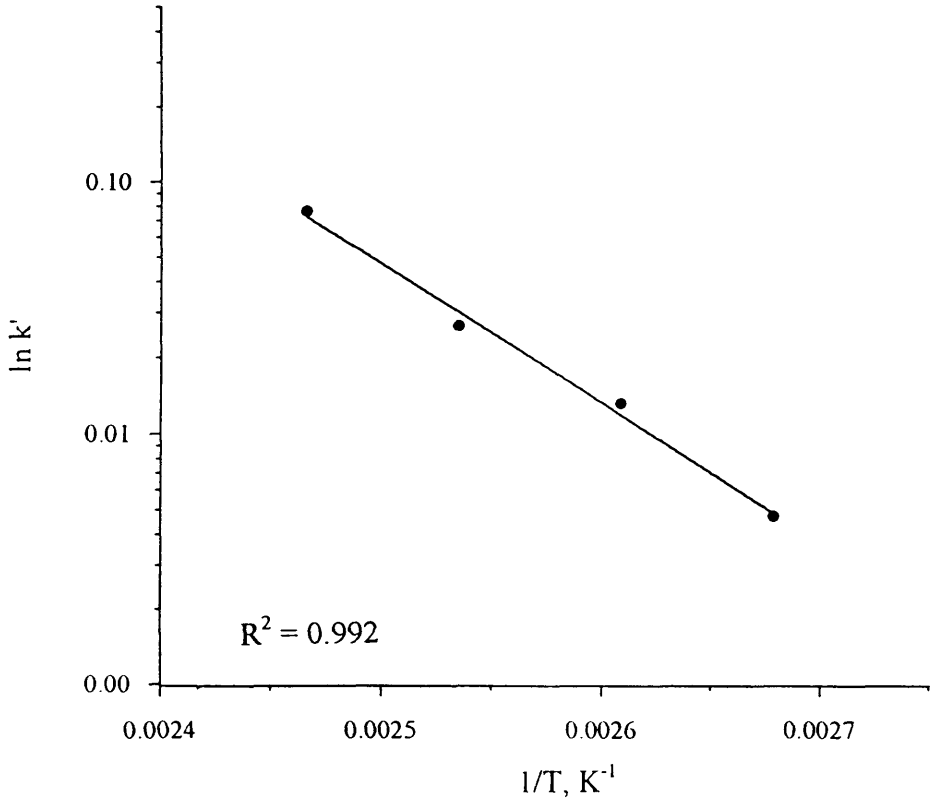

Figure 38. Temperature Dependence of k′ for Power Law Rate Expression.

Table 19. Power Law Model Statistics.

T(C)	df	R^2	SSE	F	% confidence interval
100.00	8	0.97	$3.11x10^{-7}$	1.175	>95
110.18	5	0.93	$3.11x10^{-7}$	2.015	>95
120.29	8	0.91	$2.35x10^{-6}$	2.529	95
132.40	3	0.96	$3.08x10^{-6}$	1.132	95

Kinetic Analysis for DEE: The experimental data show that dehydration of ethanol was the main side reaction for EIPE production. The objective of this part of the study was to derive a rate expression for this side reaction. Ethanol dehydration to DEE has been studied widely during the last century. Most of the previous studies have been carried out in gas phase, and no previous work has been published for the liquid phase reaction in the presence of ion exchange resins. Much of the significant work has been reviewed by Kabel and Johason (1962) and Birk (1985). Kabel proposed a LHHW rate expression for the dehydration of ethanol to DEE over acidic cation exchange resins (Dowex 50) in the gas phase. Assuming the rate-determining step is the surface reaction between two adjacent adsorbed ethanol molecules, the rate expression takes the following form:

$$-r' = \frac{kK_{Et}\left(P_{Et}^2 - P_{DEE}P_w / K_{eq}\right)}{\left(1 + K_{Et}P_{Et} + K_w P_w + K_{DEE}P_{DEE}\right)^2} \qquad \text{------(21)}$$

This reaction was investigated experimentally in the down-flow packed-bed micro-reactor system. When ethanol was passed through the reactor system without catalyst, no conversion of ethanol was detected. When ethanol alone was passed through the acidic resins, only two products were obtained, water, and DEE. This indicated that no side reaction of ethanol dehydration to form ethylene occurred.

To study ethanol dehydration kinetics, pure ethanol was passed through the catalyst in different W/F_{Ao} ratios at three different temperatures. Detailed experimental data for each run are reported in Appendix C.2.5. Conversion levels for these reactions were high. The range of conversions were in the range of 20 to 60%, hence to determine the reaction rate the conversion versus W/F_{Ao} data at constant temperature had to be differentiated. The results of these runs are shown in Figure 39.

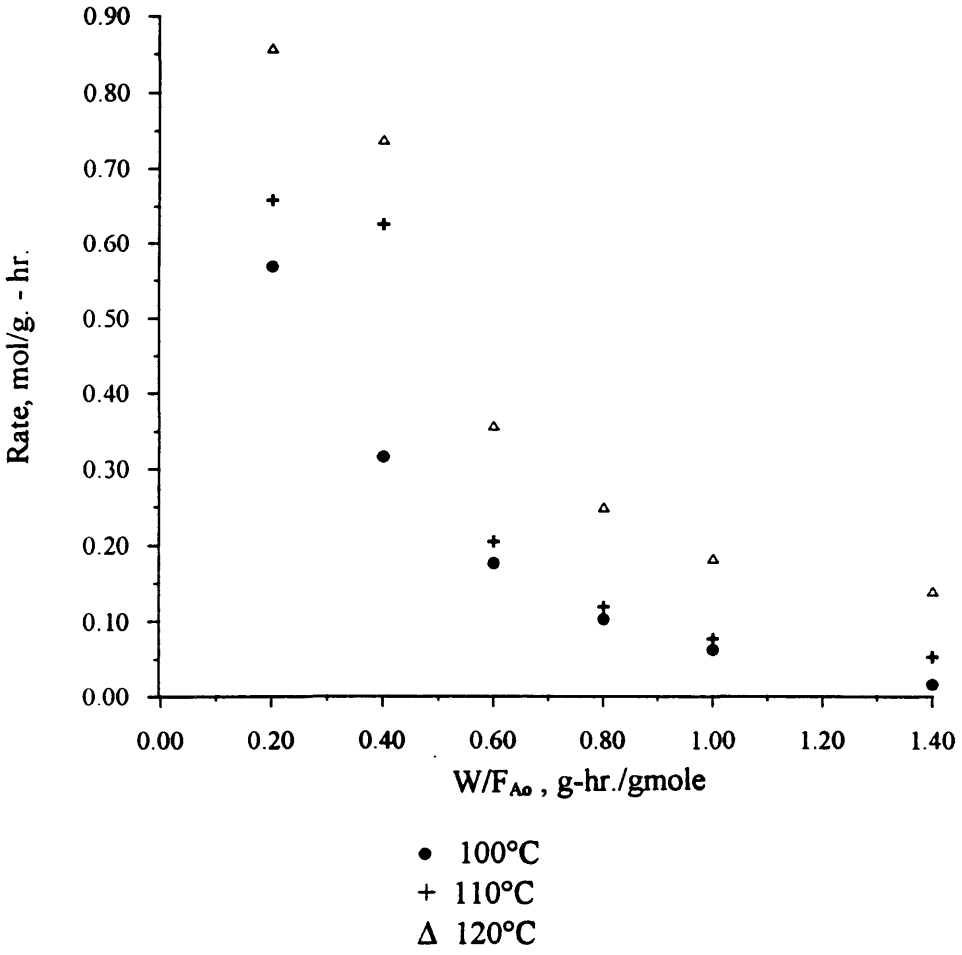

Figure 39. Reaction Rate for EtOH Dehydration to DEE.

Two kinetic models were evaluated for this reaction. Both rate expressions were derived assuming surface reaction was the controlling step. The difference between these two expressions concerns the mechanism for the surface reaction: model 5 is a single-site surface reaction while model 6 assumes a dual-site mechanism.

Model 5

$$-r' = \frac{kK_{Et}\left(C_{Et}^2 - C_{DEE}C_w / K_{eq}\right)}{\left(1 + K_{Et}C_{Et} + K_w C_w\right)} \quad \text{------(22)}$$

Model 6

$$-r' = \frac{kK_{Et}\left(C_{Et}^2 - C_{DEE}C_w / K_{eq}\right)}{\left(1 + K_{Et}C_{Et} + K_w C_w + K_{DEE}C_{DEE}\right)^2} \quad \text{------(23)}$$

Under the conditions utilized for these runs, the thermodynamic equilibriums constants for this reaction which were computed by ASPEN (9.0) were not extremely high. Therefore, the reverse reaction terms could not be eliminated. Kabel (1962) found that the polar ethanol and water molecules are preferentially adsorbed on the ion exchange resin catalyst as compared to the relatively nonpolar DEE and that fraction of unoccupied sites was small. Hence, it was assumed that

$$K_{DEE}\,C_{DEE} << 1 + K_wC_w + K_{Et}C_{Et}$$

leading to the following simplified dual-site model:

$$-r' = \frac{kK_{Et}\left(C_{Et}^2 - C_{DEE}C_w / K_{eq}\right)}{\left(1 + K_{Et}C_{Et} + K_w C_w\right)^2} \quad \text{------(23.2)}$$

Non-linear least squares was used to analyze the kinetic data and to determine parameters for these models. The results of calculated kinetic parameters are shown in Tables 20 and 21. As can be seen, the dual-site model generally was found to be more

Table 20. Kinetic Parameters for Model 5 Computed by Non-linear Least Squares DEE Formation, Surface Reaction Controlling, Single Site.

$$-r' = \frac{kK_{Et}\left(C_{Et}^2 - C_{DEE}C_w / K_{eq}\right)}{\left(1 + K_{Et}C_{Et} + K_w C_w\right)}$$

T (°C)	kinetic parameter	SSE	R^2
100	$k' = 0.017$ $K_{Et} = 0.10$ $K_w = 5$	0.0055	0.955
110	$k' = 0.023$ $K_{Et} = 0.10$ $K_w = 3$	0.0238	0.881
120	$k' = 0.040$ $K_{Et} = 0.4$ $K_w = 1$	0.0373	0.810

Table 21. Kinetic Parameters for Model 6 Computed by Non-linear Least Squares DEE Formation, Surface Reaction Controlling, Dual Site.

$$-r' = \frac{kK_{Et}\left(C_{Et}^2 - C_{DEE}C_w/K_{eq}\right)}{\left(1 + K_{Et}C_{Et} + K_w C_w\right)^2}$$

T (°C)	kinetic parameter	SSE	R^2
100	$k' = 0.082$ $K_{Et} = 0.20$ $K_w = 2.0$	0.0053	0.957
110	$k' = 0.201$ $K_{Et} = 0.20$ $K_w = 2.1$	0.0060	0.981
120	$k' = 0.463$ $K_{Et} = 0.30$ $K_w = 2.0$	0.0075	0.981

adequate with higher R^2 and lower error sum of squares (SSE) values. The k′ values from the dual-site mechanism were used to determine the apparent activation energy for this reaction. The k′ values were plotted as shown in Figure 40. From this line the apparent activation energy for ethanol dehydration to DEE was estimated to be 98.93 kJ/g-mole. Compared to the activation energy of 125.40 kJ/g-mol reported by Kabel (1962) for gas-phase dehydration, the activation energy for this study was lower. It can be expected that the solvation by liquid ethanol might improve the reaction rate by decreasing the activation energy due to stabilization of the oxonium ion intermediate. The kinetic constant k for this reaction can hence be expressed as

$$k' = 6.95x10^{12} \exp\left(\frac{-11{,}900}{T}\right) \text{...-----(24)}$$

A parity plot for this model is presented in Figure 41, which indicates that the expression provides an adequate representation to the observed data.

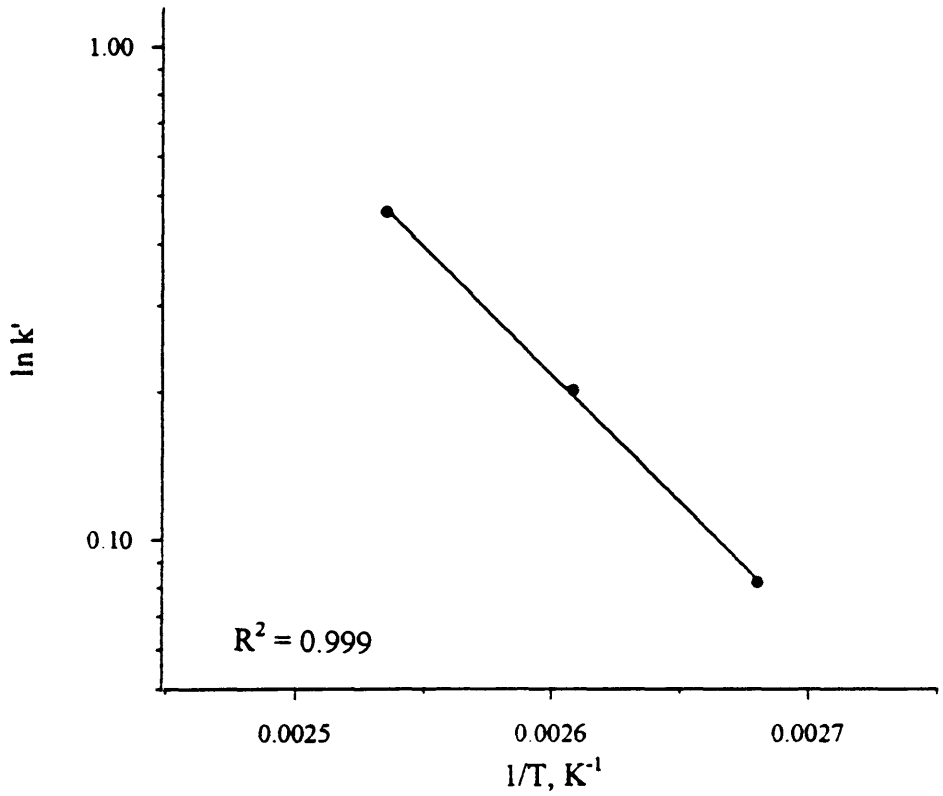

Figure 40. Temperature Dependence of k' for DEE Formation.

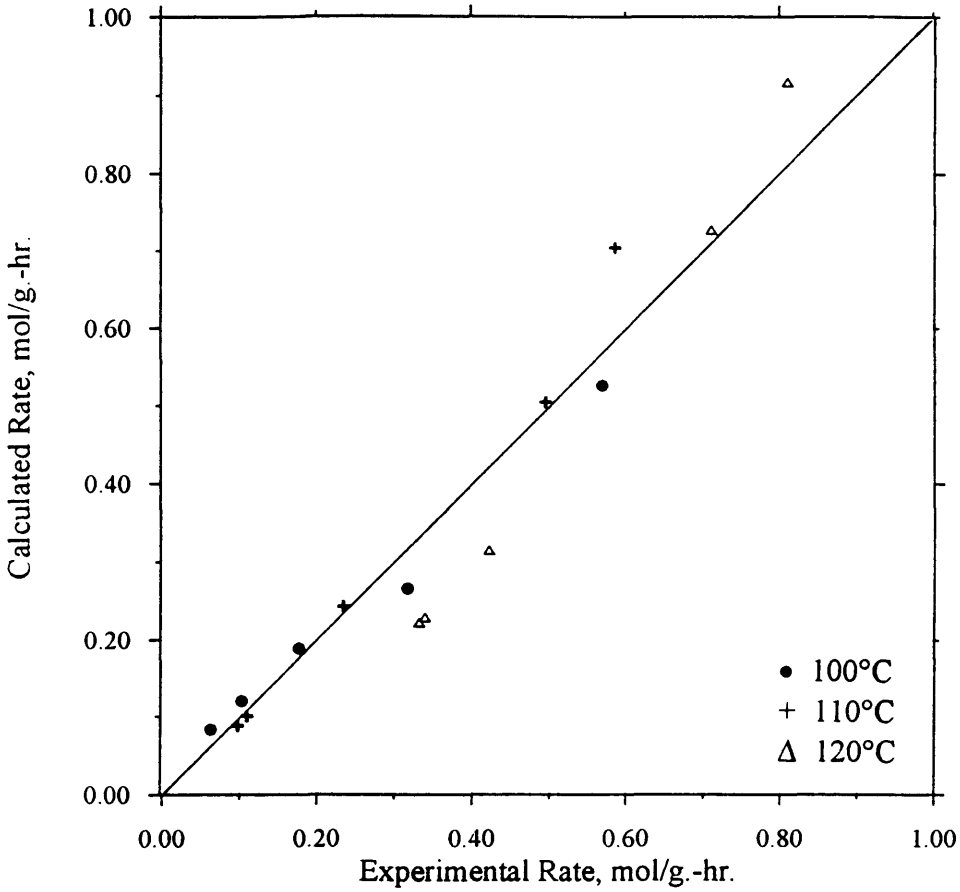

Figure 41. Parity Plot for Model 6: Ethanol Dehydration to DEE.

5.2-6 Modeling of Integral Reactor Experimental Data

The rate expression model for EIPE formation obtained from the differential reactor experimental data has been discussed in detail (sections 5.2-5). In this section, the model will be tested against experimental data from integral reactor experiments in order to confirm the reliability of the model. For this part of the investigation, the simplest rate expression from model 3 (as shown in equation 20) was used. In order to derive an expression in which data could be tested, it was necessary to rearrange the integral reactor design equation into the following form:

$$W = F_{Ao} \int_0^x \frac{dx}{-r_A'} \qquad \text{-------(25)}$$

From experimental conditions of W, F_{Ao}, P, T, this expression can be integrated and the resulting equation used to calculate conversion. The ethanol conversions obtained from this model were plotted against the experimental ethanol conversions as shown in Figure 42.

It was found that, in the low conversion range, conversions obtained from the model were very close to conversions obtained from the experimental apparatus. The differences between experimental and predicted conversions were in the range of ±10%, which indicates agreement within the range covered by experimental error. For the higher conversion tests it was found that ethanol conversions obtained from the experimental apparatus were lower than the predicted ethanol conversion by 10-15%. These discrepancies could be due to two effects concerned with mass transfer and thermodynamic equilibrium.

According to model 3 as Equation 26 which was derived from the full model as Equation 27, it shows that ethanol conversions were predicted with only the part of forward reaction rate;

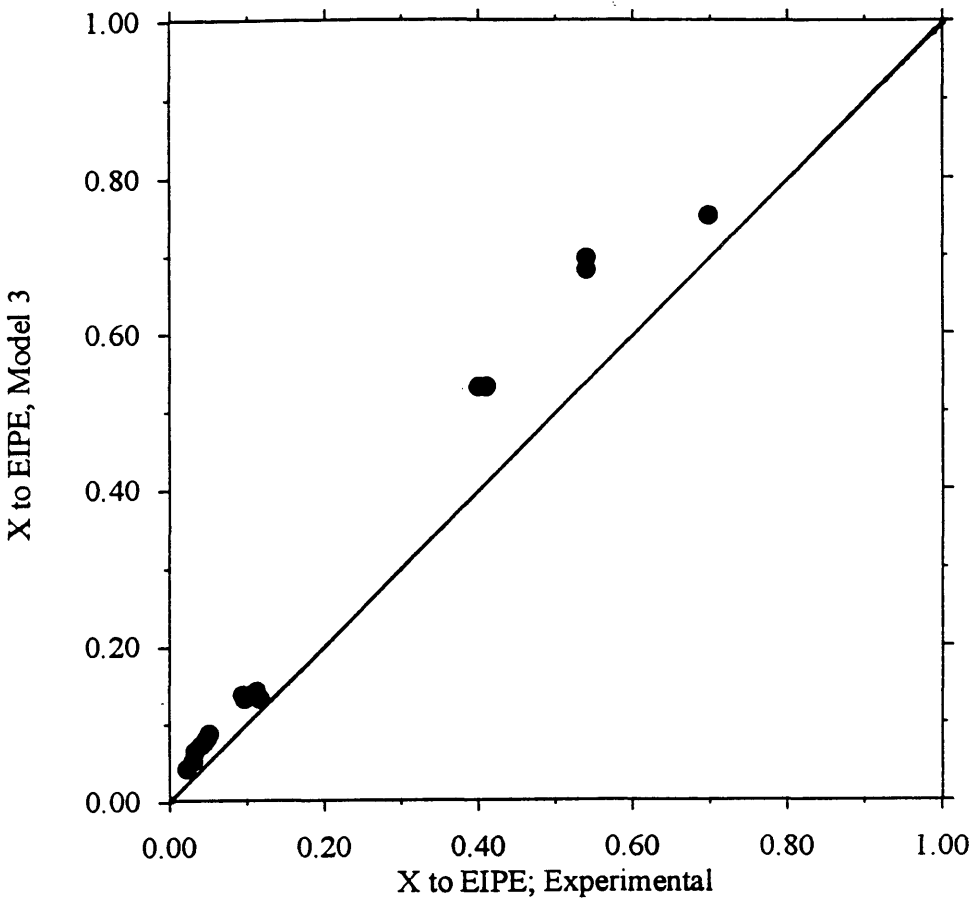

Figure 42. Experimental Conversion Against Computed Conversion Obtained from Model 3.

$$-r = \frac{k' C_{g,\mathrm{Pr}} C_{l,Et}}{\left(1 + \frac{K_{\mathrm{Pr}}}{H} C_{g,\mathrm{Pr}} + K_{Et} C_{l,Et}\right)^2} \quad \text{----(26)}$$

$$-r = \frac{k_s C_{*tot}\left(K_{\mathrm{Pr}} K_{Et} C_{Et} C_{\mathrm{Pr}} - \frac{K_E}{K} C_E\right)}{\left(1 + K_{\mathrm{Pr}} C_{\mathrm{Pr}} + K_{Et} C_{Et} + K_E C_E\right)^2} \quad \text{---(27)}$$

However, at high conversion or the reaction was close to thermodynamic equilibrium limitation, EIPE concentration increase which then decrease the reaction rate by driving the reaction back which could make ethanol conversion lower than what the model predicts. In addition, mass transfer effect could decrease the surface concentration of ethanol and propylene and the reaction rate, afterwards. Therefore, the model then overpredicts the ethanol conversions.

5.2-7. Selectivity Consideration.

The previous sections (5.2-5) were concerned with determination of rate expressions for EIPE and DEE formation. With these rate expressions in hand, it is possible to investigate qualitatively those conditions that would maximize the yield of EIPE with respect to DEE. The parameter which was used for this purpose was the rate selectivity parameter, S_{xy}., which is the ratio of the rate of formation of desired product X to the undesired product Y. For this study, X refers to EIPE and Y refers to DEE.

The rate selectivity parameter can be determined from model 3 divided by rate model 6:

$$S_{xy} = \frac{k_{EIPE} C_{g,\mathrm{Pr}} C_{l,Et}}{\left(1 + K_{Et} C_{l,Et}\right)^2} \frac{\left(1 + K_{Et} C_{Et} + K_w C_w\right)^2}{k_{DEE}\left(C_{Et}^2 - C_w C_{DEE} / K_{eq}\right)} \quad \text{---(28)}$$

The rate selectivity parameter shown above is complicated and from this expression it is difficult to draw exact conclusions regarding appropriate conditions for maximizing the yield of EIPE. The above expression can however be used to suggest conditions under which selectivity improvement might be achieved by considering two parameters (C_{Pr}, C_{DEE}). Increasing the concentration of propylene (C_{Pr}) will serve to maximize selectivity, thus leading to the necessity of operating at high pressures as has been previously suggested. Similarly, keeping the concentration of diethylether (C_{DEE}) as high as possible will also increase the selectivity. This effect can be achieved by recycling by-product DEE to the reactor.

To investigate this possibility, an experiment was carried out under simulated recycle conditions by feeding a mixture of ethanol and DEE to the reactor. Mixtures of DEE and ethanol in ratio of 0.5 and 1.0 (mole basis) were used. The selectivity results were then compared to the results obtained from feeding pure ethanol as shown in Figure 43.

By increasing the ratio of DEE to ethanol in the feed, the selectivity to EIPE was found to be increased at both temperatures investigated (100 and 110°C). Runs using feed compositions in the range of DEE:EtOH up to 1.00 (mole basis) were effective in increasing the selectivity by about 10-20%. The experiment was run at a higher ratio of DEE to ethanol (1.5 on a molar basis), however difficulties were encountered in pumping the mixture since it had a tendency to vaporize in the pump head which caused cavitation.

5.2-8 Catalyst Deactivation

From the preliminary catalyst screening studies described above (section 5.2-4), significant deactivation of catalyst could not be seen, possibly because the experiment were performed over a fairly short period of time (40 hours). In this portion of the study, the same method was used to evaluate deactivation for the Dowex resin with a much

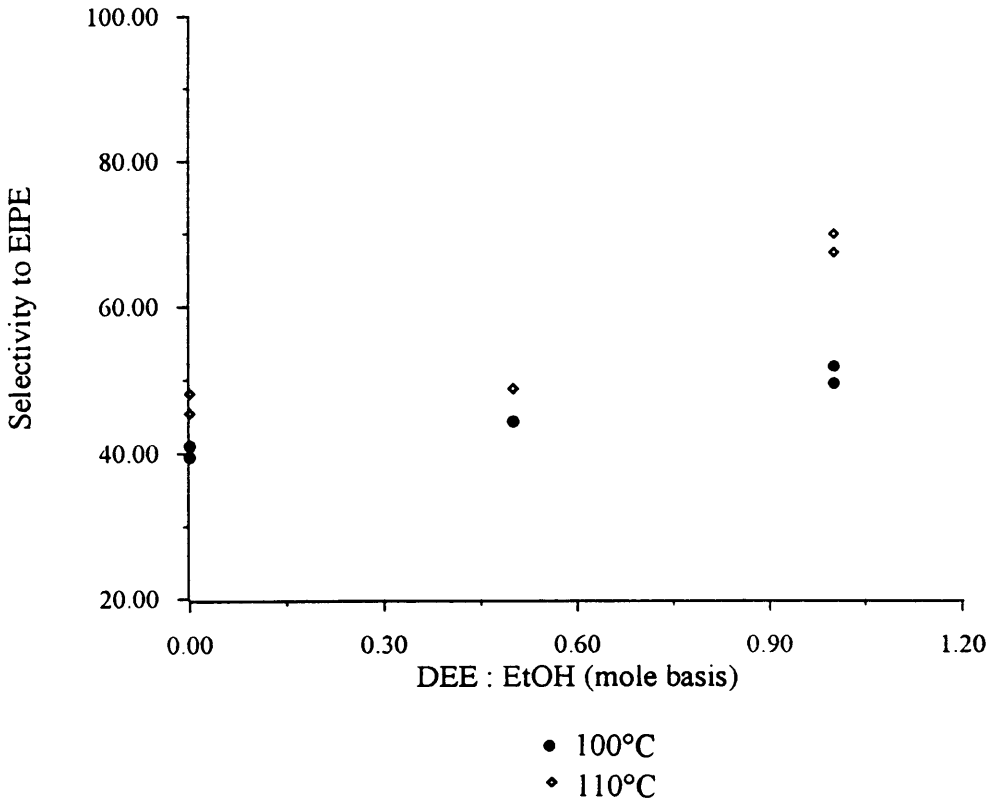

Figure 43. Selectivity for Different Ratios of DEE to Ethanol.

longer test period. The results for conversion and selectivity before and after tests were compared along with the physical evidence obtained by total carbon analysis and the ion exchange capacity.

The reactor vessel was loaded with 2.00 grams of catalyst, 40-70 mesh size, and the deactivation test was carried out at a pressure of 500 psi and a WHSV (based on ethanol) of 0.8 hr^{-1} . Testing at 100°C proceeded for 15 hours, followed by an increase to 140°C with a hold for 100 hours before a temperature decrease to back to 100°C as shown in Figure 44(a). Conversion and selectivity results are shown in Figure 44(b). As can be seen, conversion and selectivity at 100°C both decreased after running at the maximum allowable temperature (140°C) for 100 hours. Conversion decreased by 20% (from 10% to 8%) while selectivity decreased from 60% to 50%. The resin after testing appeared darker than was observed during the catalyst screening runs suggesting carbon or polymer buildup. Catalyst after testing was tested for ion exchange capacity and total carbon analysis using the same procedures discussed previously in section 5.2-4. The results in Table 22 show that the ion exchange capacity decreased about 10% while the total carbon increased by about 4%. These data indicate that periodic replacement or regeneration of the resin may be necessitated due to deactivation by either carbon deposition and/or loss of ion exchange capacity.

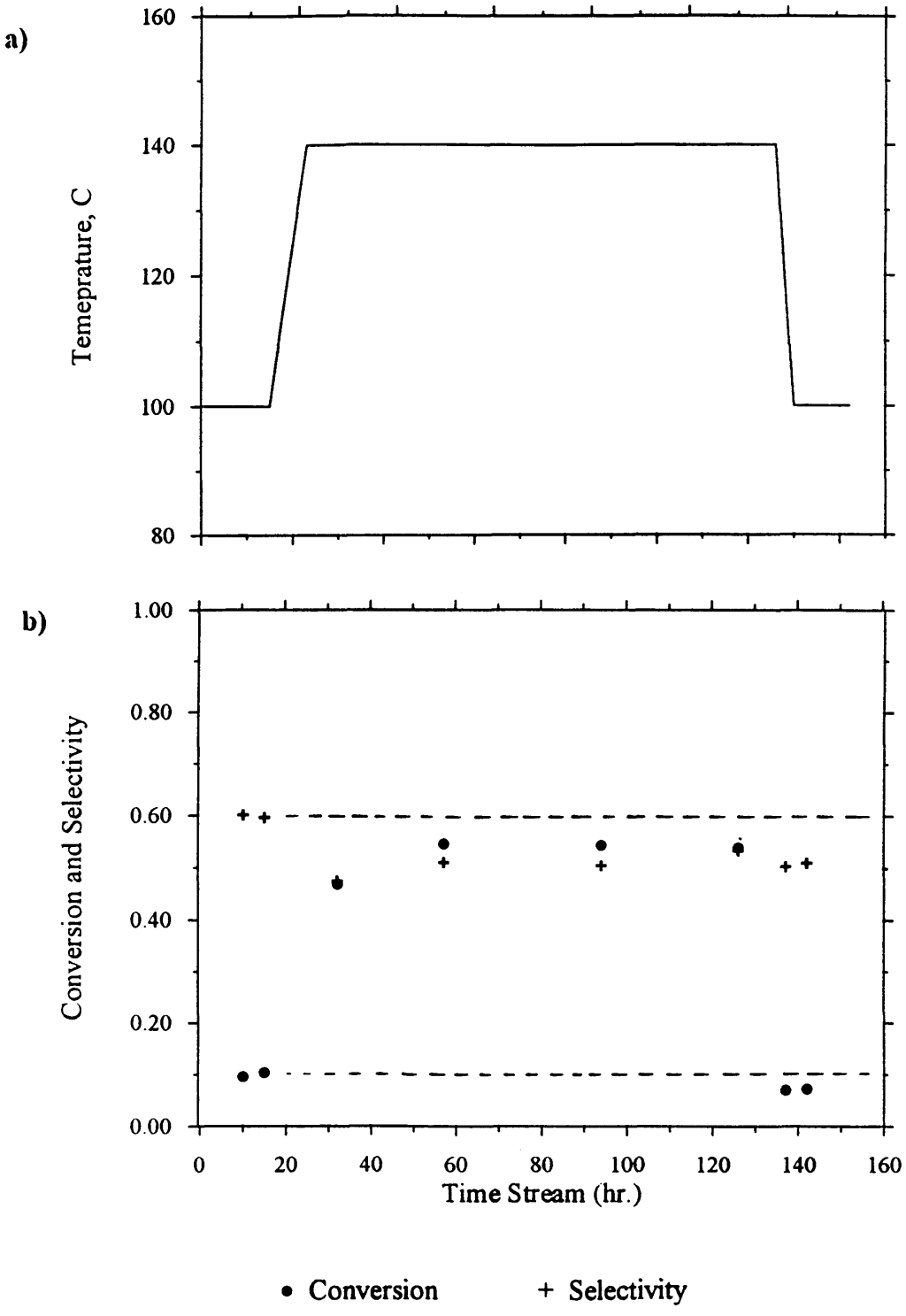

Figure 44. Catalyst Deactivation Test. a) Temperature Sequence b) Conversion and Selectivity.

Table 22. Ion Exchange Capacity and Total Carbon Analysis.

Test	
Ion Exchange Capacity; meq/g.	Fresh = 5.08 Used* = 4.55
Total Carbon Analysis; %C	Fresh = 40.63 Used* = 43.68

Note: *: after 150 hours reaction time.

Chapter 6
CONCLUSIONS AND RECOMMENDATIONS

6.1 Conclusions.

The mixed phase addition of ethanol to propylene to synthesize ethyl isopropyl ether (EIPE) was studied over acid ion exchange resin catalysts at the conditions where ethanol was in the liquid phase and propylene was in the gas phase. The study was divided into two phases: 1) batch reactor investigation and; 2) continuous flow micro-reactor studies. The batch reactor was used to investigate the feasibility of the formation of EIPE and for screening of reaction process conditions, while the continuous flow reactor was used to study the kinetics of the reaction. In a batch reactor using an initial pressure of 1000 psi at temperature 125°C, 1.5:1.0 propylene/ethanol mole ratio, and 1:1 catalyst/ethanol loading, the feasibility of EIPE production was demonstrated with an ethanol conversion of over 80% with an EIPE selectivity of 85%. The major reaction by-product was found to be diethylether (DEE).

For the continuous flow system, a trickle-bed downflow reactor was used. The kinetic study was performed at conditions of WHSV greater than 0.2 hr^{-1} (based on ethanol flow rate) and with a catalyst of 40-70 mesh size mixed with a diluent of inert quartz chips. Rate effects due to internal and external mass transfer diffusional limitations and heat transfer effects were shown to be insignificant both analytically and experimentally. Effects on the reactor due to the presence of axial dispersion were also found to be negligible.

The formation of EIPE was investigated over four catalysts. The commercially available ion exchange resins Dowex HCR-w2 and Amberlyst-15 were found to give

similar results for selectivity to EIPE, but the activity of Dowex was considerably higher due to the higher allowable maximum operating temperature for this material. Supported FCSA gave a better conversion than the ion exchange resins, but lower selectivity. An experimental catalyst containing P/Al 0.8 was found to not give good conversion and selectivity results for this reaction. Investigation of the kinetics of EIPE synthesis was then carried out over Dowex catalyst.

The kinetic studies were carried out at 100-130°C and 300-650 psi. Rate data showed that the reaction was highly temperature sensitive and propylene had an enhancing effect on the rate whereas ethanol had an inhibiting effect. Four rate expressions based on a LHHW mechanism were analyzed by non-linear least squares: 1) adsorption of propylene as the rate-limiting step; 2) adsorption of ethanol as a rate-limiting step; 3) dual-site surface reaction as a rate-limiting step; 4) desorption of EIPE as a rate-limiting step. Fitting differential reaction rate data to each of these four models indicated that both the surface reaction and adsorption of propylene models gave adequate representations to the observed data. The LHHW rate expression when surface reaction was the rate-limiting step was also reduced to a power law expression, resulting in a rate law which was first order with respect to propylene concentration and minus one order with respect to ethanol concentration. The apparent activation energies using pseudo-homogenous and heterogeneous models were found to be 105.42 kJ/mol and 97.60 kJ/mol respectively.

The production of DEE was also studied since it was a major by-product. This study was carried out over the same catalyst, and in the liquid phase. Two LHHW rate expressions were derived and tested for this reaction: 1) single-site, surface reaction as the rate-limiting step and; 2) dual-site, surface reaction as the rate limiting step. The apparent activation energy was determined to be 98.94 kJ/mol. The rate selectivity parameter suggested that keeping propylene and DEE concentrations high increased the selectivity.

It was shown experimentally that a molar feed ratio of DEE:ethanol of 1.0 increased the selectivity for EIPE by 10-20%.

Finally, the Dowex catalyst was tested for the formation of EIPE continuously for 100 hours at the maximum allowable temperature for the catalyst, 140°C. Temperature sequence tests, total carbon analysis, and ion exchange capacity were used to characterize the catalyst before and after the run. A 4% wt. total carbon in the catalyst increase caused a modest decrease in both activity and selectivity. The increase in total carbon was expected from coke or polymer formation which reduced the resin capacity for ion exchange.

Using the conclusions above, the results of this thesis can be used for industrial application as follows:

1. The reaction has been shown to have a moderate activation energy, similar to the published value for MTBE. The rate expression models developed in this study can be used to scale-up the process.
2. The reaction rate is somewhat slow compared to MTBE process, therefore using Dowex HCR-w2 as the catalyst could be effective in speeding the reaction rate due to the higher maximum operating temperature for this material.
3. From the selectivity comparison (section 5.2-7), it was shown that the selectivity of the reaction for EIPE could be improved simply by the recycling DEE to the reactor feed stream. Figure 45 shows a simple schematic for EIPE synthesis which incorporates a separation unit to recover EIPE and return DEE to the reactor.

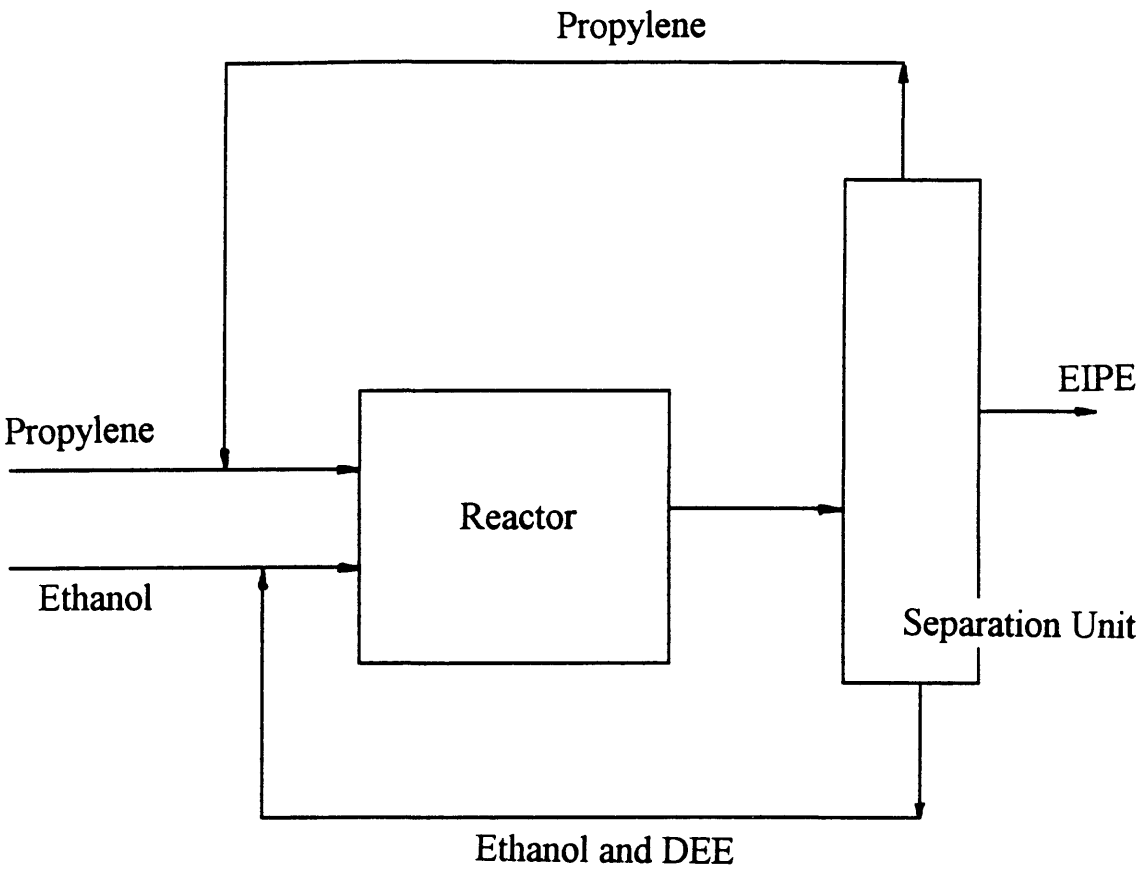

Figure 45. A Schematic Diagram for EIPE Process Development.

6.2 Recommendations.

Finding new octane additives to reduce air pollution caused by car exhausts will be a main research objective for the gasoline industry in future years. This research project is both practical and meaningful in finding viable solutions to this problem. Recommendations for the further research on this project are:

1. Since the thermodynamic calculations in this work were based on group contribution theory, thermodynamic studies from practical laboratory experiments should be carried out.
2. The model from this work was found to fit differential experimental data very well but fell somewhat far from the integral experimental data. In order to make the model universal (corresponding to the conditions in an industrial packed-bed reactor), it will be interesting to study this reaction in an integral reactor with subsequent analysis.
3. Data analysis indicated that the adsorption equilibrium constant for propylene was very small compared to that of ethanol. This result needs to be verified by laboratory chemisorption studies.
4. Study of EIPE over catalysts effective for MTBE and ETBE production like ZSM-5 should be conducted since ZSM-5 has small pore opening which may improve the selectivity.
5. Deactivation effects, such as coking and chemical poisoning during the reaction should be studied in more detail.
6. According to the thermodynamic calculations, both conversion and selectivity to EIPE are very high at lower temperatures and moderate pressures at which ethanol and propylene both behave as liquids. Therefore, liquid phase synthesis kinetics should be studied more extensively.

REFERENCES CITED

Ancillotti, F., Mauri, M..M., and Perscarollo, E. 1977. Ion Exchange Resin Catalyzed Addition of Alcohols to Olefins. J. Catal. 46: 49-57.

Baldwin, R.M., and Cowley, S. 1994. Personel Communication with Author. June 7.

Bell, W.K. 1989. Ether Synthesis with Zeolite Beta. EP.App. 0 309 177 A1.

Bell, W.K. 1987. Production of Ethers from Linear Olefins. EP.App. 0 213 844 A2.

Bennett, G.M. and Phillip, W.G. 1928. The Influence of Structure on the Solubilities of Ether Part I Aliphatic Ethers. J.Chem. Soc. : 1930.

Birk, R.H. Thomas, W.J. and Yue, P.L. 1985. Effect of Mass Transport and Catalyst Deactivation on the Kinetics of Ethanol Dehydration on Zeolite 13X. Chem.Eng.Res.Des. 63 (9) : 338-344.

Brockwell, H.L., Sarathy, P.R. and Trotta, R. 1991. Synthesize Ethers. Hydrocarbon Processing 70 (9): 133-141.

Chang, C.D. and Morgan, N.J. 1980. Hydration of Olefins Using Zeolite Catalyst. US Patent 4 214 107.

Chang, E.J. and Leiby, S.M. 1992. Ethers Help Gasoline Quality. Hydrocarbon Processing 71 (2): 41-44.

Chang, K-H., Kim, G-J.,and Ahh, W-S. 1992. Methyl tert-Butyl Ether Synthesis over Titanium-Silicate I Catalyst. Ind.Eng.Chem.Res. 31: 125-130.

Chu, P. Kuehl, G.H., and Hill, C. 1986. Process for the Preparation of Alkyl Tert-Alkyl Ethers. US Patent 4 605 787.

Chu, P. and Kuehl, G.H. 1987. Preparation of Methyl tert-Butyl Ether (MTBE) over Zeolite Catalyst. Ind.Eng.Chem.Res. 26: 365-369.

Cowley, S. 1995. Personel Communication with Author. August 14.

Davis, B.C. 1992. Adventures in Clean Air Act Amendments Implementation. Hydrocarbon Processing 71 (5): 91-94.

Datta, R. and Zhang, T. 1995. Integral Analysis of Methyl Tert-Butyl Ether Synthesis Kinetics. Ind.Eng.Chem.Res. 34: 730-740.

Dorfner, K. 1972. Ion Exchange Properties and Application. Ann Arbor Science. New York: 66.

_____. Product Data Catalysts Dow Type 1 Superacid Catalyst. Dow Chemical manual 1994.

Dunn, L. 1993. HP Impact: Isobutylene Leads C4 Hydrocarbon Growth. Hydrocarbon Processing 72 (1): 33.

Eokhoff, S. 1993. 10th International Symposium on Alcohol Fuels "The Road to Commercialization". Colorado Spring. (November 7-10).

Evans, T.W. and Edlund, K.R. 1936. Tertiary Alkyl Ethers-Preparation and Properties. Ind.Eng.Chem. 28 (10): 1186-88.

Fogler, H.S. 1992. Elements of Chemical Reaction Engineering 2nd Edition. Prentice Hall International Series. New Jersey. : 209-212.

Francis, A.W. and Woodbury. 1937. Method of Making Ethers. US Patent. 2 077 042.

Froment, G.F. and Bischoff, K.B. 1990. Chemical Reactor Analysis and Design 2nd edition. John Wiley & Son. New York. : 99.

Gates, B.C. and Rodriguez, W. 1973. General and Specific Acid Catalysis in Sulfonic Acid Resin. J.Cata. 31 : 27-31.

Goto, S. Matoug, M. and Tagawa, T. 1993. Liquid-Phase Synthesis of MTBE on Heterogeneous Heteropoly Acid Catalyst. J.Chem. Eng. Japan. 26 (3) : 254-258

Graboski, M.S. 1994. Personel Communication with Author. February 7.

Hammett, L.P. and Deyrup, A.J. 1932. A Series of Simple Basic Indicator I. Acidity Functions of Sulfuric and Perchloric Acids. J.Am Chem Soc. 54 (7): 2721-2739.

Hart's 21st Century Fuels. 1994. Methanol Watch. :14 (8): 20.

Hiestand, J.H. 1961. Hydration of Propylene with a Cation Exchange Resin Catalyst. PhD Dissertation University of Michigan.

Hoffman, U. , Rehfinger, A. 1990. Kinetics of Methyl Tertiary Ether Synthesis Catalyzed by Ion Exchange Resin-I Intrinsic Rate Expression in Liquid Phase Activities. Chem.Eng.Science. 45 (6):1605-1617.

Huang et al. 1989. Process for the Production of Ether and Alcohol. U.S.Patent 4 857 664.

Huang, Sorenson, T.J.H., and Mitchel, C.Jr. 1989. Production of Ethers from Light Olefins and Aqueous Alcohols. EP.Patenet App.EP 323 138.

Huffman, E. W. D, Jr. 1977. Performance of a New Automatic Carbon Dioxide Coulometer. Microchemical Journal. 22: 567-573.

Gray, C.L.,Jr. and alson, J.A. 1989. The Case of Methanol. Scientific American. 5:108-114.

Iborra, M. Izquierdo, J.F., Tejero, J., and Cunill, F. 1988. Getting the Lead out with Ethyl Tert-Butyl Ether. ChemTech (2): 120-122.

Iborra, M. Izquierdo, J.F. Cunill, F. and Tejero, J. 1992. Application of the Response Surface Methodology to the Kinetic Study of the Gas-Phase Addition of Ethanol to Isobutene on a Sulfonated Styrene-Divinylbenzene Resin. Ind.Eng.Chem.Res. 31 : 1840-1848.

Imaizumi, M. 1980. Process for Continuously Producing Diisopropyl Ether. US Patent 4 182 914.

Josephson, J. 1992. Biofuel Development. Environ Sci Tech. 26 (4): 660-663.

Kabel, R. L. and Johason, L. N. 1962. Reaction Kinetics and Adsorption Equilibria in the Vapor-Phase Dehydration of Ethanol. AIChE Journal. 8 (5): 621-624.

Kirk-Othmer. 1980. Ether. Encyclopedia of Chemical Technology 3rd Edition. John Willey&Sons. New York. 9: 381-392.

Kunin, R. 1958. Ion Exchange Resins. John Wiley&Son, Inc. New York. : 78 -79.

Lien, A. P. 1946. Etherification Process. U.S.Patent 2 299 126.

Maholland, M.K. 1987. Synthesis, Characterization and Activity Evaluation of Phosphate-Modified Hydroprocessing Catalysts for Benzofuran Hydrodeoxgenation. Ph.D Desertation. Colorado School of Mines.

Mears, D.E. 1971. Tests for Transport Limitations in Experimental Catalytic Reactors. Ind. Eng. Chem. Process Des. Develop. 10 (4): 541.

Monfils, J.L., Barendregt, S, Kapur, S.K., and Woerde, H.M. 1992 Upgrade Isobutane to Isobutylene. Hydrocarbon Processing. 71 (2): 47-50.

Neir, W. and Woellner, J. 1972. Use Cation Catalyst for IPA. Hydrocarbon Processing. 51: 113-116.

Ng, K.M. and Chu, C.F. 1987. Trickle-Bed Reactors. Chem. Eng. Progress. (11) : 55-63.

Norris, J.F. and Rigby, G.W. 1932. The Reactivity of Atom and Group in Organic Compounds. XII The Preparation and Properties of Mixed Aliphatic Ethers with Special Reference to Those Containing the Tert-Butyl Radical. J.Am.Chem.Soc. 54: 2088-2100.

Otoma, Y.H., Arai, H. and Ukihashi. 1969. Bull. Chem.Soc.Jap. 42: 2449.

Perry, J. A. 1981 Introduction to Analytical GC: History, Principles and Practice. Marcel Deckker, Inc. New York. : 341-345.

Piccoli, R.L. and Lovisi, H.R. 1995. Kinetic and Thermodynamic Study of the Liquid-Phase Etherification of Isoamylenes with Methanol. Ind.Eng.Chem.Res. 34 : 510-515.

Pien, S.I. and Hatcher, W.J. 1990. Synthesis of Methyl Tert-Butyl Ether on HZSM-5 Zeolite. Chem.Eng.Comm. 93: 257-265.

Reed, D. 1994. Methanol Dangers are Cited as U.S. Indicates Increase; Pipeline Spills at School. Fuels for the Future News. May 16.

Reid, R.C., Prausnitz, J.M. and Poling, B.E. 1987. The Properties of Gases and Liquids. 4th Edition. McGraw-Hill, Co.New York : 95-150.

Rys, P. and Steinegger, W.J. 1979. Acidity Function and Solid-Bound Acid. J. Am. Chem. Soc. : 4801-4806.

Saterfield, C.N. 1970. Mass Transfer in Heterogeneous Catalysis. M.I.T.Press Cambridge. : 41.

Saterfield, C.N. 1975. Trickle -Bed Reactors. AIChE Journal. 21(2) : 209-228.

Seddon, D. 1992. Reformulated Gasoline, Opportunities for New Catalyst Technology. Catalysis Today. 15 : 1-21.

Selwittz et al.. 1981. Novel Etherification Process. U.S.patent. 4 262 145.

Shelley, S. and Fouhy, K. 1994. The Drive for Cleaner-Burning Fuel. Chem Eng. : 61-63.

Shuterman, D. 1993. Methanol Toxicity. American Family Physician. 47 : 163-171.

Sonnemans, M.H.W. 1993. Hydration and Etherification of Propene over H-ZSM-5 1. A Kinetic Study. Ind.Eng.Chem.Res. 32: 2506-2511.

Smith, J.M. and Herskowitz, M. 1983. Trickle-Bed Reactors: A Review. AIChE Journal. 29 (1) : 1-17.

Smith, J.M. 1985. Chemical Engineering Kinetics 3rd Edition. McGrawHill. New York. : 434.

Szabo, J. and Perrotey, J. 1991. Isomerization of n-Butenes into Isobutene over Fluorinated Aluminas: Influence of Experimental Conditions upon Selectivity. J of Molecular Catalysis. 67 : 79-90.

Tau, L-M. and Davis, B.H. 1989. Acid Catalyzed Formation of Ethyl TertiaryButyl Ether (ETBE). Applied Catalysis. 53 (2-3) : 263-271.

Tejero, J. Fite, C. Iborra, M. Izquierdo, J.F. and Cunill, F. 1994. Kinetics of the Liquid-Phase Synthesis of ETBE. Ind.Eng.Chem.Res. 33 : 581-591

Unzelman, G.H. 1991. U.S. Clean Air Act Expands Role for Oxygenates. OGJ. April 15 : 44-48.

Waller, F.J. and Scoyoc, R.W.V. 1987. Catalysis with Nafion. ChemTech. (7): 438-441.

Ward, J.W. (editor). 1988. Catalysis 1987. Elsevier Science Publisher. : 483-489.

Weaver, J.D. Tasset, E.L., and Fry, W.E. 1992. Supported Fluorocarbonsulfonic Acid Catalysts. Catalysis Today. 14 : 195-210.

Wyman, C.E. 1993. An Overview of Ethanol Production for Transportation Fuels. 1st Biomass Conference. : 1010-1024.

Xu, X., Zheng, Y. and Zheng, G. 1995. Kinetics and Effectiveness of Catalyst for Synthesis of Methyl tert-Butyl Ether in Catalytic Distillation. Ind.Eng.Chem.Res. 34 : 2232-2236.

Yaws, C.L. 1992. Thermodynamic and Physical Property Data. Gulf Publishing Comp. Houston. : 18, 35, 128, 145.

APPENDIX A
EIPE PHYSICAL AND THERMODYNAMIC PROPERTIES

A.1 Critical properties, T_c and P_c

The calculation of EIPE critical properties was estimated by modified Joback method (Reid et al., 1987)

	Δ_T	Δ_P
(3) -CH3	0.0141	-0.0012
(1) >CH2-	0.189	-
(1) -O- non ring	0.0168	0.0015
(1) >CH-	0.0164	0.002
Σ	0.0944	-0.0001

$T_c = T_b [0.584 + 0.965 \Sigma\Delta_T - (\Sigma\Delta_T)^2]^{-1}$

$= 491.08$ K

$P_c = (0.113 + 0.0032 n_A - \Sigma\Delta_P)^{-2}$

where n_A (number atoms) = 18

$= 34.3$ bar

A.2 EIPE Thermodynamic Properties

The group contribution which is used to estimate its ideal-gas properties is the method of Joback (Reid et al., 1987) as shown below.

	H_f	G_f	C_{pa}	C_{pb}	C_{pc}	C_{pd}
(3) - CH_3	-76.45	-43.96	19.500	-0.00808	0.000153	-9.67e-8
(1) >CH_2	-20.64	8.42	-0.909	0.09500	-5.44e-5	1.19e-8
(1) -O- nonring	29.89	58.36	-23.000	0.20400	-0.000265	1.20e-7
(1) >CH-	-132.22	-105.00	25.500	-0.06320	0.000111	-5.48e-8
summation	-352.32	-170.10	60.091	0.21156	0.000251	-2.13e-7
correction factor	68.29	53.88	-37.930	0.21000	-0.000391	2.06e-7
	-284.03	-116.22	22.161	0.42156	-0.00014	-7.00e-9

$\Delta H_{f,298}$ = -284.03 kJ/mol (-283.8 kJ/mol , Spartan Software)

$\Delta G_{f,298}$ = -116.22 kJ/mol

$\Delta C^{o}_{p,298}$ = 22.161 + 0.42156 T - 0.00014 T^2 - 7.0x10^{-9} T^3 J/mol-K

To find the heat and Gibbs of formation for the liquid phase, the heat and entropy of vaporization need to be determined using an equation proposed by Kobayashi (1972)

$$\frac{\Delta H_v}{RT_c} = 7.08\,(1-T_r)^{0.354} + 10.95\omega\,(1-T_r)^{0.456}$$

at T = 298.15 K or Tr = 0.607

$$\omega = \frac{3}{7}\frac{T_{br}}{1-T_{br}}\log(P_c - 1) = 0.312$$

$H_{f,298\,(l)} = H_{f,298\,(g)} + \Delta H_v$

$\Delta S_v = \Delta H_v / T$

hence, $H_{f,298\,(l)} = -315.71$ kJ/mole and $G_{f,298\,(l)} = -128.849$ kJ/mole

$Cp\,(T) = 162.04 - 0.17341\,T + 0.000738\,T^2$ J/mole-K (MTBE property)

A.3 Data for computing the equilibrium constant (Yaws, 1993).

	state	$H_{f,298}$ kJ/mole	$G_{f,298}$ kJ/mole	C_{pA}	C_{pB}	C_{pC}	C_{pD}
C_3H_6	*g*	20.43	62.76	3.71	0.234	-1.2e-4	2.2e-8
H_2O	*g*	-242.00	-228.80	32.24	1.9e-3	1.1e-5	-3.6e-9
	l	-285.832	-234.976	75.6	-	-	-
EtOH	*g*	-235.00	-168.40	9.014	0.214	-8.4e-5	1.4e-9
	l	-276.302	-171.097	100.92	-0.111	-5e-4	-
DEE	*g*	-252.40	-122.4	21.42	0.336	-1e-5	-9.4e-9
	l	-277.283	-120.837	152.25	-0.184	8.6e-4	-
IPA	*g*	-272.60	-173.50	32.43	0.189	6.4e-5	-9.3e-8
	l	-317.031	-180.094	146.16	-0.193	0.007	-
DIPE	*g*	-319.00	-122.00	7.505	0.585	-3e-4	5.8e-8
	l	-351.163	-128.686	183.45	-0.250	9.4e-4	-

where $Cp = Cpvap\ A + (Cpvap\ B)T + (Cpvap\ C)T^2 + (Cpvap\ D)T^3$; J/mol-K

A.4 Estimation of Rvp of EIPE

Since there are RVP data available for EIPE, it is necessary to use group contribution to estimate the value.

Vapor pressure of EIPE at 100°F by the Gomez-Thodos method.

T_b = 327.15 K (for experimental data)

and T = 100°F (311.11 K)

$T_{br} = T_b/T_c = 0.666$

$T_r = T/T_c = 0.633$

$$h = T_{br}\left(\frac{\ln(P_c / 1.01325}{1 - T_{br}}\right) = 7.03$$

M (molecular weight) = 88.15

$m = 0.0052\ M^{0.29}\ T_c^{\ 0.72} = 1.651$

$$\gamma = \frac{2.464}{M} \exp(9.8 \times 10^{-6}\ M\ T_c) = 0.0427$$

$$a = \frac{1 - 1/T_{br}}{T_{br}^7 - 1} = 0.532$$

$$b = \frac{1 - 1/T_{br}^m}{T_{br}^7 - 1} = 1.0145$$

$$\beta = \frac{\gamma}{b} - \frac{ah}{b} = -3.645$$

$$\ln P_{vpr} = \beta\left[\frac{1}{T_r^m} - 1\right] + \gamma\left[T_r^m - 1\right]$$ This equation will be used to estimate the vapor pressure for EIPE.

In case of determining the RVP

$\ln P_{vpr} = -4.14$

P_v = 0.546 bar

= 7.90 psi <==== estimated RVP for EIPE

APPENDIX B
EQUILIBRIUM CONSTANT, CONVERSION CALCULATIONS AND PROPYLENE-ETHANOL PHASE DIAGRAMS

B.1 Equilibrium Constant for EIPE Formation

Ethanol(g) + Propylene(g) <=====> EIPE (g)

Data	H, kJ/mole	G,kJ/mole	J/ mole-K			
			Cp,a	Cp,b	Cp,c	Cp,d
Ethanol	-235	-168.4	9.014	0.2141	-8.4E-05	1.37E-09
Propylene	20.43	62.76	3.71	0.2345	-0.00012	2.2E-08
EIPE	-284.03	-116.22	-37.93	0.42156	-0.00014	-7E-09

Hf,rxn	**Gf,rxn**	**Ka,298**	**Delta Cp**			
-69.46	-10.58	71.5438	-50.654	-0.02704	6.39E-05	-3E-08

T, K	**Integral Cp**	**Del Cp**	**H,T**	**K2/K1**	*Ka, T*
298.15	-15799.805		**kj/mole**		*71.5438*
313.15	-16607.041	-807.2358	-70.26724	0.257217	*18.40229*
323.15	-17144.708	-1344.902	-70.8049	0.109722	*7.849916*
333.15	-17681.9	-1882.095	-71.34209	0.048624	*3.478759*
343.15	-18218.55	-2418.745	-71.87875	0.022312	*1.596285*
353.15	-18754.592	-2954.787	-72.41479	0.01057	*0.75622*
363.15	-19289.962	-3490.156	-72.95016	0.005156	*0.368896*
373.15	-19824.595	-4024.79	-73.48479	0.002584	*0.18487*
383.15	-20358.433	-4558.628	-74.01863	0.001328	*0.09498*
393.15	-20891.417	-5091.611	-74.55161	0.000698	*0.049933*

NOTE: *Italic* represents the results.

B.2 Equilibrium Constant for DEE Formation

2 Ethanol(g) <=====> DEE (g) + H2O (g)

Data	H, kJ/mole	G,kJ/mole	J/ mole-K			
			Cp,a	Cp,b	Cp,c	Cp,d
Ethanol	-235	-168.4	9.014	0.2141	-8.4E-05	1.37E-09
water	-242	-228.8	32.24	0.001924	1.1E-05	-3.6E-09
DEE	-252.4	-122.4	21.42	0.3359	-1E-05	-9.4E-09

Hf,rxn	**Gf,rxn**	**Ka,298**	**Delta Cp**			
-24.4	-14.4	334.3345	35.632	-0.090376	0.000169	-1.6E-08

T, K	Integral Cp	Del Cp	H,T	K2/K1	*Ka, T*
298.15	8066.9262		kJ/mole		*334.632*
313.15	8416.89829	349.9721	-24.05003	0.628299	*210.0619*
323.15	8651.48757	584.5614	-23.81544	0.475554	*158.994*
333.15	8887.45542	820.5292	-23.57947	0.368119	*123.0748*
343.15	9125.10845	1058.182	-23.34182	0.290875	*97.24953*
353.15	9364.75231	1297.826	-23.10217	0.234223	*78.30883*
363.15	9606.69171	1539.766	-22.86023	0.191919	*64.16519*
373.15	9851.23041	1784.304	-22.6157	0.159811	*53.43041*
383.15	10098.6712	2031.745	-22.36825	0.135082	*45.16241*
393.15	10349.316	2282.39	-22.11761	0.115782	*38.70979*

NOTE: *Italic* represents the result.

B.3 Equilibrium Constant for IPA Formation

H2O(g) + Propylene(g) <=====> IPA (g)

Data	H, kJ/mole	G,kJ/mole	J/ mole-K			
			Cp,a	Cp,b	Cp,c	Cp,d
Water	-242	-228.8	32.24	0.001924	1.1E-05	-3.6E-09
Propylene	20.43	62.76	3.71	0.2345	-0.00012	2.2E-08
IPA	-272.6	-173.5	32.43	0.1885	6.4E-05	-9.3E-08

Hf,rxn	**Gf,rxn**	**Ka,298**	**Delta Cp**			
-51.03	-7.46	20.30795	-3.52	-0.047924	0.000173	-1.1E-07

T, K	Integral Cp	Del Cp	H,T	K2/K1	*Ka, T*
298.15	-1871.2513		kJ/mole		*20.30795*
313.15	-1949.0354	-77.78416	-51.10778	0.37247	*7.564093*
323.15	-1997.4646	-126.2133	-51.15621	0.202589	*4.11417*
333.15	-2042.9956	-171.7443	-51.20174	0.114173	*2.318616*
343.15	-2085.5018	-214.2506	-51.24425	0.066471	*1.349881*
353.15	-2124.8633	-253.6121	-51.28361	0.039872	*0.809714*
363.15	-2160.9667	-289.7155	-51.31972	0.024584	*0.499245*
373.15	-2193.7055	-322.4542	-51.35245	0.015548	*0.315742*
383.15	-2222.9796	-351.7284	-51.38173	0.010067	*0.204443*
393.15	-2248.6959	-377.4447	-51.40744	0.006663	*0.135302*

NOTE: *Italic* represents the results.

B.4 Equilibrium Constant for DIPE Formation

2 IPA(g) <=====> DIPE (g) + H2O (g)

Data	H, kJ/mole	G,kJ/mole	J/ mole-K			
			Cp,a	Cp,b	Cp,c	Cp,d
IPA	-272.6	-173.5	32.43	0.1885	6.4E-05	-9.3E-08
water	-242	-228.8	32.24	0.001924	1.1E-05	-3.6E-09
DIPE	-319	-122	7.505	0.5849	-0.0003	5.8E-08

Hf,rxn	**Gf,rxn**	**Ka,298**	**Delta Cp**			
-15.8	-3.8	4.635572	-25.115	0.209824	-0.000417	2.4E-07

T, K	Integral Cp	Del Cp	H,T	K2/K1	*Ka, T*
298.15	-1371.1346		**kJ/mole**		***4.6356***
313.15	-1267.3113	103.8234	-15.69618	0.73837	*3.422766*
323.15	-1195.5909	175.5437	-15.62446	0.614076	*2.846595*
333.15	-1122.3065	248.8282	-15.55117	0.51732	*2.398076*
343.15	-1047.8186	323.316	-15.47668	0.440974	*2.044167*
353.15	-972.47361	398.661	-15.40134	0.379976	*1.761406*
363.15	-896.60327	474.5314	-15.32547	0.330677	*1.532876*
373.15	-820.525	550.6096	-15.24939	0.290406	*1.346198*
383.15	-744.54178	626.5929	-15.17341	0.257184	*1.192194*
393.15	-668.94217	702.1925	-15.09781	0.229523	*1.063971*

NOTE: *Italic* represents the results.

B.2 Equilibrium Conversion Calculation for Competing Reactions, EIPE and DEE.

$$EtOH + \text{Pr}opylene \xleftrightarrow{K_1} EIPE \qquad \delta = -1$$

$$2\,EtOH \xleftrightarrow{K_2} DEE + H_2O \qquad \delta = 0$$

Species	Symbol	Initially	Change	Remaining
EtOH	A	F_{Ao}	$-F_{Ao}X_1 - F_{Ao}X_2$	$F_{Ao}(1-X_1-X_2)$
Propylene	B	F_{Bo}	$-F_{Bo}X_1$	$F_{Bo}(1-X_1)$
EIPE	C	0	$F_{Bo}X_1$	$F_{Bo}X_1$
DEE	D	0	$F_{Ao}X_1/2$	$F_{Ao}X_1/2$
H_2O	E	0	$F_{Ao}X_1/2$	$F_{Ao}X_1/2$

where X_1 , X_2 are ethanol conversions with respect to EIPE and DEE formation

ν (reactor volume) = ν_o (1 - 0.5 X_1)

Let : C_{Ao} = 1 mole/liter

Molar ratio of A to B = 1

Assuming that all components behave as ideal gas and as ideal solution, the activities of each species then are expressed as concentration. Therefore, the equilibrium expressions become

$$\frac{X_1(1-0.5X_1)}{(1-X_1-X_2)(1-X_1)} = K_1$$

$$\frac{(X_2/2)^2}{(1-X_1-X_2)^2} = K_2$$

where K_1 and K_2 are equilibrium constants for the above reactions. These values refer to the results from ASPEN (9.0), which are shown in Figure 12, 14. To solve equations

simultaneously, mathematical software (Mathematica) was used. One example of the calculation using Mathematica is shown below:

Given: 330 K 1 atm.

K_1 for EIPE formation = 273.822

K_2 for DEE formation = 165.699

In[1]:=

```
Solve [ {(x1*(1-0.5*x1))/((1-x1-x2)*(1-x1))==273.822 ,
         (x2/2)/(1-x1-x2) == 165.699^0.5}, {x1,x2}]
```

Out[1]=

```
{{x2 -> -0.207715, x1 -> 1.21578},
  {x2 -> 0.207715, x1 -> 0.784217}}
```

B.6 Propylene-Ethanol Phase Equilibrium.

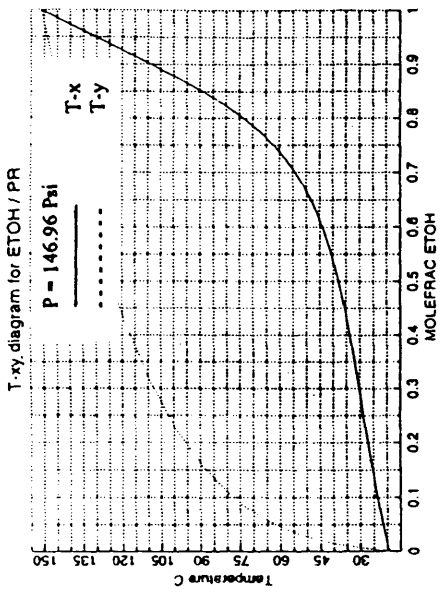

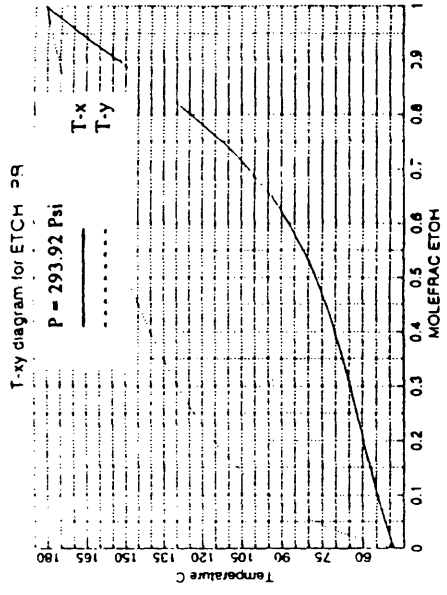

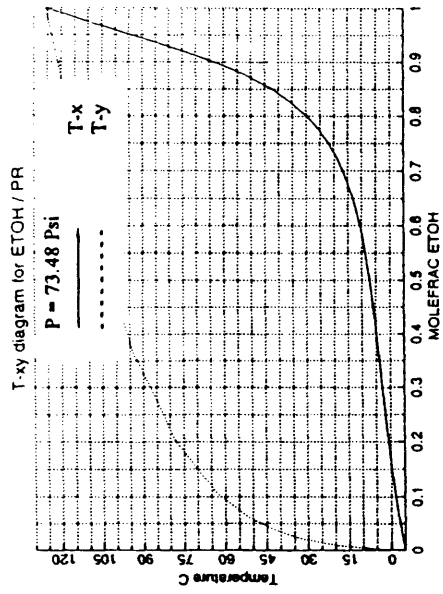

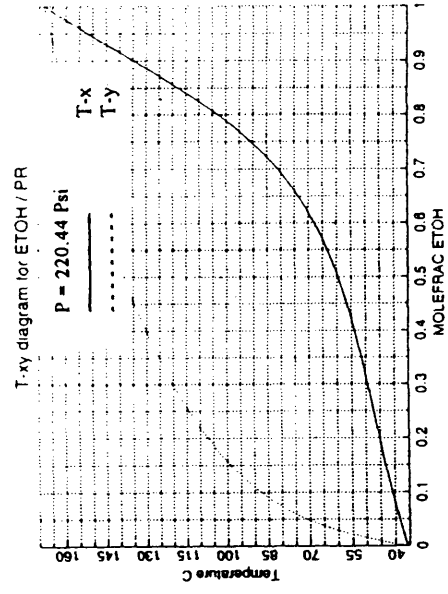

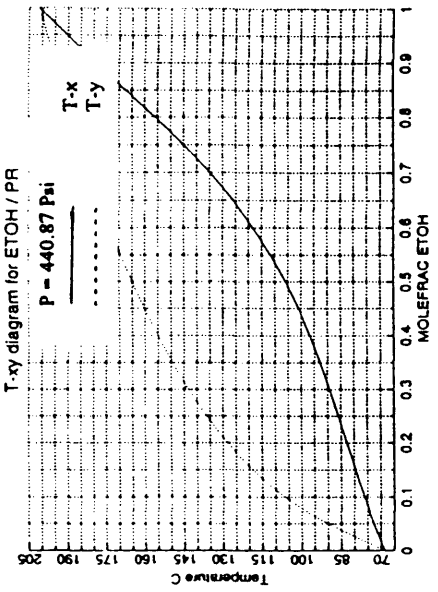
T-xy diagram for ETOH / PR
P = 440.87 Psi
T-x
T-y
Temperature C
MOLEFRAC ETOH

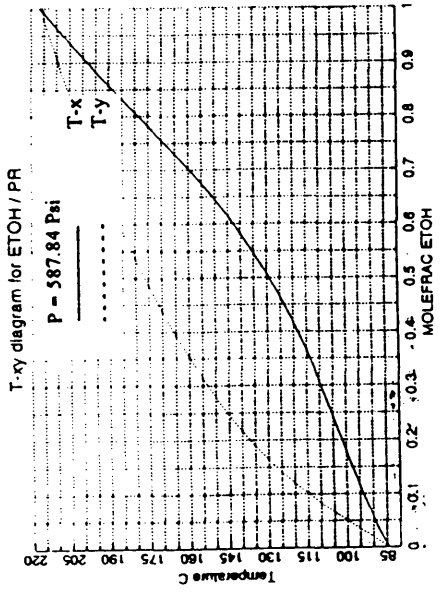
T-xy diagram for ETOH / PR
P = 587.84 Psi
T-x
T-y
Temperature C
MOLEFRAC ETOH

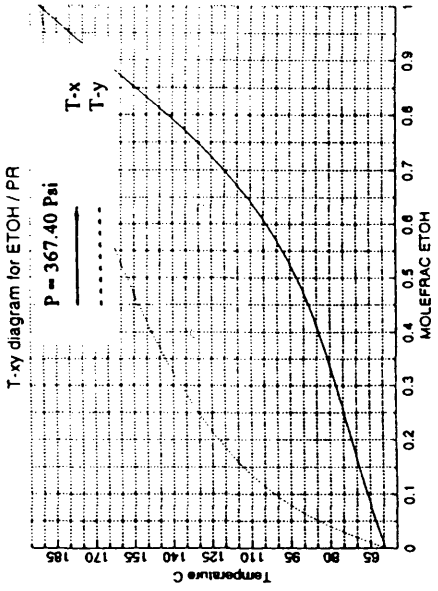
T-xy diagram for ETOH / PR
P = 367.40 Psi
T-x
T-y
Temperature C
MOLEFRAC ETOH

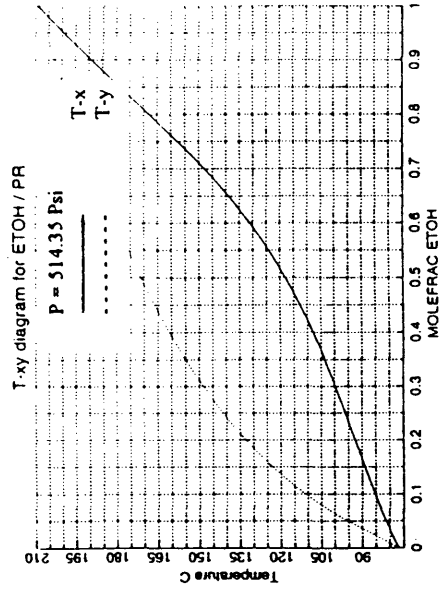
T-xy diagram for ETOH / PR
P = 514.35 Psi
T-x
T-y
Temperature C
MOLEFRAC ETOH

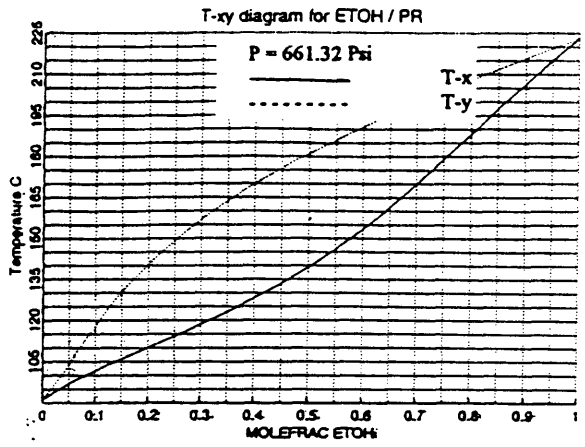
T-xy diagram for ETOH / PR
P = 661.32 Psi
T-x
T-y
Temperature C
MOLEFRAC ETOH

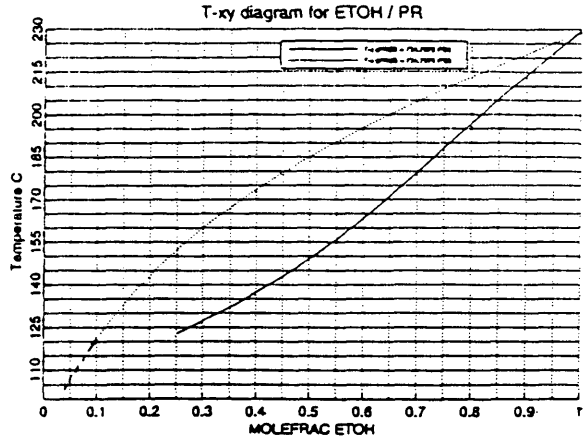
T-xy diagram for ETOH / PR
Temperature C
MOLEFRAC ETOH

APPENDIX C
GC CALIBRATION AND INDIVIDUAL RUNS

C.1 GC Relative Response Factors

The results from a gas chromatograph are given as area percents. To relate area percent to weight percent in a normalized analysis (Perry, 1981), we calibrate with a mixture having known concentrations of the components we wish to determine. We can then use the resultant response factors to determine the concentrations of these components in mixtures. A standard sample is classified into two ways for determining its response factors. One is for a liquid-standard sample consisting of water, ethanol, isopropyl alcohol, DEE, EIPE, and DIPE. Another one is a gas-standard sample, propylene and 4-methyl-2pentene which were injected individually along ethanol.

1) Response factors for liquid sample

A liquid standard mixture was prepared under low temperature in a reagent bottle sealed with a rubber stopper and an aluminum crimp cap. This sample was pumped through a gas chromatograph.

2) Response factor for propylene

A gas-standard propylene or 4-methyl-2-pentene was passed to a sample-loop of known volume, 1.00 ml.. Under the same conditions 100 psig and 70°F, pure ethanol was fed with the same mass flow rate to the same column.

Using the normalized analysis to determine their response factors for each component :

Rf_i (Response factor) = weight percent$_i$ / area percent$_i$

weight product$_i$ = Rf_i * area$_i$ of unknown mixture

weight percent$_i$ = weight product$_i$ / ($\sum$ weight product$_i$)

Retention time and weight response factors of expected components in the catalyst evaluation are listed in Table C.1. The response factors were used to analyze experimental data as shown the typical chromatogram in Figure C.1.

Table C.1. Retention Times and Weight Response Factors of Gas and Liquid Standards.

Compond	Retention time (min)	Response Factor
4-methyl-2 pentene	0.88±0.09	0.707
Propylene	2.04±0.15	0.649
Water	2.95±0.20	0.993
Ethanol	6.37±0.14	0.931
Diethylether	7.55±0.06	0.848
Isopropyl alcohol	8.05±0.07	0.966
Ethyl isopropyl ether	8.70±0.15	1.091
Diisopropyl ether	11.03±0.08	1.474

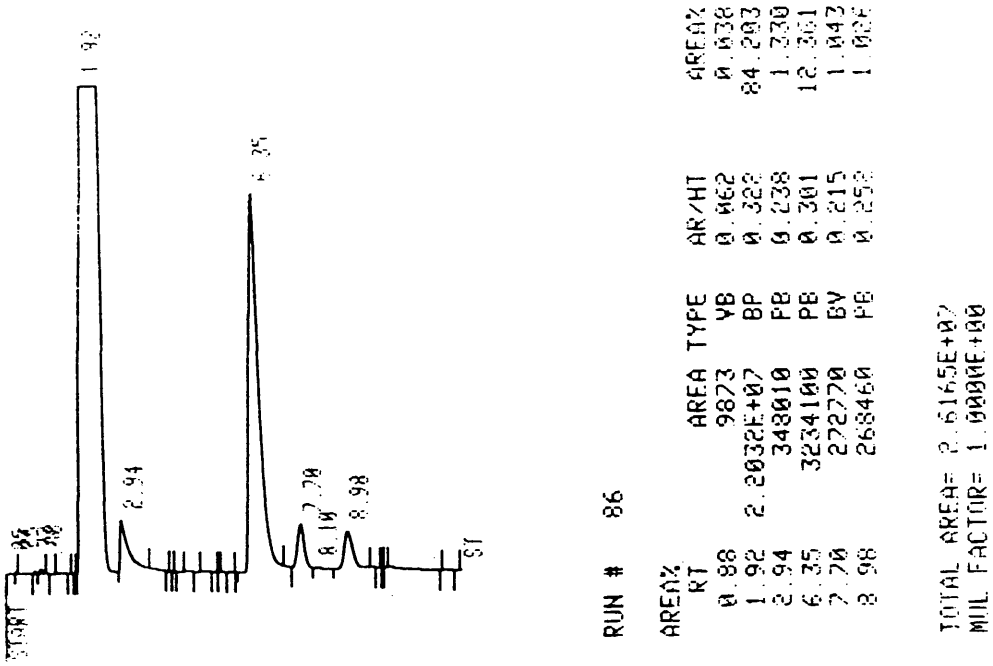

Figure C.1. A Typical Chromatogram.

Appendix C.2 Individual Runs.

Appendix C.2.1 Batch Reactor Experimental Data.

Catalyst: Dowex HCR-w2
Size catalyst : 20-50 mesh
Reactor: Batch

Run: / Component (mole %)	1	2	3	4	5	6	7	8	9
Propylene	-	-	-	-	-	-	-	-	-
Ethanol	94.41	66.05	64.83	79.98	31.39	12.17	16.66	17.98	4.72
DEE	-	3.35	2.79	1.93	8.49	11.35	11.30	14.25	15.82
Water	5.59	23.64	24.34	9.47	5.87	4.45	4.65	-	-
EIPE	-	3.02	3.54	3.30	28.08	59.08	44.74	57.14	65.55
IPA	-	3.93	4.49	5.30	26.15	10.13	22.65	0.29	5.71
DIPE	-	-	-	-	-	6.82	-	10.33	8.19
Conversion	-	12.84	12.33	8.22	58.94	87.04	80.16	82.64	95.36
Selectivity	-	31.09	38.83	46.07	62.30	66.44	66.43	66.72	67.45
COMPONENT MASS BALANCE %									
Carbon	-	92.40	93.54	93.10	96.63	90.07	94.21	99.10	94.01
Hydrogen	-	91.32	91.07	93.64	92.47	96.31	90.16	95.16	93.61
Oxygen	-	95.60	97.51	90.47	98.14	93.30	97.55	98.37	90.33
OPERATING CONDITIONS									
T(C)	80-120	125	115	115	115	125	125	125	125
Intial Pressure (psi)	800	850	815	815	900	800	700	1000	1000
Catalyst/EtOH (mass)	-	0.10	0.10	0.20	0.62	0.80	0.80	0.80	1.00
Propylene/EtOH(mass)	1.0-4.0	1.5	1.5	1.5	1.5	1.5	1.5	1.5	2.15

continue next page

C.2.1 (continue)

Run: / Component (mole %)	10	11	12	13	14	15
Propylene	-	-	-	-	-	-
Ethanol	1.87	48.35	96.59	90.18	19.57	8.23
DEE	20.13	11.61	-	-	23.31	21.50
Water	4.79	19.66	-	0.93	0.33	-
EIPE	64.18	13.21	1.45	6.12	54.56	62.84
IPA	1.87	7.16	0.81	1.41	1.50	6.31
DIPE	13.12	-	1.13	-	1.03	1.11
Conversion	99.82	42.97	3.41	9.82	80.43	91.77
Selectivity	61.45	36.26	100.00	100.00	53.92	59.37
COMPONENT MASS BALANCE %						
Carbon	94.58	96.12	97.89	98.12	95.77	95.54
Hydrogen	90.11	89.99	91.02	97.73	94.76	95.56
Oxygen	97.32	97.13	90.47	98.15	97.75	96.55
OPERATING CONDITIONS						
T(C)	125	125	125	125	125	125
Intial Pressure (psi)	1300	1200	1000	1000	1000	1000
Catalyst/EtOH (mass)	1.00	0.50	1.00	1.00	1.00	1.00
Propylene/EtOH(mass)	2.15	0.52	1.5	1.5	1.5	1.5
Time Stream (min)			20	35	50	65

Appendix C.2.2 Internal and External Mass Transfer Study

Catalyst: Dowex HCR-w2
Reactor: A Trickle Flow Reactor

Run: / Component (mole %)	16	17	18	19	20	21	22	23	24	25	26	27
Propylene	78.20	85.60	80.42	82.88	78.60	61.41	57.83	50.46	43.43	54.82	49.93	52.66
Ethanol	17.74	12.02	10.38	8.71	10.91	36.02	38.92	45.51	52.44	40.04	44.53	42.73
DEE	0.94	0.69	2.57	2.09	2.25	0.48	0.66	0.55	0.91	0.68	1.03	1.05
Water	0.87	0.89	2.04	2.92	3.08	0.38	0.82	0.067	0.93	0.89	1.27	1.21
EIPE	2.25	0.79	4.27	3.34	4.77	1.52	1.61	2.27	2.15	1.94	2.17	1.44
IPA	-	-	0.29	0.04	0.38	0.19	0.08	0.04	0.03	0.02	0.02	-
DIPE	-	-	-	-	-	-	0.06	0.02	0.09	0.05	0.04	-
Conversion	18.85	15.41	47.56	46.34	45.95	6.44	7.03	6.91	7.03	7.60	8.69	7.64
Selectivity	54.54	36.20	45.34	44.44	51.48	61.27	54.78	67.19	54.15	58.85	51.26	40.64
COMPONENT MASS BALANCE %												
Carbon	94.21	97.01	96.46	97.08	97.24	94.67	95.54	97.16	98.48	93.35	93.48	94.66
Hydrogen	90.11	89.99	91.55	91.02	94.56	95.56	90.18	96.55	91.88	91.27	93.00	93.46
Oxygen	97.32	97.13	94.29	94.16	94.28	97.16	96.55	99.57	94.76	92.48	95.45	95.56
OPERATING CONDITIONS												
T(C)	120	120	120	120	120	100	100	100	100	100	100	100
Pressure (psi)	150	150	150	150	150	500	500	500	500	500	500	500
Catalyst (mass)	1.74	2.13	4.21	7.00	5.77	2.00	2.00	2.00	2.00	2.00	2.00	2.00
Ethanol (ml/hr.)	1.00	1.00	1.00	1.00	1.00	1.60	1.60	1.60	1.60	1.60	1.60	1.60
Propylene (ml/hr.)	2.15	0.52		1.5	4.05	4.05	4.05	4.05	4.05	4.05	4.05	4.05
Catalyst Size (mesh)	20-50	20-50	20-50	20-50	20-50	20-40	20-40	40-70	70-100	70-100	40-70	40-70
WHSV (hr-1)	0.46	0.37	0.19	0.12	0.14	0.64	0.64	0.64	0.64	0.64	0.64	0.64

Appendix C.2.3 Catalyst Screening.

Catalyst: Dowex HCR-w2
Reactor: A Trickle Flow Reactor

Run:	28	29	30	31	32	33	34	35
Component (mole %)								
Propylene	52.66	77.98	60.90	54.46	45.08	74.94	58.02	67.61
Ethanol	42.83	19.89	35.24	22.59	27.74	12.22	37.87	29.71
DEE	0.95	0.46	0.82	5.29	6.06	3.15	0.84	0.61
Water	1.26	0.58	0.85	4.49	4.59	2.30	0.77	0.50
EIPE	2.17	1.08	2.18	11.31	16.17	7.22	2.42	1.48
IPA	0.08	-	-	0.98	0.31	0.14	-	-
DIPE	0.05	-	-	0.87	0.05	0.03	0.09	-
Conversion	8.66	9.16	9.77	49.21	50.50	52.54	9.75	8.35
Selectivity	53.36	54.05	57.18	51.65	57.15	53.35	59.07	54.55
COMPONENT MASS BALANCE %								
Carbon	95.10	97.55	98.81	97.00	98.78	96.41	98.87	99.20
Hydrogen	91.28	90.44	95.46	92.48	94.56	94.56	95.56	91.08
Oxygen	105.12	99.87	94.39	96.60	92.44	95.52	97.21	96.58
OPERATING CONDITIONS								
T(C)	100	100	100	140	140	140	100	100
Pressure (psi)	500	500	500	500	500	500	500	500
Catalyst (mass)	2.00	2.00	2.00	2.00	2.00	2.00	2.00	2.00
Ethanol (ml/hr.)	2.00	2.00	2.00	2.00	2.00	2.00	2.00	2.00
Propylene (ml/hr.)	4.5	4.5	4.5	4.5	4.5	4.5	4.5	4.5
Catalyst Size (mesh)	40-70	40-70	40-70	40-70	40-70	40-70	40-70	40-70
WHSV(hr-1)	0.8	0.8	0.8	0.8	0.8	0.8	0.8	0.8
Time Strem (hr.)	10	11	12	22	23	30	40	41

continued next page

C.2.3 (continued)

Catalyst: Amberlyst-15
Reactor: A Trickle Flow Reactor

Run: / Component (mole %)	36	37	38	39	40	41	42	43
Propylene	78.41	83.95	72.36	72.74	68.78	68.87	73.83	62.91
Ethanol	19.46	13.81	25.35	20.14	25.18	25.74	23.91	34.48
DEE	0.30	0.30	0.36	1.08	0.97	0.97	0.34	0.49
Water	0.38	0.27	0.37	1.12	0.99	0.96	0.41	0.051
EIPE	1.38	1.56	1.52	4.14	3.39	3.36	1.11	1.54
IPA	-	0.07	-	0.73	0.65	0.05	0.38	0.04
DIPE	0.05	0.02	0.02	0.03	0.03	0.03	0.01	0.01
Conversion	9.25	13.61	8.16	23.85	17.52	17.07	6.97	6.85
Selectivity	69.85	71.98	67.63	65.69	63.48	63.43	61.84	60.67
COMPONENT MASS BALANCE %								
Carbon	97.23	98.88	95.50	97.74	95.52	97.15	96.41	94.07
Hydrogen	91.23	96.64	94.37	94.68	92.34	94.00	94.79	90.59
Oxygen	101.56	97.33	100.02	99.26	97.10	98.11	102.45	99.95
OPERATING CONDITIONS								
T(C)	100	100	100	120	120	120	100	100
Pressure (psi)	500	500	500	500	500	500	500	500
Catalyst (mass)	2.00	2.00	2.00	2.00	2.00	2.00	2.00	2.00
Ethanol (ml/hr.)	2.00	2.00	2.00	2.00	2.00	2.00	2.00	2.00
Propylene (ml/hr.)	4.5	4.5	4.5	4.5	4.5	4.5	4.5	4.5
Catalyst Size (mesh)	40-70	40-70	40-70	40-70	40-70	40-70	40-70	40-70
WHSV(hr-1)	0.8	0.8	0.8	0.8	0.8	0.8	0.8	0.8
Time Strem (hr.)	10	11	12	22	23	30	40	41

continued next page

C.2.3 (continued)

Catalyst: Supported FCSA
Reactor: A Trickle Flow Reactor

Run:	44	45	46	47	48	49	50	51
Component (mole %)								
Propylene	72.78	54.78	52.88	66.12	49.36	52.37	74.75	54.71
Ethanol	23.87	4.00	43.09	7.48	11.29	6.39	21.46	40.86
DEE	1.16	1.76	1.47	7.71	12.26	13.82	0.79	1.40
Water	1.36	1.96	1.71	6.29	7.21	6.12	2.43	2.23
EIPE	0.835	1.52	0.08	10.66	17.04	18.05	0.56	0.79
IPA	-	-	-	1.15	1.88	2.06	-	-
DIPE	-	-	-	0.57	0.94	1.11	-	-
Conversion	11.65	11.19	8.05	77.70	78.62	87.73	9.11	8.08
Selectivity	26.53	30.12	22.05	40.87	41.01	39.51	26.07	22.09
COMPONENT MASS BALANCE %								
Carbon	95.16	97.14	94.56	97.11	95.01	96.00	92.31	94.56
Hydrogen	94.23	94.01	90.23	91.51	90.45	92.22	91.78	93.79
Oxygen	99.56	97.34	100.42	96.77	88.13	87.02	102.45	105.79
OPERATING CONDITIONS								
T(C)	140	140	140	180	180	180	140	140
Pressure (psi)	500	500	500	500	500	500	500	500
Catalyst (mass)	2.00	2.00	2.00	2.00	2.00	2.00	2.00	2.00
Ethanol (ml/hr.)	2.00	2.00	2.00	2.00	2.00	2.00	2.00	2.00
Propylene (ml/hr.)	4.5	4.5	4.5	4.5	4.5	4.5	4.5	4.5
Catalyst Size (mesh)	40-70	40-70	40-70	40-70	40-70	40-70	40-70	40-70
WHSV(hr-1)	0.8	0.8	0.8	0.8	0.8	0.8	0.8	0.8
Time Strem (hr.)	10	11	12	22	23	30	40	41

continued next page

C.2.3 (continued)

Catalyst: P/Al 0.8
Reactor: A Trickle Flow Reactor

Run: / Component (mole %)	52	53	54	55	56	57	58	59
Propylene	60.03	55.96	61.81	81.17	58.78	62.56	48.40	42.05
Ethanol	34.58	37.86	32.61	13.92	31.08	26.95	42.95	50.55
DEE	2.54	2.62	2.08	2.32	4.59	4.25	3.86	3.14
Water	2.07	2.73	2.64	2.09	4.60	5.37	3.86	3.35
EIPE	0.76	0.83	0.86	0.49	0.94	0.87	0.85	0.90
IPA	-	-	-	-	-	-	-	-
DIPE	-	-	-	-	-	-	-	-
Conversion	14.48	13.81	13.33	26.92	24.58	25.81	16.63	12.45
Selectivity	13.06	13.64	17.20	9.65	9.24	9.30	9.91	12.55
COMPONENT MASS BALANCE %								
Carbon	96.15	97.82	98.76	99.00	96.70	97.51	100	98.83
Hydrogen	92.34	91.23	96.17	95.70	95.55	97.20	100	97.57
Oxygen	96.66	94.42	100.12	99.33	98.80	103.48	100	99.97
OPERATING CONDITIONS								
T(C)	140	140	140	240	240	240	140	140
Pressure (psi)	500	500	500	500	500	500	500	500
Catalyst (mass)	2.00	2.00	2.00	2.00	2.00	2.00	2.00	2.00
Ethanol (ml/hr.)	2.00	2.00	2.00	2.00	2.00	2.00	2.00	2.00
Propylene (ml/hr.)	4.5	4.5	4.5	4.5	4.5	4.5	4.5	4.5
Catalyst Size (mesh)	40-70	40-70	40-70	40-70	40-70	40-70	40-70	40-70
WHSV(hr-1)	0.8	0.8	0.8	0.8	0.8	0.8	0.8	0.8
Time Strem (hr.)	10	11	12	22	23	30	40	41

Appendix C.2.4 Experimental EIPE Kinetic Data.

Catalyst: Dowex HCR-w2
Reactor: A Trickle Flow Reactor

Run: / Component (mole %)	60	61	62	63	64	65	66	67	68
Propylene	83.50	65.78	77.65	59.10	59.84	67.17	67.38	79.90	61.68
Ethanol	15.96	32.78	21.58	39.41	38.37	31.28	31.18	18.79	36.18
DEE	0.16	0.33	0.24	0.53	0.47	0.42	0.42	0.28	0.58
Water	0.17	0.65	0.25	0.51	0.85	0.41	0.43	0.52	0.56
EIPE	0.19	0.42	0.28	0.47	0.46	0.55	0.58	0.50	0.76
IPA	-	-	-	-	-	-	-	-	-
DIPE	-	-	-	-	-	-	-	-	-
Conversion	3.13	3.17	3.38	3.73	3.51	4.27	4.35	5.30	5.05
Selectivity	36.91	39.14	36.62	30.50	32.93	39.49	40.96	47.56	39.38
COMPONENT MASS BALANCE %									
Carbon	98.33	97.26	95.58	98.03	96.74	97.82	95.57	96.37	99.46
Hydrogen	92.35	95.14	93.15	91.05	92.00	95.12	93.20	94.18	91.19
Oxygen	102.47	110.20	100.06	97.25	111.30	98.16	99.60	105.50	97.63
OPERATING CONDITIONS									
T(C)	100	100	100	100	100	100	100	100	100
Pressure (psi)	370	370	420	42	425	510	510	610	620
Catalyst (mass)	0.50	0.50	0.50	0.50	0.50	0.50	0.50	0.50	0.50
Ethanol (ml/hr.)	2.00	2.00	2.00	2.00	2.00	2.00	2.00	2.00	2.00
Propylene (ml/hr.)	4.50	4.50	4.50	4.50	4.50	4.50	4.50	4.50	4.50
Catalyst Size (mesh)	40.70	40.70	40.70	40.70	40.70	40.70	40.70	40.70	40.70

continued next page

C.2.4 (continued)

Catalyst: Dowex HCR-w2
Reactor: A Trickle Flow Reactor

Run: / Component (mole %)	69	70	71	72	73	74	75	76	77
Propylene	70.22	57.34	77.80	60.04	61.95	68.10	77.95	59.44	58.22
Ethanol	28.46	40.45	21.04	38.00	35.92	30.04	20.52	36.77	39.03
DEE	0.44	0.69	0.31	0.59	0.62	0.51	0.46	0.88	0.89
Water	0.53	0.71	0.28	0.53	0.63	0.47	0.54	1.81	0.80
EIPE	0.44	0.75	0.57	0.98	0.93	0.80	0.56	1.11	1.07
IPA	-	-	-	-	-	-	-	-	-
DIPE	-	-	-	-	-	-	-	-	-
Conversion	4.46	5.01	5.33	5.36	5.68	5.69	6.71	7.22	6.79
Selectivity	33.37	34.98	48.03	45.38	42.87	44.08	37.99	38.75	37.68
COMPONENT MASS BALANCE %									
Carbon	96.57	97.85	99.66	98.73	97.51	98.17	97.14	99.64	98.15
Hydrogen	92.37	93.57	96.78	95.81	94.15	94.43	93.47	92.18	93.48
Oxygen	102.24	103.48	97.52	98.61	100.01	95.68	99.46	112.47	98.63
OPERATING CONDITIONS									
T(C)	110.18	110.18	110.18	110.18	110.18	110.18	121.30	121.30	121.30
Pressure (psi)	400	475	520	520	560	560	400	422	422
Catalyst (mass)	0.50	0.50	0.50	0.50	0.50	0.50	0.50	0.50	0.50
Ethanol (ml/hr.)	2.00	2.00	2.00	2.00	2.00	2.00	2.00	2.00	2.00
Propylene (ml/hr.)	4.50	4.50	4.50	4.50	4.50	4.50	4.50	4.50	4.50
Catalyst Size (mesh)	40.70	40.70	40.70	40.70	40.70	40.70	40.70	40.70	40.70

continued next page

C.2.4 (continued)

Catalyst: Dowex HCR-w2
Reactor: A Trickle Flow Reactor

Run: / Component (mole %)	78	79	80	81	82	83	84	85	86
Propylene	75.09	60.03	62.57	63.38	55.04	54.77	74.54	61.02	78.42
Ethanol	22.95	37.18	34.46	33.07	40.93	41.21	21.02	33.34	18.58
DEE	0.60	0.92	0.85	0.91	1.07	1.06	0.85	1.21	0.82
Water	0.63	0.90	0.90	0.97	1.10	1.00	2.04	1.96	0.93
EIPE	0.74	1.27	1.18	1.60	1.96	2.01	1.30	2.39	1.21
IPA	-	-	-	-	-	-	-	-	-
DIPE	-	-	-	-	-	-	-	-	-
Conversion	7.82	7.70	7.72	9.35	9.09	9.13	12.50	12.59	13.33
Selectivity	38.06	40.95	40.78	46.91	47.85	48.66	43.38	49.81	42.45
COMPONENT MASS BALANCE %									
Carbon	98.50	97.21	95.16	97.16	94.57	98.00	97.82	94.27	97.59
Hydrogen	92.67	95.18	90.57	96.74	91.27	95.46	92.19	90.29	96.17
Oxygen	101.54	99.78	102.42	101.01	100.20	99.10	109.31	105.24	101.48
OPERATING CONDITIONS									
T(C)	121.30	121.30	121.30	121.30	121.30	121.30	132.40	132.40	132.40
Pressure (psi)	515	515	515	550	620	620	420	420	500
Catalyst (mass)	0.50	0.50	0.50	0.50	0.50	0.50	0.50	0.50	0.50
Ethanol (ml/hr.)	2.00	2.00	2.00	2.00	2.00	2.00	2.00	2.00	2.00
Propylene (ml/hr.)	4.50	4.50	4.50	4.50	4.50	4.50	4.50	4.50	4.50
Catalyst Size (mesh)	40.70	40.70	40.70	40.70	40.70	40.70	40.70	40.70	40.70

continued next page

C.2.4 (continued)

Catalyst: Dowex HCR-w2
Reactor: A Trickle Flow Reactor

Run: / Component (mole %)	87	88	89	90	91	92
Propylene	67.29	58.07	59.07	63.67	61.75	56.54
Ethanol	28.72	29.89	28.65	25.33	26.39	31.45
DEE	1.23	0.80	0.83	0.79	31.45	1.06
Water	1.23	11.04	11.21	10.04	10.67	10.27
EIPE	2.08	0.25	0.38	0.22	0.44	0.67
IPA	-	-	-	-	-	-
DIPE	-	-	-	-	-	-
Conversion	13.66	5.83	6.66	6.67	8.37	8.53
Selectivity	45.73	13.38	18.67	12.27	18.63	22.77
COMPONENT MASS BALANCE %						
Carbon	98.50	97.21	95.16	97.16	94.57	98.00
Hydrogen	92.67	95.18	90.57	96.74	91.27	95.46
Oxygen	101.54	99.78	102.42	101.01	100.20	99.10
OPERATING CONDITIONS						
T(C)	121.30	100	100	100	100	100
Pressure (psi)	550	425	520	520	590	590
Catalyst (mass)	0.50	0.50	0.50	0.50	0.50	0.50
Ethanol (ml/hr.)	2.00	2.00	2.00	2.00	2.00	2.00
Propylene (ml/hr.)	4.50	4.50	4.50	4.50	4.50	4.50
Catalyst Size (mesh)	40.70	40.70	40.70	40.70	40.70	40.70

Appendix C.2.5 Experimental DEE Kinetic Data

Catalyst: Dowex HCR-w2
Reactor: A Trickle Flow Reactor

Run: / Component (mole %)	93	94	95	96	97	98	99	100	101
Ethanol	87.85	77.37	79.36	79.55	66.08	62.47	71.94	61.39	54.58
DEE	5.95	10.95	12.02	11.28	14.82	17.75	13.96	17.46	22.32
Water	6.20	11.68	8.62	9.16	19.10	19.78	14.10	21.15	23.10
Conversion	11.93	22.07	23.25	22.10	30.96	36.23	27.96	36.25	44.99
COMPONENT MASS BALANCE %									
Carbon	96.35	97.22	95.66	97.61	94.37	98.20	99.45	97.34	95.78
Hydrogen	94.01	92.57	91.58	94.00	90.37	96.01	91.27	94.03	91.11
Oxygen	102.53	105.34	95.64	92.14	102.37	105.10	101.03	107.34	101.32
OPERATING CONDITIONS									
T(C)	100.00	110.18	121.30	100.00	110.18	121.30	100.00	110.18	121.30
Pressure (psi)	500	500	500	500	500	500	500	500	500
Catalyst (mass)	0.02	0.02	0.02	0.04	0.04	0.04	0.05	0.05	0.05
Ethanol (ml/hr.)	5.00	5.00	5.00	5.00	5.00	5.00	5.00	5.00	5.00
Catalyst Size (mesh)	40.70	40.70	40.70	40.70	40.70	40.70	40.70	40.70	40.70

continued next page

C.2.5 (continued)

Catalyst: Dowex HCR-w2
Reactor: A Trickle Flow Reactor

Run: / Component (mole %)	102	103	104	105	106	107	108	109	110
Ethanol	70.90	60.12	50.48	67.50	57.71	35.76	66.58	55.03	38.88
DEE	15.13	20.59	24.80	15.68	21.31	21.66	16.50	21.96	28.84
Water	13.97	19.29	24.71	16.82	20.97	42.57	16.91	23.02	32.28
Conversion	29.91	40.66	49.56	31.72	42.48	54.77	33.14	44.39	59.74
COMPONENT MASS BALANCE %									
Carbon	99.13	96.79	96.46	98.10	97.71	99.17	95.58	98.55	96.22
Hydrogen	92.55	95.73	90.99	91.64	94.22	91.64	94.26	91.01	92.38
Oxygen	97.33	98.66	99.28	103.20	98.77	112.48	100.83	102.44	103.79
OPERATING CONDITIONS									
T(C)	100.00	110.18	121.30	100.00	110.18	121.30	100.00	110.18	121.30
Pressure (psi)	500	500	500	500	500	500	500	500	500
Catalyst (mass)	0.07	0.07	0.07	0.09	0.09	0.09	0.13	0.13	0.13
Ethanol (ml/hr.)	5.00	5.00	5.00	5.00	5.00	5.00	5.00	5.00	5.00
Catalyst Size (mesh)	40.70	40.70	40.70	40.70	40.70	40.70	40.70	40.70	40.70

Appendix C.2.6 Selectivity Study and Catalyst Deactivation Test

Catalyst: Dowex HCR-w2
Reactor: A Trickle Flow Reactor

Run: / Component (mole %)	111	112	113	114	115	116	117	118	119	120	121	122	123	124
Propylene	70.25	69.66	67.18	68.71	67.47	71.65	52.66	77.98	60.90	54.46	45.08	74.94	58.02	67.61
Ethanol	19.01	16.14	17.36	20.60	13.78	12.81	44.61	19.89	35.24	21.01	20.57	11.56	43.62	29.71
DEE	9.14	12.39	14.04	8.93	16.64	13.52	0.95	0.46	8.17	6.18	6.06	3.15	0.84	0.65
Water	0.62	0.62	0.44	0.60	0.37	0.39	1.26	0.58	8.52	6.08	5.83	2.30	0.77	0.49
EIPE	1.79	1.20	0.96	1.15	1.73	1.63	2.85	1.36	14.78	12.84	12.34	7.22	1.69	1.29
IPA	-	-	-	-	-	-	0.08	-	-	1.00	0.31	0.14	0.04	0.01
DIPE	-	-	-	-	-	-	0.05	-	-	0.87	0.06	0.03	0.09	0.06
Conversion	10.44	13.07	9.67	9.35	15.23	15.84	9.60	10.27	46.90	54.54	54.33	53.92	7.17	7.82
Selectivity	44.28	49.51	51.81	46.91	70.01	67.46	60.04	59.52	47.48	50.94	50.45	53.35	50.34	51.19
MASS BALANCE %														
							97.16	95.87	98.08	98.06	99.10	96.66	96.18	97.06
C-H-O	90-100	90-100	90-100	90-100	90-100	90-100	94.51	92.00	94.10	92.37	95.13	94.44	91.20	96.17
							105.55	101.36	100.88	97.16	97.64	96.48	96.11	98.00
OPERATING CONDITIONS														
T(C)	100	100	100	110.18	110.18	110.18	100	100	140	140	140	140	100	100
Pressure (psi)	500	500	500	500	500	500	500	500	500	500	500	500	500	500
Catalyst (mass)	0.50	0.50	0.50	0.50	0.50	0.50	2.00	2.00	2.00	2.00	2.00	2.00	2.00	2.00
Mixture Ethanol (ml/hr.	2.00	2.00	2.00	2.00	2.00	2.00	2.00	2.00	2.00	2.00	2.00	2.00	2.00	2.00
Propylene (ml/hr.)	4.50	4.50	4.50	4.50	4.50	4.50	4.50	4.50	4.50	4.50	4.50	4.50	4.50	4.50
DEE:Ethanol	0.50	1.00	1.00	0.50	1.00	1.00								
Time Stream(hr.)							10	15	32	57	94	126	137	142

C.2-7 Derivation of LHHW Rate Expressions.

Model 1 Adsorption of EtOH controlling

$$Et + * \underset{k'_{Et}}{\overset{k_{Et}}{\rightleftharpoons}} Et*$$

$$Pr + * \overset{K_{Pr}}{\rightleftharpoons} Pr*$$

$$Et* + Pr* \overset{K}{\rightleftharpoons} E* + *$$

$$E* \overset{K_E}{\rightleftharpoons} E + *$$

$$-r = k_{Et}C_{Et}C_* - k'_{Et}C_{Et*}$$

where $K_{Pr} = \dfrac{C_{Pr*}}{C_{Pr}C_*}$, $K = \dfrac{C_{E*}C_*}{C_{Et*}C_{Pr*}}$, $K_E = \dfrac{C_{E*}}{C_E C_*}$

$$C_{*tot} = C_* + C_{Et*} + C_{Pr*} + C_{E*}$$

therefore, $C_{Et*} = \dfrac{K_E C_E C_*}{K K_{Pr} C_{Pr}}$, $C_* = \dfrac{C_{*tot}}{1 + K_{Pr}C_{Pr} + K_E C_E + \dfrac{K_E C_E}{K K_{Pr} C_{Pr}}}$

substitute;

$$-r = \frac{C_{*tot}\left(k_{Et}C_{Et} - \dfrac{k'_{Et}K_E C_E}{K K_{Pr} C_{Pr}}\right)}{1 + K_{Pr}C_{Pr} + K_E C_E + \dfrac{K_E C_E}{K K_{Pr} C_{Pr}}}$$

consider only the forward reaction term (for low conversions)

$$-r = \frac{k' C_{l,Et}}{1 + \dfrac{K_{Pr}}{H} C_{g,Pr}} \quad \text{where} \quad k' = k_{Et} C_{*tot}$$

Model 2 Adsorption of Propylene controlling

$$Et + * \overset{K_{Et}}{\rightleftharpoons} Et^*$$

$$Pr + * \underset{k'_{Pr}}{\overset{k_{Pr}}{\rightleftharpoons}} Pr^*$$

$$Et^* + Pr^* \overset{K}{\rightleftharpoons} E^* + *$$

$$E^* \overset{K_E}{\rightleftharpoons} E + *$$

$$-r = k_{Pr} C_{Pr} C_* - k'_{Pr} C_{Pr^*}$$

where $K_{Et} = \dfrac{C_{Et^*}}{C_{Et} C_*}$, $K = \dfrac{C_{E^*} C_*}{C_{Et^*} C_{Pr^*}}$, $K_E = \dfrac{C_{E^*}}{C_E C_*}$

$$C_{*tot} = C_* + C_{Et^*} + C_{Pr^*} + C_{E^*}$$

therefore, $C_{Et^*} = \dfrac{K_E C_E C_*}{K K_{Et} C_{Et}}$, $C_* = \dfrac{C_{*tot}}{1 + K_{Et} C_{Et} + K_E C_E + \dfrac{K_E C_E}{K K_{Et} C_{Et}}}$

substitute;

$$-r = \frac{C_{*tot}\left(k_{Pr\,t} C_{Pr} - \dfrac{k'_{Pr} K_E C_E}{K K_{Et} C_{Et}}\right)}{1 + K_{Et} C_{Et} + K_E C_E + \dfrac{K_E C_E}{K K_{Et} C_{Et}}}$$

consider only the forward reaction term (for low conversion)

$$-r = \frac{k' C_{g,Pr}}{1 + K_{Et} C_{Et}} \quad \text{where} \quad k' = k_{Pr} C_{*tot}$$

Model 3 Surface reaction controlling

$$Et + * \overset{K_{Et}}{\rightleftharpoons} Et^*$$

$$Pr + * \overset{K_{Pr}}{\rightleftharpoons} Pr^*$$

$$Et^* + Pr^* \underset{k'_s}{\overset{k_s}{\rightleftharpoons}} E^* + *$$

$$E^* \overset{K_E}{\rightleftharpoons} E + *$$

$$-r = k_s C_{Et^*} C_{Pr^*} - k'_s C_{E^*} C_*$$

where $K_{Pr} = \dfrac{C_{Pr^*}}{C_{Pr} C_*}$, $K_{Et} = \dfrac{C_{Et^*}}{C_{Et} C_*}$, $K_E = \dfrac{C_{E^*}}{C_E C_*}$

$$C_{*tot} = C_* + C_{Et^*} + C_{Pr^*} + C_{E^*}$$

therefore,

$$C_{Et^*} = K_{Et} C_{Et} C_* \,,\; C_{E^*} = K_E C_E C_* \,,\; C_{Pr^*} = K_{Pr} C_{Pr} C_* \,,\; C_* = \frac{C_{*tot}}{[1 + K_{Pr} C_{Pr} + K_E C_E + K_{Et} C_{Et}]}$$

substitute;

$$-r = \frac{k_s C_{*tot} \left(K_{Et} K_{Pr} C_{Et} C_{Pr} - \dfrac{K_E}{K} C_E \right)}{\left(1 + K_{Pr} C_{Pr} + K_{Et} C_{Et} + K_E C_E\right)^2}$$

consider only the forward reaction term (for low conversion)

$$-r = \frac{k' C_{g,Pr} C_{l,Et}}{\left(1 + \dfrac{K_{Pr}}{H} C_{g,Pr} + K_{Et} C_{l,Et}\right)^2} \quad \text{where} \quad k' = k_s K_{Et} \frac{K_{Pr}}{H} C_{*tot}$$

Model 4 Desorption of EIPE controlling

$$Et + * \overset{K_{Et}}{\rightleftharpoons} Et^*$$

$$Pr + * \overset{K_{Pr}}{\rightleftharpoons} Pr^*$$

$$Et^* + Pr^* \overset{K}{\rightleftharpoons} E^* + *$$

$$E^* \overset{k_E}{\underset{k'_E}{\rightleftharpoons}} E + *$$

$$-r = k_E C_{E^*} - k'_E C_E C_*$$

where $K_{Pr} = \dfrac{C_{Pr^*}}{C_{Pr} C_*}$, $K = \dfrac{C_{E^*} C_*}{C_{Et^*} C_{Pr^*}}$, $K_{Et} = \dfrac{C_{Et^*}}{C_{Et} C_*}$

$$C_{*tot} = C_* + C_{Et^*} + C_{Pr^*} + C_{E^*}$$

therefore, $C_{E^*} = K K_{Pr} K_{Et} C_{Pr} C_{Et} C_*$, $C_* = \dfrac{C_{*tot}}{1 + K_{Pr} C_{Pr} + K_{Et} C_{Et} + K K_{Pr} K_{Et} C_{Pr} C_{Et}}$

substitute;

$$-r = \frac{C_{*tot}\left(k_E K K_{Pr} K_{Et} C_{Pr} C_{Et} - k'_E C_E\right)}{1 + K_{Pr} C_{Pr} + K_{Et} C_{Et} + K K_{Pr} K_{Et} C_{Pr} C_{Et}}$$

consider only the forward reaction term (for low conversion)

$$-r = \frac{k' C_{g,PR} C_{l,Et}}{1 + \dfrac{K_{Pr}}{H} C_{g,Pr} + K_{Et} C_{l,Et} + K'' C_{g,Pr} C_{l,Et}}$$ where

$k' = k_E C_{*tot}$, $K'' = K K_{Pr} K_{Et} / H$

APPENDIX D
ESTIMATION OF
MASS AND HEAT TRANSFER EFFECTS

Given Data:

density of catalyst particle = 1 g/cm^3

void faction (ε, θ) = 0.5

surface area of catalyst Dowex HCR-w2 = 0.1 m^2/g

solubility of propylene in ethanol at 1 atm and 17°C = 16 cm^3/ 100 cm^3

Henry's Law constant (H) = 148.743 l-atm/mol

Maximum reaction rate = 0.02 mol/hr-g(cat)

(-ΔH) of reaction = 68 kJ/mol

R gas constant = 82.057 cm^3-atm/mol-K

Maximum flow rate of propylene = 5 cm^3/hr

Maximum flow rate of ethanol = 2 cm^3/hr $M_{ethanol}$ = 46

T = 390 K; P = 500 psi

d_p (catalyst particle) = 0.078 cm

Superficial Gas Flow Rate, G

$\rho_{propylene}$ @ 500 psi and 390 K = 90 g./cm^3

$$G = \frac{90\ g/cm^3 * 5\ cm^3/hr * 100^2\ cm^2/m^2 * 1kg}{0.85177\ cm^2 * 1000g}$$

$= 5.3 \times 10^3$ kg/ m^2-hr

Superficial Liquid Flow Rate, L

$$L = \frac{1.6\ kg/hr * 100^2}{1000 * 0.85177\ m^2}$$

= 18.80 kg/ m^2-hr

D.1 Interphase Mass Transfer.

The criteria which is used to study the external mass transfer effect from the bulk gas and liquid to the catalyst surface was proposed by Satterfield (1970). It was proposed that when $\frac{10\, d_p}{C^*\, k_{LS}}\, r\,(1-\varepsilon) \;<\; 1$ external mass transfer effects can be neglected.

where k_{Ls} (overall external mass transfer coefficient) [cm/s]

C^* (saturation concentration of propylene in ethanol) [mol/L]

$k_{Ls} = \frac{2 D_{12}\, a}{\varepsilon}$

where a (interfacial area for mass transfer) = 1000 [1/cm]

D_{12} (molecular diffusivity; from Appendix D.2) = 1.634×10^{-5} cm^2/s

Therefore, k_{Ls} = 0.065 cm/s

C* = P/H (Henry's Law)

$$= \frac{500 / 14.7\ atm}{148.743\ L - atm / mol} = 0.2286\ \text{mol/L}$$

Substitute in the criteria equation

$$LHS: \quad \frac{10 * 0.078 cm * 0.02\ \frac{mol}{hr - g.} * 0.5 * 1000\ g / cm^3}{0.2286 mol / L * 0.065\ cm / s\ 3600\ s / hr} = 0.146$$

D.2 Intraparticle Mass Transfer.

The Weisz parameter was modified by Satterfiled (1970) for trickle-bed reactor:

$$\frac{(d_p / 2)^2}{D_{eff}\, C_s}\, r\,(1-\varepsilon) \;<\; 1$$

then if the criteria holds, intraparticle transport can be neglected.

where D_{eff} (effective diffusivity; cm2/s) = $\frac{1}{\frac{1}{D_{K,eff}} + \frac{1}{D_{12,eff}}}$

$$D_{K,eff}\text{(Knuden diffusion)} = 194000\frac{\theta^2}{\tau_m s \rho_p}\sqrt{\frac{T}{M}}$$

$$= 4.519 \text{ cm}^2/\text{s} \sqrt{\frac{T}{M}}$$

$$D_{12} = \frac{7.4x10^{-8} (\varphi M)^{0.5} T}{\mu V^{0.6}} \text{ cm}^2/\text{s}$$

φ (associate factor) for ethanol = 1.5 (Reid, 1990)

μ (viscosity of ethanol at reaction conditions) = 1.1 cP

V (propylene molar volume at reaction conditions) = 75 cm^3/mol

then, D_{12} = 1.634 x 10^{-5} cm^2/s

$$D_{12,eff} = \frac{D_{12}\theta}{\tau_m} = 3.3 \text{ x } 10^{-6} \text{ cm}^2/\text{s}$$

Therefore, D_{eff} = 3.3 x 10^{-6} cm^2/s

C_s (ethanol concentration at surface) $\cong$ Concentration of ethanol * effectiveness factor (asumed 0.5)

$\cong$ 8.70 x 10^{-3} mol/cm^3

Substitute into the criteria

$$\frac{(0.078/2)^2 \text{ x } 0.02 \text{ x } 0.5}{3.3x10^{-6} \text{ x } 8.7x10^{-3} \text{ x } 3600} = 0.15$$

D.3 Heat Transfer Limitation

From the energy balance, the difference between surface temperature and bulk temperature is defined as

$$T_s - T_b = \frac{r(-\Delta H)(C_p \mu / k_f)^{\frac{2}{3}}}{s j_H C_p L}$$

where C_p (ethanol heat capacity at reaction conditions) = 159 J/K-mol

k_f (thermal conductivity of ethanol) = 0.135 W/m-K

j_H (heat transfer factor; assumed to be equal to j_D) = $\frac{0.458}{\varepsilon}\left(\frac{d_p L}{\mu}\right)^{-0.407}$

The difference can be acceptable if it is less than 5 °C.

substitute

$$T_s - T_b = \frac{0.02\ (mol/hr-g.cat)x\ 68000(J/mol)\left(\frac{159/46\ x\ 1.1\ x\ 0.01\ x\ 100}{0.135}\right)^{-0.407}}{0.1(m^2/g.cat)\ x\ 8.947\ x\ 159/46\ x\ 18780(g/hr-m^2)}$$

$$= 0.22\ K$$

D.4 Axial Dispersion.

Mears (1974) presents the following criterion for the axial dispersion as

$$\frac{h}{d_p} > \frac{20\,m}{Pe_L}\ln\frac{1}{1-x}$$

where h (height of reacotr) = 2.5 cm

m (reaction order; asume to be first order) = 1

Pe_L (pelect No.) = $d_p L_v/D_l$

The value of Peclet No. was general used at

= 2 for fully developed turbulent flow

= 0.15 for Reynolds No. less than 0.4 which is applicable in this case.

x (conversion) = 0.15 for the maximum sutdy

substitute

LHS. = 32

RHS. = 21

It was found that the axial dispersion can be ignored in the range of study.

APPENDIX E
NON-LINEAR LEAST SQUARES

SSE (sum of the squares of error) = $\sum_{1}^{N} \frac{(r_{ic} - r_{im})^2}{N - K - 1}$

where N = number of runs

K = number of parameters to be determined

r_{im} = measured reaction rate for run i

r_{ic} = calculated reaction rate for run i

The program is modified to minimize the value of SSE (Folgler, 1992).

```
      Program Nonlinear Least Squares
      implicit none
      integer i,j,k
      real x(9),y(9),z(9),a,b,c,sum,dif,coma(1000),min1,mina,minb
      real sse,min2,v,comb(1000),comc(1000),minc,min3,m,N
      open (unit=20,file='raw.d',status='unknown')
      open (unit=21,file='pro.d',status='unknown')
      read(20,*) (x(i),i=1,9)
      read(20,*) (y(i),i=1,9)
      read(20,*) (z(i),i=1,9)
      coma(1)=1
      comb(1)=1
      comc(1)=1
      do 40 m=2,1000
              b=0.000001
      do 30 k=2,1000
              c=c+0.001
              a=0.0001
      do 10 j= 2,2000
              sum=0.0
              i=j-1
              N=9
              do 20 i=1,9
              dif=sum+(((a*x(i)*y(i)/(1+b*y(i)+c*x(i))**2)-z(i))**2/(N-4))
              sum=dif
20            continue
              coma(j)=sum
              if (abs(coma(j)/coma(j-1)) .gt. 1.) then
              min1=coma(j-1)
              mina=a
              else
              endif
              a=a+0.001
10    continue
      comb(k)=min1
      if(abs(comb(k)/comb(k-1)) .gt. 1.) then
              min2 = comb(k-1)
              minc=c
              else
              endif
30    continue
```

```
        comc(m)=min2
        if(abs(comc(m)/comc(m-1)) .gt. 1.) then
                min3 =comc(m-1)
                minb=b
                else
                endif
                b=b+0.000001
40      continue
        write (21,100) (mina,minb)
        write (21,101) (minc,min3)
100     format (1x,'mina=',e10.3,'minb=',e10.3)
101     format (1x,'minc=',e10.3,'min3=',e10.3)
        end
```